MASSEY UNIVERSITY
TE KUNENGA KI PŪREHUROA
UNIVERSITY OF NEW ZEALAND

Effect of Air Temperature on the Thermal Degradation of Heat Liable Products in Spray Drying and Monodisperse Drying

A thesis presented in partial fulfilment of the requirements for the degree of

Master of Food Technology

at Massey University, Manawatū, New Zealand

Xiaoqi Sang

2018

Abstract

Three heat liable protein-based materials β-galactosidase, whey protein isolate (WPI) and egg white (with 30-35% w/w total solids) were dried through conventional spray drying and monodisperse drying respectively with constant inlet air temperature 200 ℃ and different outlet air temperature. The purpose was to test the hypothesis that monodisperse droplet drying could produce more control over time-temperature experience during drying, resulting in reduced loss of structure or activity. The residual enzyme activity of the dried lactase product was determined by ONPG β-galactosidase assay, and the extent of denaturation of WPI and egg white was determined by differential scanning calorimetry (DSC). Particle size and morphology were also measured and observed.

The results showed that for both spray drying and monodisperse drying, the extent of protein denaturation increased as outlet air temperature increased. In comparison with spray drying, monodisperse drying had a longer residence time using our particular apparatus and gave rise to higher extent of heat degradation for all three materials. The dried products from monodisperse drying showed a narrower particle size distribution but had larger particle size compared to the products from spray drying. The majority of monodisperse dried powders had a multivesicular hallow morphology due to high interior temperature and coalescence of neighbouring particle in flight. The feasibility of using monodisperse drying in real industry is still under investigation. Although the results obtained from this study denied the expectation that monodisperse drying can reduce the thermal degradation of product during drying process, they are still useful in developing the monodisperse drying system and optimizing the operating parameters.

Acknowledgements

Firstly, I would like to express my sincere gratitude to my supervisors Professor Richard Archer and Dr. Jeremy Smith for them giving me the chance to conduct this project and guiding me the direction to broaden my thinking. I am also thankful for their help and support throughout the whole project. The knowledge and experiences that I achieved from this project are invaluable.

My special thanks go to Dr. Jim Q Chen for helping me with understanding the rationale of reaction kinetic and calculations; and Professor Patrick Morel for the assistance on data analysis and statistical problems.

I sincerely appreciated the support from the following people:

- Mr John Pedley for helping with the electrical issues, heating system and insulation of the heater stack.
- Mr Garry Radford, Mr Byron McKillop and Mr Warwick Johnson for their support on spray drying and other equipment in the pilot plant.
- Ms Michelle Tamehana for the help with spectrophotometer and rheometer.
- Mr Steve Glasgow for his guidance on Kjeldahl determination, moisture content and water activity measurement.
- Mr Chris Hall for the training and help with DSC measurement.
- Mr John Sykes for his assistance on particle size measurement.
- Mr Trevor Loo for training me on nano-DSC technique.

I would also like to thank the other postgraduate students and interns who helped me during the project, especially Jolin Morel, Lukas Frieler who helped me a lot on the monodisperse drying system and Sarah Priour who gave me advice on DSC measurement.

Thanks also to Dr. Michael Parker, Ms Yvonne Parkes, Ms Pip Littlejohn and Ms Hannah Hutchinson for their administrative assistance. Mr Matt Levin for his IT and network support.

I am also grateful for the support and understanding from all my friends and flatmates especially Xin Wang, Lisanne Fermin and Xuan Song. Special thanks to my parents for giving me continuous love and encouragement. I could not have done it without you all.

Table of Contents

List of Figures

List of Tables

Chapter 1 Introduction

Drying of foods is an important food processing operation used to preserve foods for extended periods of time. Spray drying is a mild and effective convective drying method that is widely used in food industry. During a spray drying process, food materials experience a series of physical, chemical and biological changes which may affect their properties and natural attributes such as colour, texture, flavour and nutritional value (Woo & Bhandari, 2013). As a thermal process, heat denaturation of heat sensitive material may also occur during spray drying. These properties are to a large extent determined by the control of variables of the entire drying process. A greater control of spray drying process can lead to improvement of energy efficiency and product quality (Rogers, Wu, Lin, & Chen, 2012). Therefore, optimizing of spray drying method in order to produce products with better quality and functionality is a significant objective and also a great challenge of drying studies.

The conventional polydisperse spray drying process leads to a broad size distribution of the feed droplets, resulting in variability of the drying history between droplets (Watson & Harper, 1988). This will increase the difficulty in controlling the product quality and may give rise to burning and incomplete dried particles at the same drying conditions. Single droplet drying is a novel technique that has been developed in the last decades for investigating the drying kinetics and monitoring the drying process. Free-fall single droplet drying, also known as monodisperse drying, acts as an improved process for conventional spray drying (Fu, Woo, & Chen, 2012). During monodisperse drying, each droplet is believed to have uniform size and properties, experiencing similar air conditions inside the drying chamber. Therefore, the drying process becomes more predictable (Rogers, Fang, Lin, Selomulya, & Chen, 2012). A few research studies have been conducted by using different single droplet drying methods to investigate the

drying kinetics and the product properties (Fu et al., 2012; Schutyser, Perdana, & Boom, 2012; Werner, Edmonds, Jones, Bronlund, & Paterson, 2008). However, rarely did study focus on the overall quality of the powder produced by monodisperse spray drying in comparison with polydisperse spray drying. It is expected that with better-controlled drying process, monodisperse drying technique can be advantageous in producing high-quality powder and is beneficial to heat liable product for retaining their activity.

Three materials WPI, egg white and β-galactosidase (expressed as "lactase" in the following content) are selected to be applied in this study to investigate the heat degradation of different drying techniques on heat liable components. Several previous studies have been conducted in terms of the effect of spray drying conditions on their functionalities (Anandharamakrishnan, Rielly, & Stapley, 2007; Ayadi, Khemakhem, Belgith, & Attia, 2008; Campbell, Raikos, & Euston, 2003). However, most of the research focused on adjusting the inlet air temperature or both of the inlet and outlet air temperature together, few of them works on the impact of either inlet or outlet air temperature only with the other one constant.

This work seeks to address the above questions and investigate suitable conditions for operating the monodisperse drying system. In addition, compare the two drying techniques and figure out the feasibility of monodisperse drying to act as an advanced process of spray drying.

Chapter 4 investigates the effect of air temperature, mainly outlet air temperature, on the thermal degradation of the three materials during conventional spray drying. Chapter 5 demonstrates the set-up and operation of monodisperse drying system, including the development of the system and troubleshooting. The effect of air temperature on the extent of protein denaturation is also investigated and discussed during monodisperse

drying. Factors that affect the size of monodisperse droplets and the particle size of the dried powders have also been explored. Chapter 6 includes an overall discussion and a comparison between the two drying techniques in the aspect of residence time, particle size, drying kinetics and thermal related properties of the products. Suggestions for improving the experimental parameters of monodisperse drying to achieve higher product quality are also demonstrated in Chapter 6.

Chapter 2 Literature Review

2.1 Drying

Drying is one of the oldest methods and major procedures of food preservation. The effectiveness of drying as a food preservation technique is due to the removal of water that acts as an essential requirement for microbial growth and enzyme activity, thereby extending the shelf-life of the product. Adjusting the activity of residual moisture to the desired level helps to retain the quality of food products by inhibiting the growth of microorganisms and the function of enzymes which may lead to the deterioration of the products. Apart from achieving longer storage stability and reducing perishability, drying of foods is also advantageous for reduction of the weight and volume of the product as water is often the principal component of most foods. This will bring about economic benefits by reducing the cost of product packaging, handling, transportation, distribution, and storage. Furthermore, dried foods provide convenience in certain circumstance where weight and space are the major concern for instance military and long-haul journey. In these cases, dried foods need to be reconstituted easily to their original composition at the time of consumption.

Water in foods usually presents in the free or bound state. The removal of moisture from the food material depends on the degree of binding of water to the food matrix. It initially starts with the vaporization of free water until the critical moisture content is reached. During this stage of drying the drying rate remains constant, known as constant rate period. However, in reality, most food products do not exhibit a constant rate period. This is because in many cases water is not always present in the unbounded state in foods, they are found to be loosely bound to various extent (Rotstein & Crapiste, 1997). A comparison of the drying rates of sand, a material with mostly free water, with minced meat containing more bound water is shown in Figure 2.1.

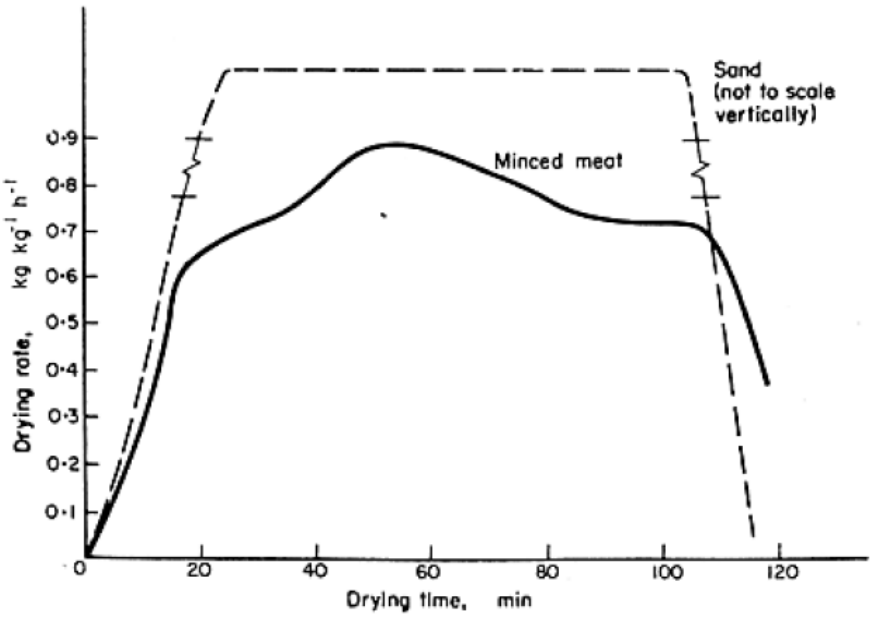

Figure 2.1 *Drying rate curves for sand and minced meat (Earle & Earle, 1983).*

When the moisture content drops to below the critical moisture content, drying then requires the vaporization of bound water. The latent heat of evaporation of the bound water is usually higher than that of free water, as a result, the drying rate will decrease, known as falling rate period (van't Land, 2011a). Figure 2.2 shows the theoretical pattern of drying rate as a function of moisture content (a) and time (b) respectively, in which X is the initial moisture content, Xc is the critical moisture content, X^* is the equilibrium moisture content, and t_c is the duration of constant rate period. The drying rate in the falling-rate stage depends on the changing of energy binding pattern of the water molecules and the diffusion through the food (Earle & Earle, 1983).

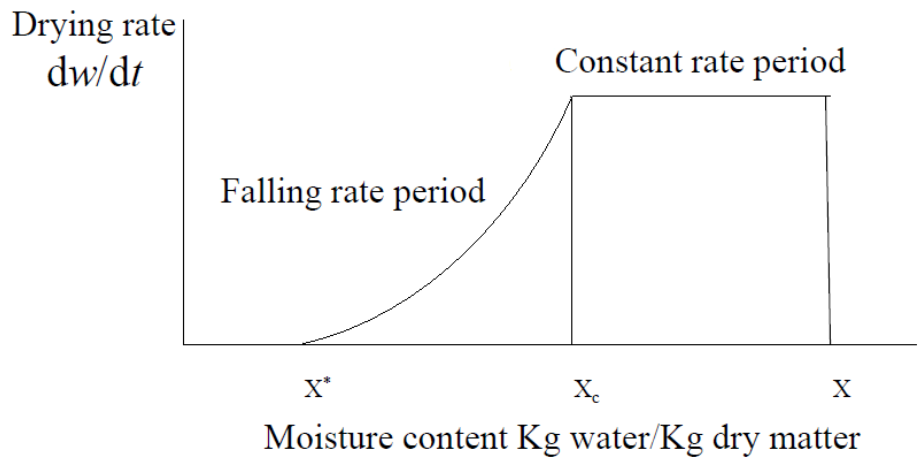

(a)

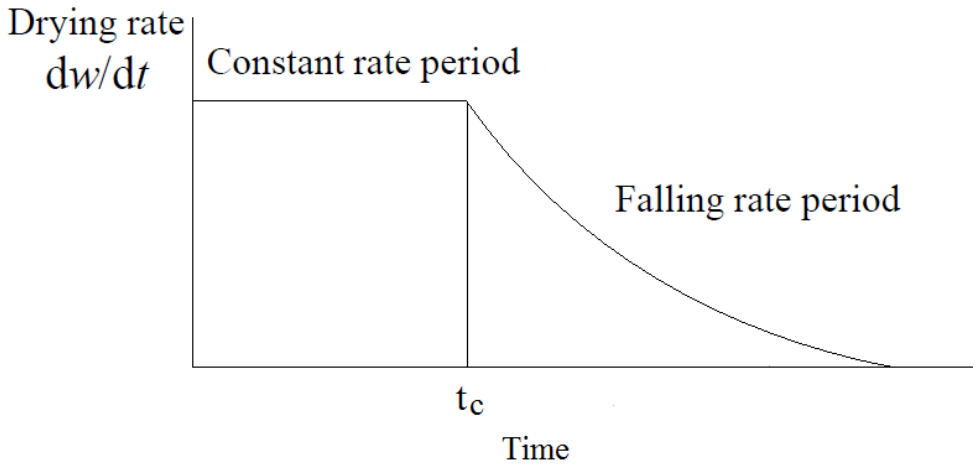

(b)

Figure 2.2 *Typical drying rate of a hygroscopic product (the time scale of the different periods are exaggerated to indicate the different drying period).*

Drying processes can be classified into three categories: air drying under atmospheric pressure, usually using a heated air (gas) as the heat source; vacuum drying occurs at lower pressure, resulting in more ready evaporation of water and lower energy consumption; and freeze drying in which water is removed by sublimation from frozen foods under suitable temperature and pressure. The removal of water during the drying process is achieved by heat and mass transfer. The heat required for drying is

transferred by three different mechanisms: convection, conduction, and radiation. The predominance of the mechanisms varies from one drying process to another. Based on different design and purpose, there are various types of dryer applied in a wide variety of industries. Typical dryer types and their applications in food processing are summarized in Table 2.1. In this article, we will mainly focus on the conventional spray drying process and the applying of a monodisperse droplet generator as the potential atomizer for spray drying technology.

Table 2.1 *Applications of typical dryers in food processing (Rotstein & Crapiste, 1997).*

Dryer type	**Product application**
Tray or cabinet	Fruit, vegetables, meats, confectionery
Tunnel	Fruits, vegetables
Belt conveyor	Grains, vegetables, fruits, cereals, nuts
Rotary	Seeds, grains, starch, sugar crystals
Pneumatic or flash	Starch, pulps, crops, granules, powders
Fluid bed	Vegetables, granules, grains, peas
Spray	Milk, cream, coffee, tea, juices, eggs, extracts, syrups
Drum	Milk, soups, flakes, baby cereals, juices, purees
Foam mat	Fruit juices and purees
Puffing	Fruits and vegetables
Freeze	Flakes, juices, meat, shrimp, coffee, vegetables, extracts

2.2 Spray drying

Spray drying is the most widely used drying technique for liquid food products. This technique involves spraying small droplets of fluids or slurries into a continuous stream of hot convective medium (usually hot air or steam), which also act as a carrier medium

of water vapour evaporating from the droplets. During spray drying, the material is sprayed as fine droplet dispersion with a large total surface area, which results in rapid drying and little heat damage to the product (Brennan, 2011; Jelen, 1985). A design of spray dryer with bag filter is shown in Figure 2.3. A typical spray dryer consists of several specific elements, air handling system, atomization system and dried product discharge system (Heldman & Hartel, 1997). Typical food products produced by spray drying include milk or dairy powders, instant tea or coffee drinks, soy milk powders, yeast extracts, enzymes, etc. (Heldman & Hartel, 1997). Spray drying can also be used in microencapsulation to encapsulate active material within a protective matrix (Ré, 1998). The applications of spray drying in encapsulation in the food industry have been reviewed by Gibbs et al. (1999) and Gharsallaoui et al. (2007). In addition, spray drying as a microencapsulation technique is also applied in pharmaceutical and biotech industries to produce microparticles as reviews by Vehring (2008).

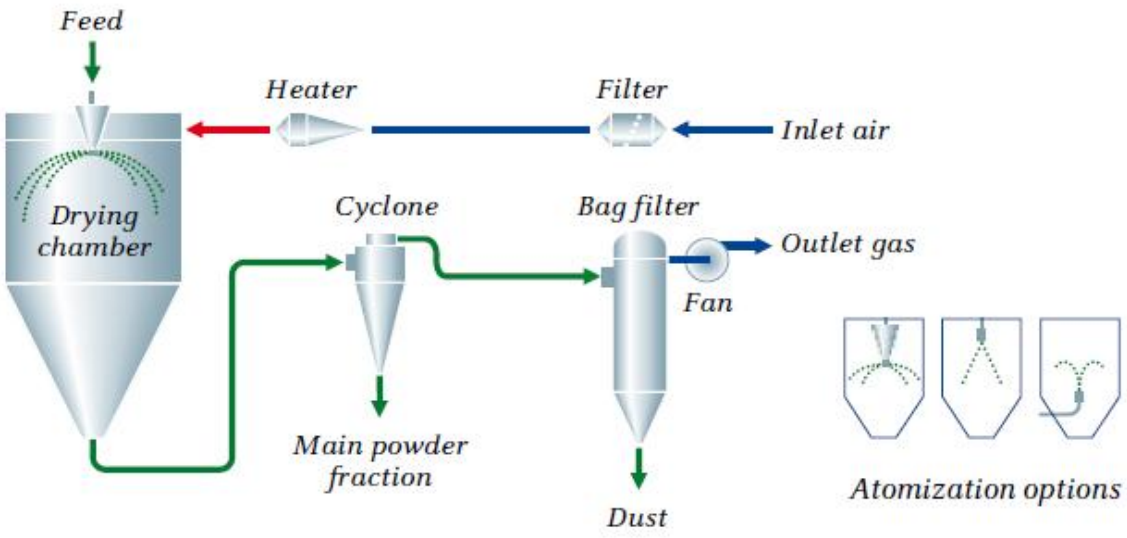

Figure 2.3 *Design mode of spray dryer with bag filter (GEA Process Engineering).*

2.2.1 Drying behaviour of droplets during spray drying

Study of the drying kinetics and drying behaviour of the droplets is important to predict the particle size of the dried product and determine the optimal operating parameters in order to achieve better product quality. During the last decades, more efforts were put into the study of drying kinetics of spray drying. Several theoretical models of heat and mass transfer base on the drying of single droplet have been introduced. Several detailed reviews of published models can be found in the literature (Chen, 2004; Fu et al., 2012; Mezhericher, Levy, & Borde, 2007, 2008a, 2010).

As stated previously, there are generally three ways of heat transfer mechanism in the drying process. During spray drying, the predominant heat transfer mechanism is convection. Even though in some drying process heat transmission inside the product may also occur by conduction due to the internal gradient of temperature (Rotstein & Crapiste, 1997). Some studies also take into consideration the effect of radiation on drying of the droplets in the heated air (Mezhericher, Levy, & Borde, 2008b). However, as the particle size in spray drying is very small, the temperature gradient within the droplets and the influence of radiation are typically negligible during spray drying process (Woo & Bhandari, 2013).

A typical drying model which involves a shrinking system has been developed and is generally accepted at present (Mezhericher et al., 2008a; Rotstein & Crapiste, 1997; Woo & Bhandari, 2013). This drying model indicates that the drying of droplets containing solid components is usually divided into two stages. In the first drying stage, the droplet with excess moisture is surrounded by the flow of heated air as shown in Figure 2.4(a). Heat is transferred from air to the droplet by convection and conduction, resulting in gaining sensible heat of the droplet, and moisture flows from the surface of the droplet to the air by evaporation until the moisture content of the particle reaches the

critical moisture content (X_{cr}). As water evaporation occurs, the diameter of the droplet is decreased and the concentration of solid components near the droplet surface is increased. The droplet temperature remains at the evaporation temperature due to high moisture content and high evaporation rate. As a consequence of evaporation, solids participate at the surface of the droplet and form a layer called 'crust', and the second drying stage commences. In the second drying stage, the resistance for mass transfer increases due to the crust layer, therefore the rate of drying is decreased. Moisture transfers from the core of the particle to the surface by water vapour diffusion as shown in Figure 2.4(b). The heat continues flowing from air to the particle, heating up the droplet until its temperature approaching air temperature in the chamber. As the result of further drying, the wet core of the particle shrinks and the thickness of the solid crust increases until the particle moisture content reaches the equilibrium moisture content (X_e). Changes of temperature and moisture content of the particle during drying process are shown in Figure 2.5.

Figure 2.4 *Schematic illustration of heat and mass transfer of single droplet in the first drying stage (a) and the second drying stage (b) of spray drying (Mezhericher et al., 2008a).*

Figure 2.5 *Typical drying behaviour of droplet temperature (a) and moisture content (b) of a single particle (Mezhericher et al., 2010).*

2.2.2 Atomization and feed droplet size

Atomization is an important process in spray drying. In order to achieve a rapid rate of drying in a spray dryer, liquid feed must be sprayed into large numbers of small droplets. Typical devices used to atomize the feed include rotary atomizers, two-fluid nozzles, and high-pressure nozzles as shown in Figure 2.6. Different nozzles can be used to achieve various droplet size distributions. The selection of atomization parameters depends on the requirement of the drying process and the properties (e.g. viscosity, concentration) of the material being dried.

In rotary atomization, the feed is accelerated by centrifugal force in the atomizer disk before being discharged into the drying chamber. The rotary atomizer is suitable for a wide range of products and all feed viscosities as long as they are pumpable into the disk. It is preferred for large feed stream and can produce relatively small droplets (typically between 30 and 120 μm) (van't Land, 2011b). The degree of atomization and droplet size depends on the feed rate, the atomizer peripheral speed, liquid properties and the design of atomizer disk. Particle size increases with decreasing rotational speed, increasing feed rate and decreasing atomizer diameter (Heldman & Hartel, 1997).

For a high-pressure nozzle, pressure is applied to the liquid feed in a small orifice within the nozzle for atomization. The atomization pressure is normally in the range of 20 to 100 bar, however, higher pressure may also occur for feeds with high concentrations (Kessler, 1981; van't Land, 2011b). High-pressure nozzles can produce droplets with size in the range of 10 to 300 μm, depending on the atomization pressure and nozzle size (Heldman & Hartel, 1997; Kessler, 1981; van't Land, 2011b). However, under certain conditions, the droplets produced by high-pressure nozzles generally have narrow diameter distribution (Kessler, 1981).

Two-fluid nozzle, also known as a pneumatic nozzle, uses a second material (usually air) as an atomizing gas to atomize the liquid feed. The feed discharged through an orifice concentric with the air, creating a ventilated effect and sprayed into the chamber (Brennan, 2011). The atomization relies on high air velocity rather than liquid velocity, therefore, the required feed pumping pressure for two-fluid nozzles is lower than that for pressure nozzles (van't Land, 2011b). The droplet size is determined by the characteristics of the feed and the ratio of air and feed (Kessler, 1981; van't Land, 2011b). The two-fluid nozzle is also suitable for all feed viscosities. It can produce droplets with a typical size distribution between 5 to 300 μm (Filkova, Huang, & Mujumdar, 2007). However, the droplets produced by two-fluid nozzle are generally not as uniform in size as those from the other two types of atomizers, especially when handling high viscosity liquids (Brennan, 2011).

(a) (b) (c)

Figure 2.6 *Different atomizers for spray drying: (a) rotary atomizer; (b) two-fluid nozzle; (c) pressure nozzle (fountain) (GEA Process Engineering).*

Droplet size is one important parameter that influences the convective heat and mass transfer rates. Smaller droplet size results in a larger surface area for a given liquid volume, leading to higher transfer rates and vice versa. The size of the droplet may also affect the evaporation temperature of the droplet. And the time that the droplet is kept at

this temperature is important for heat labile materials as the evaporation temperature is much lower than the final temperature of the particle (Anandharamakrishnan et al., 2007).

The droplet size also determines the trajectory of droplets in the chamber. Larger droplets tend to traverse the air flow due to higher momentum, whereas smaller droplets tend to follow the air flow, resulting in segregation of particles in the chamber. As a consequence, droplets with different size will experience different drying histories during drying. Typically, smaller droplets may have a longer residence time in the chamber compared with large ones (Woo & Bhandari, 2013).

2.2.3 Product and air flow pattern of spray dryer

The overall rate of heat and mass transfer is determined by the relative droplet and air contact (Woo & Bhandari, 2013). Air can be led either in the same (co-current) or in the opposite direction (counter-current) to that of feed falling down the drying chamber. Feed can also be atomized from the bottom of the drying chamber (mixed flow) by a fountain mode pressure nozzle, as shown in Figure 2.7.

As shown in the figure, in a co-current operation, the feed droplets will firstly contact the air with the highest temperature. A sudden increase of temperature and rapid evaporation will occur to the droplets at this stage, and as a result of the evaporative cooling effect, the droplets will not be heated up to above the wet-bulb temperature for the air. As the product falls, the temperature of air decreases and the humidity of air increases, the driving force of heat and mass transfer decreases. This ends up with less exposure of the product to the high temperature, hence is desirable for foods that are sensitive to thermal degradation (Heldman & Hartel, 1997; Woo & Bhandari, 2013). The thermal experience of droplets during a mixed flow process is similar to that of co-

current mode. However, the using of fountain nozzle will increase the residence time of droplets in the chamber, especially the contact time of the droplets with the hot air. As a result, the drying efficiency will increase, but the risk of heat damage to the product will be greater (Brennan, 2011).

Figure 2.7 *Typical feed and air flow modes of spray dryer (Woo & Bhandari, 2013)*

On the other hand, in a counter-current mode, the feed droplets are injected in the opposite direction of the inlet air flow. As a result, the droplets will experience a slower heating process at the beginning, and an accelerated heat and mass transfer as falling down to the bottom of the chamber due to increased air temperature and decreased air humidity (Woo & Bhandari, 2013). The advantage of counter-current drying is that the

materials can be dried to low residual moisture content and have higher thermal efficiency. However, in this case, the particles with lower moisture content will be exposed to the higher temperature. The discharge temperature of dried product from the counter-current flow method is always higher than that of the co-current method, which can be disadvantageous for heat sensitive materials (Kessler, 1981).

The direction of air flow and feed flow is an important feature that needs to be considered in the design of spray drying process as it determines the quality of the product. The determination of the flow mode needs to fulfil the thorough mixing of air and product in order to prevent insufficient drying and avoid overheating due to exposing dried product in the hot area. In most case of spray drying of foods, co-current and mixed flow processes are more widely used than counter-current due to the consideration of thermal sensitivity, whereas counter-current can be used for relatively heavy and thermally stable particles (Heldman & Hartel, 1997; Kessler, 1981; van't Land, 2011b)

The flow rate of air may also influence the residence time of droplets in the drying chamber. It is important to maintain a uniform and appropriate air velocity over the whole chamber, in order to prevent too much product being carried in the outlet air and to avoid particles falling in the chamber too quickly (Kessler, 1981).

2.2.4 Effects of operating parameters on product quality in spray drying

The quality of the final dried products is governed by the drying process and related operating conditions. In addition to the air flow mode and atomization process, other parameters of the feed and the inlet and outlet air are also significant as listed in Table 2.2.

Table 2.2 *Main operating parameters of spray drying (Woo & Bhandari, 2013).*

Feed Material	Temperature
	Flow rate
	Initial concentration
Atomization	Feed pressure (nozzle)
	Air pressure (two fluid nozzle)
	Rotation speed (rotary atomizer)
Inlet air flow	Temperature
	Flow rate
	Humidity
Outlet air flow	Temperature
	Humidity

Temperature

Heat transfer during drying is driven by the temperature difference between the droplet surface and the heated air. The higher the temperature difference, the larger the driving force of heat transfer, resulting in a greater rate of heat transfer. In addition, higher temperature increases the internal diffusion and the migration of water molecules. Therefore, increase air temperature results in a higher drying rate.

Ambient air needs to be heated to the required temperature (typically between 150 and 300 ℃) before entering the drying chamber. The determination of air temperature depends highly on the thermal stability of the product that being dried. Heat-labile products such as milk, egg and enzymes cannot withstand high temperatures (over 100 ℃) due to protein denaturation, whereas heat stable products such as coffee can be dried at a significantly higher temperature (250 ℃) without degradation (Heldman & Hartel, 1997). For quality and safety concern, the inlet air temperature for producing organic materials do not normally excess 200 ℃ (van't Land, 2011b). The quality of the

product will also be affected by the outlet air temperature. Anandharamakrishnan et al. (2007) have confirmed that lower outlet gas temperatures produce a lower degree of protein denaturation and solubility loss. Silva, Freixo, Gibbs, and Teixeira (2011b) also indicated that lower outlet temperature will increase the retention of enzyme activity and probiotic viability during drying.

Relative humidity

Mass transfer during drying is driven by the difference in vapour pressure between the droplet surface and the ambient air. Hence the humidity of the heated air will significantly affect the moisture loss of the droplet (Woo & Bhandari, 2013). Reducing the relative humidity of air increases the driving force of moisture loss in the constant-rate period of drying, therefore, enhances the rate of drying in the constant rate period. However, it has little influence on drying in the falling rate period (Heldman & Hartel, 1997). For the air with certain moisture content, relative humidity decreases as temperature increases, resulting in higher driving force for removing moisture from the product.

In addition, the drying process can also be modified by adjusting the flow rate of the feed. Increased feed flow rate brings more moisture into the drying chamber, resulting in a decrease of the outlet air temperature. This can be important to heat sensitive materials since outlet temperature is an important parameter for thermal related degradation. Quality of the product may also be influenced by different feed concentration, for the degree of solid content may affect the formation process of the dry crust during particle drying (Anandharamakrishnan et al., 2007; Rogers, Wu, et al., 2012).

2.3 Single droplet drying and monodisperse spray drying

Optimization of the spray drying process can increase energy efficiency, prevent products from overheating or incomplete drying, increase the production rate and improve product quality (Rogers, Wu, et al., 2012). A great amount of research work has been conducting in order to achieve better control of the spray drying process in past decades. Single droplet drying and monodisperse drying are novel technologies that have been introduced and developed in the last decade for the study and improvement of spray drying processes. They will be introduced respectively as follows.

2.3.1 Single droplet drying

Single droplet drying is an effective technique for investigating drying kinetics and monitoring a drying process. This technique involves generating of a single isolated droplet under a controlled drying condition, imitating the convective drying process of the droplet in spray drying (Fu et al., 2012). This technique has been widely applied in studying the behaviour and heat and mass transfer of droplet during drying, as mentioned in the previous section. It can also be used for investigating the morphological changes of the droplet during drying and the effects of different parameters such as droplet size and air temperature. More studies have been conducted in the modelling of single droplet drying (Farid, 2003; Werner et al., 2008), applying single droplet drying for optimizing spray drying of proteins, enzymes and probiotics (Lorenzen & Lee, 2012; Pajander et al., 2015; Schutyser et al., 2012), and for observing of the crystallization of taurine (Lin, Woo, Fu, Selomulya, & Chen, 2013).

There are different methodologies for single droplet drying, mainly include acoustic levitation method, glass filament method and free falling method. The comparison of three different single droplet drying methods is shown in Table 2.3. Schematic

illustrations of these three methods are shown in Figure 2.8, of which the free fall method will be introduced in the next section.

Figure 2.8 *Three types of single droplet drying system: (a) droplet levitated by acoustic or aerodynamic fields; (b) droplet suspended on the tip of a glass filament; (c) free-falling droplet in a tall tower (Fu et al., 2012).*

The acoustic levitation method is also known as noncontact levitation, during which the droplet is freely suspended in the air by acoustic or aerodynamic force (Adhikari, Howes, Bhandari, & Truong, 2000; Schutyser et al., 2012). One of the devices for acoustic single droplet levitation known as drying kinetics analyzer™ is shown in Figure 2.9.

Table 2.3 *Comparison between the different single droplet drying techniques (Fu et al., 2012).*

Figure 2.9 *Systematic diagram of drying kinetics analyzer™ and zoom on the levitated droplet in the ultrasonic field (helix) (Pajander et al., 2015).*

The acoustic levitation method allows more easily and visually monitoring of drying conditions, morphological changes and residence time. Several studies have been conducted to evaluate the diameter changes, estimate the evaporation rate, and investigate the drying characteristics of droplet using the acoustic levitation (Brenn, Rensink, Tropea, & Yarin, 1997; Kastner, Brenn, Rensink, & Tropea, 2001; Mondragon, Jarque, Julia, Hernandez, & Barba, 2012; Sloth et al., 2006). However, there are some limitations of the method. One practical challenge is that it is hard to accurately control the droplet levitation (Schutyser et al., 2012). It is also reported that the droplet drying behaviour can be affected by the acoustic field, resulting in larger heat and mass transfer coefficients and higher drying rate measurements (Al Zaitone & Tropea, 2011; Groenewold, Möser, Groenewold, & Tsotsas, 2002; Yarin, Brenn, Kastner, & Tropea, 2002). In addition, the acoustic stream may have influences on the inactivation of heat sensible materials, for instance, microbial inactivation (Dijkstra et al., 2011).

The alternative way of acoustic levitation is contact suspension, with a droplet suspended at the tip of a glass filament or deposited on a flat hydrophobic surface as shown in Figure 2.10 (a) and (b) respectively (Schutyser et al., 2012). The mass of the droplet is monitored by connecting a mass balance to the filament, and the morphological changes can be recorded and visually monitored by a camera (Schutyser et al., 2012). The contact between the droplet and the glass filament or surface could affect the drying rate and the heat and mass transfer during drying (Fu et al., 2012; Schutyser et al., 2012). However, this method is still practical and has been used in investigating the drying kinetics and behaviour (Fu, Woo, & Chen, 2011; Jimmy Perdana, Fox, Schutyser, & Boom, 2013).

(a) (b)

Figure 2.10 *Illustration of contact levitation: (a) glass filament single droplet drying system (Fu et al., 2012); (b) single droplet on a hydrophobic surface (Perdana et al., 2013).*

2.3.2 Monodisperse spray drying

Single droplet drying system using free fall method is also known as monodisperse drying. This method involves the generation of a unique stream of droplets with identical size that freely falls through a tall tower to be dried (Adhikari et al., 2000; Fu

et al., 2012; Schutyser et al., 2012). Figure 2.11 shows the generation of a monodisperse droplet stream. In comparison with the first two methods which are more microcosmic and that can only look at the properties of a single droplet, monodisperse drying is more closely reproduce the drying system in the real industry and can be used to investigate the effects of single droplet drying on the overall product quality rather than just on one droplet.

Figure 2.11 *Photograph of monodisperse droplet stream (The nozzle is originally pointed downwards) (Fu, Zhou, et al., 2011).*

As stated previously, droplets with different size will have different drying history during spray drying and result in different degrees of drying. Each droplet may undergo a different route and experience various temperature-time and humidity-time profiles. During the conventional poly-disperse atomizing process, collisions and trajectories may also happen within the droplets and between the droplets and the chamber walls. These all lead to variability of the residence time and thermal experience of droplets during drying (Wu, Patel, Rogers, & Chen, 2007). However, with monodisperse drying technique, each droplet produced by the generator will have identical initial size, properties, and falls vertically from the top of the tall drying chamber by gravitational

force. Therefore, every droplet is assumed to experience similar and predictable conditions during drying, preventing overheating or incomplete drying, assuring more controllable drying process and uniform particles with similar properties to be produced (Rogers, Wu, et al., 2012).

Several monodisperse droplet generators have been developed as potential atomizers for spray drying during the past few years, include ink-jet droplet generators, microfluidic droplet generators, piezoceramics-driven glass nozzles, and multi orifices atomizing plate. Detailed introduction of these monodisperse droplet generators and their advantages and limitations can be found in the articles of Wu et al. (2007), K. C. Patel, Wu, and Chen (2007), Wu, Lin, and Chen (2011) and van Deventer, Houben, and Koldeweij (2013).

Monodisperse spray drying has been used in drying research for various materials in the aspects of particle morphology, solubility, wettability and other properties and their governing factors. A drawback for monodisperse drying is that in order to achieve typical residence time in the spray dryer, a tall column is required (Schutyser et al., 2012). In addition, it is difficult to monitor the drying kinetics, the mass and temperature changes of a individual droplet during drying (Adhikari et al., 2000; Fu et al., 2012). However, it can well mimic what happens to a droplet during spray drying, and can at the same time ensure that each droplet undergoes the same and better-controlled drying condition. It can also produce a relatively large amount of product which can be used for quality assessment. Therefore, the aim of this study is to investigate how single droplet drying will affect the thermal-related behaviour and quality of heat liable products in comparison with conventional spray drying.

2.3.3 Factors affecting product quality in single droplet drying

The factors that govern the drying experience and heat and mass transfer in single droplet drying are similar to that for spray drying, as demonstrated in Figure 2.12 as follows.

Study of Rogers, Fang, et al. (2012) indicated that skim milk powder produced by a monodisperse spray dryer had poor wettability and solubility at high inlet air temperatures (above 140 ℃); changes in residence time or particle size may have a significant effect on product quality. Another study conducted by their group towards morphology also found that skim milk powder produced with higher feed solid concentration had less collapsed particles (Rogers, Wu, et al., 2012). Fu, Zhou, et al. (2011) found that epigallocatechin gallate microparticles produced by monodisperse spray drying at low temperature have retained most of the antioxidant activities.

Figure 2.12 *Factors affecting convective heat and mass transfer and the solidification process of the single droplet (Woo & Bhandari, 2013).*

2.4 Thermal-related denaturation and loss of activity of heat labile compounds during drying

Although spray drying is generally considered as a relatively gentle drying process, heat damage may still occur to thermally sensitive materials during the heat treatment. Protein denaturation is one of the most significant degradation during the drying process. In the production of milk powder, protein denaturation may affect the resolubilization of the milk and affect the quality of the product. Therefore, milk products are normally dried at a low temperature of around 65 to 70 °C (Heldman & Hartel, 1997). Denatured protein may also lead to aggregations and result in insoluble components in the product.

Research indicates that protein denaturation may be significantly affected by the drying history rather than only the final condition of the particles (Ameri & Maa, 2006; Fang, Rogers, Selomulya, & Chen, 2012; Woo & Bhandari, 2013). Protein denaturation in food powder is governed by the moisture and temperature balance, and the degree of denaturation for α-amylase decreases with higher feed rate (Samborska, Witrowa-Rajchert, & Gonçalves, 2005). As stated previously, outlet air temperature is an important parameter in determining the degree of protein denaturation. Lower outlet air temperature and lower residence time result in a lower degree of protein denaturation and higher retention of enzyme activity of the final products (Anandharamakrishnan et al., 2007; Anandharamakrishnan, Rielly, & Stapley, 2008; Schutyser et al., 2012). It is also reported that the activity of enzymes retained at lower air temperature and smaller droplets (Yamamoto & Sano, 1992); the stability of α-amylase is increased at low moisture during drying (Meerdink & Van't Riet, 1991); and that the denaturation of whey protein is slightly increased with higher feed concentration (Anandharamakrishnan et al., 2007).

The stability of proteins and enzymes can be increased by the addition of carbohydrates, typically sugars, such as maltodextrins. The possible mechanisms include (a) carbohydrates provide a glassy and amorphous matrix, increasing the immobilisation of proteins; (b) carbohydrates replace the hydrogen bonds between the protein and water molecules. Therefore, the addition of carbohydrates prevents proteins from directly contacting with the high-temperature air, as a result, protects proteins from overheating by the hot air (Costa-Silva, Nogueira, Fernandes Souza, Oliveira, & Said, 2011; Schutyser et al., 2012).

Lorenzen and Lee (2012) reported that the kinetics of inactivation of protein droplets can be divided into three stages. In the first stage of constant rate period, only marginal inactivation occurs in the solution; the second stage starts at the critical point of drying when the surface temperature also increases rapidly, but still only further marginal inactivation of the protein occurs; rapid inactivation happens in the third stage and the inactivation can be modelled by first-order kinetics. This result suggests that the residual moisture content of the particle determines the point of onset of protein denaturation.

Apart from protein denaturation, loss of amino acids may also occur during spray drying. Schmitz-Schug et al. have modelled the reaction kinetics of lysine loss during spray drying of dairy products and found that the loss of lysine is affected by temperature, water content and physical state of lactose. They also indicated that the spray drying process can be optimized by coupling lysine loss kinetics with drying kinetics and computational fluid dynamics simulation of the process (Schmitz-Schug, Kulozik, & Foerst, 2016a).

2.5 Other quality-related properties of the dried products

Apart from thermal related properties, the quality of dried powders can also be assessed in many other aspects. These include morphology, bulk density, moisture content, particle size, flow characteristics, wettability during reconstitution, dispersibility, and solubility in water, rehydration properties, and sensory properties such as colour, texture, and flavour. As a result of heat treatment, loss of volatile flavour compounds may occur, resulting in a change in flavour. However, in some cases, the decomposition of sensitive organic compounds may also give a desirable flavour to the product. Browning reactions may also occur at high temperature and result in changes in colour. For products with high lipid content, lipid oxidation may occur that affects the quality and flavour of the product. The main characteristics involved in this study are particle size and moisture content.

2.5.1 Particle size distribution

Based on different drying process, the particles produced can result in different sizes. Table 2.4 shows the typical particle size distribution from various spray dryers (Woo & Bhandari, 2013).

Table 2.4 *Size range of particles by various spray drying process.*

	Average size (μm)
Bench spray dryers	5-20
Pilot spray dryers	20-40
Commercial spray dryers (two stage)	200-400

The most distinct and important difference between conventional spray drying and monodisperse spray drying is the particle size distribution. It is expected that monodisperse spray drying will have a consistent particle size of the finished powder. However, in the real case, the absolute uniform particle diameter distribution is difficult to achieve. A histogram of particle diameters of milk powder produced by monodisperse spray dryer has been shown in Figure 2.13 from the study of Rogers, Fang, et al. (2012). Some outliers can be seen on the histogram caused by two or more particles close to each other and being resolved as a single large particle by the software. However, it can be seen that the distribution of the particle diameter produced by a monodisperse spray dryer is much narrow compared to the conventional spray dryer, and the peak value is highlighted.

Figure 2.13 *Histogram of particle diameters for monodisperse dried skim milk powder (Rogers, Fang, et al., 2012).*

2.5.2 Moisture content

Spray dried powders are not completely dry in most cases. Typically, milk powder contains 2 to 4% by weight of moisture after drying, and the value for egg powder is up

to 8% (van't Land, 2011b). The level of residue moisture in the powder depends on the characteristics of the material (e.g. water binding capacity) and drying conditions. High residue moisture content may indicate inadequate drying or reabsorption of moisture during handling of the powder. In the case that outlet air has high relative humidity, moisture condensation may occur if the temperature of powder separation section is much lower than that inside the dryer.

2.6 Differential Scanning Calorimetry (DSC)

Evaluation of the thermal degradation of heat liable components during the drying process is one of the most important purposes of this study and it is achieved by Differential Scanning Calorimetry (DSC). DSC is a thermos-analytical technique for evaluating the thermal effects over a large temperature range. It can be used in different areas of research. In this study, DSC is applied to assess the degree of protein denaturation based on the detection of absorbing heat during the transition of protein unfolding (Lepock, 2005). In order to achieve this objective, sample of spray dried powders is placed in a small disk with medium thermal conductivity and temperature sensors and placed in the heat flux DSC system together with proper reference as shown in Figure 2.14. When heat is applied, heat flows through the disk to the sample and to the reference; the differential signal is then generated which is proportional to the difference between the heat flow rates to the sample and to the reference (Höhne, Hemminger, & H.-J., 2004). During DSC analysis, any remaining undenatured protein in the sample undergoes denaturation and the enthalpy of denaturation is measured (Anandharamakrishnan et al., 2007). DSC provides a direct physical measurement of protein denaturation. The result of a DSC is a curve of heat flow versus temperature,

with a positive or negative peak indicating the temperature when protein denaturation occurs and the extent of the peak represents the amount of undenatured protein in the sample.

Figure 2.14 *Schematic illustration of heat flux DSC with disk-type measuring system (Höhne et al., 2004).*

Chapter 3 Materials and Methods

3.1 Materials

3.1.1 Whey protein isolate

The whey protein isolate (WPI 895) used in this study was provided by Fonterra Cooperative Ltd, (Auckland, New Zealand). WPI 895 has a protein content of 94%. It is an instant soluble, un-denatured whey protein manufactured by proprietary ion exchange and ultra-filtration techniques. The WPI samples used in this study were originally stored in a tight container at room temperature.

3.1.2 Lactase

The lactase sample used in this study is Maxilact L2000 (DSM Food Specialties Pty Ltd, Sydney, Australia). It is a purified liquid lactase preparation derived from the dairy yeast *Kluyveromyce lactis*. The enzyme activity was no less than 2000 NLU/g as claimed by the manufacturer, and the crude protein content in this product was 3.4% (w/w) as determined by the Kjeldahl method. This sample was stored in the original sealed containers at 4 ℃.

3.1.3 Egg white

Egg white used throughout this study was pasteurised liquid egg white (980ml pouch) from Zeagold Foods (Auckland, New Zealand). Due to the limitations of its size and shelf life, the samples were purchased from Countdown supermarket (Palmerston North, New Zealand) the day before every single drying experiment and kept refrigerated in the lab. Therefore, distinctions of different batches may occur. The composition of the egg white was 11.7% protein, 0.4% sugar, 0.18% ash, as shown on its package.

3.1.4 Maltodextrin

Maltodextrin CR10, used in this study was manufactured by Archer Daniels Midland (Chicago, United States). It is a non-sweet saccharide derived by partial hydrolysis of corn starch. Maltodextrin CR10 was added to the drying feed to acquire the desired total solid content. It also acted as a carrier of protein during the drying process.

3.1.5 2-Nitrophenyl β-D-galactopyranoside (ONPG)

ONPG acted as the colourimetric substrate for the enzyme activity test for lactase. It is hydrolysed to o-nitrophenol by β-galactosidase and appeared a yellow colour in alkaline solution that can be quantitated at 420 nm. The ONPG (N1127) used in this study was provided by Sigma-Aldrich Inc. (St. Louis, USA). It was a pale powder and was stored at -20 ℃. The maximum solubility of ONPG in water is 10 mg/ml. Gentle heating was required when making the solution for complete dissolution. In this study, a 1% ONPG stock solution was prepared in 0.1 M phosphate buffer with a pH of 7.3, and stored at -20 ℃ for up to 3 months from the preparation date. The stock solution was diluted 1:5 and preheated to 40 ℃ before use.

3.1.6 Other chemicals

All chemicals used in the study were of analytical grade with 99% minimum purity. A list of chemicals involved in this study is shown in Table 3.1.

Table 3.1 *List of chemicals and their suppliers.*

Chemical/Reagent	Supplier
di-sodium hydrogen orthophosphate anhydrous (Na_2HPO_4)	Univar, Downers Grove, Illinois, United States
sodium dihydrogen orthophosphate anhydrous (NaH_2PO_4)	Labserv Ltd, Longford, Ireland
sodium carbonate anhydrous (Na_2CO_3)	Labserv Ltd, Longford, Ireland
sodium hydroxide (NaOH) pellets	Fisher Scientific Inc., Loughborough, Leics, UK
sulphuric acid concentrated	Fisher Scientific Inc., Loughborough, Leics, UK
boric acid	Fisher Scientific Inc., Loughborough, Leics, UK
Kjeltabs S/3,5	Foss Analytical A/S, Hillerød, Denmark
hydrochloric acid (HCl)	Labserv Ltd, Longford, Ireland

3.2 Equipment and Methods

The major equipment and generic methods applied in this study are listed in the following section. The specific settings and experimental design for spray drying and monodisperse drying are described in the following corresponding chapters.

3.2.1 Spray drying

The spray drying process in this study was carried out on a pilot plant scale spray dryer MOBILE MINOR™ '2000', Models D & H (GEA Niro, Soeborg, Denmark) (Figure 3.1). A two-fluid fountain nozzle was used in the drying process, in which the atomization is achieved pneumatically by high-velocity compressed air impacting the

liquid feed. The inlet air temperature was set from the control panel, while the outlet air temperature was adjusted by controlling the feed flow rate.

It is noteworthy that as an alternative design to that shown in Figure 3.1, a pipe was used to connect the chamber from its bottom directly to the cyclone. That means instead of collecting powder from the chamber and cyclone separately, the powder was mixed up and collected mostly from the cyclone. Due to high air temperature and feed flow rate were applied in this study, condensation was found in the jar underneath the chamber as a result of high moisture content in the carrier air and large temperature difference between the jar and the chamber. By adopting the setting as mentioned above, condensation can be effectively prevented in the process.

Figure 3.1 *Image of spray drier, MOBILE MINOR, GEA.*

3.2.2 Monodisperse drying

The monodisperse droplet generating system (printing system) consists of a GBC LC1150 HPLC pump (GBC Scientific Equipment Pty Ltd, Melbourne, Australia); a FeelTech FY2200S dual channel signal generator (FeelTech Technology Cooperative Ltd, Henan, China); a signal amplifier (designed and built by John Pedley, Technical Officer of Institute of Food Science and Technology, Massey University) which magnifies the signal by a gain of ten; a single nozzle printing head developed at TNO (Nederlandse Organisatie Voor Toegepast Natuurwetenschappelijk Onderzoek, The Hague, Netherlands), a LED light, a PM 5712 pulse generator (Koninklijke Philips N.V., Amsterdam, Netherlands), a HD digital camera (Senitech, Japan) and a lens. A schematic image of the printing system is shown in Figure 3.2.

The drying stack has a height of 12 meters and diameter of 0.2 meter was covered by heat insulation material. A finned heating element HBF1129U2000 (Hislop & Barley Electrical Ltd, Auckland, New Zealand) was used as the inlet air heater of this system. The inlet air temperature was measured by a temperature sensor placed opposite to the air heater (not direct contact). A PID controller was applied and using this temperature signal to act on the inlet air heater. Two resistance thermometers (three wire RTDs) were placed at the halfway and the bottom of the drying tower respectively, connected to a USB-Temp DAQ device (Measurement Computing Corporation, Massachusetts, United States), measuring the air temperature at the middle and the bottom of the drying tower. Apart from the main air heater, there are two trace heating tapes which heat up the upper and lower chamber wall to limit the heat loss from air to wall in the drying chamber. Two wall temperature sensors were mounted for measuring the stainless steel temperature of the top and bottom half of the tower. These wall heaters and temperature

sensors were also connected to and controlled by the temperature PID controller on the control panel.

The air circulation of the system was driven by two vacuum cleaners Pullman A-031b (acted as induced draught exhaust fan) and Pullman commander 900 (acted as a forced draught blower). Air velocity in the stack was measured by Dwyer VT-300 Anemometer (Dwyer Instruments Inc., Indiana, United States). Air velocity was measured at the top, middle and bottom of the drying stack, multiplied by the area from where the air coming through, to obtain the flow rate of air. Figure 3.3 shows a Schematic diagram of the design for the whole drying system.

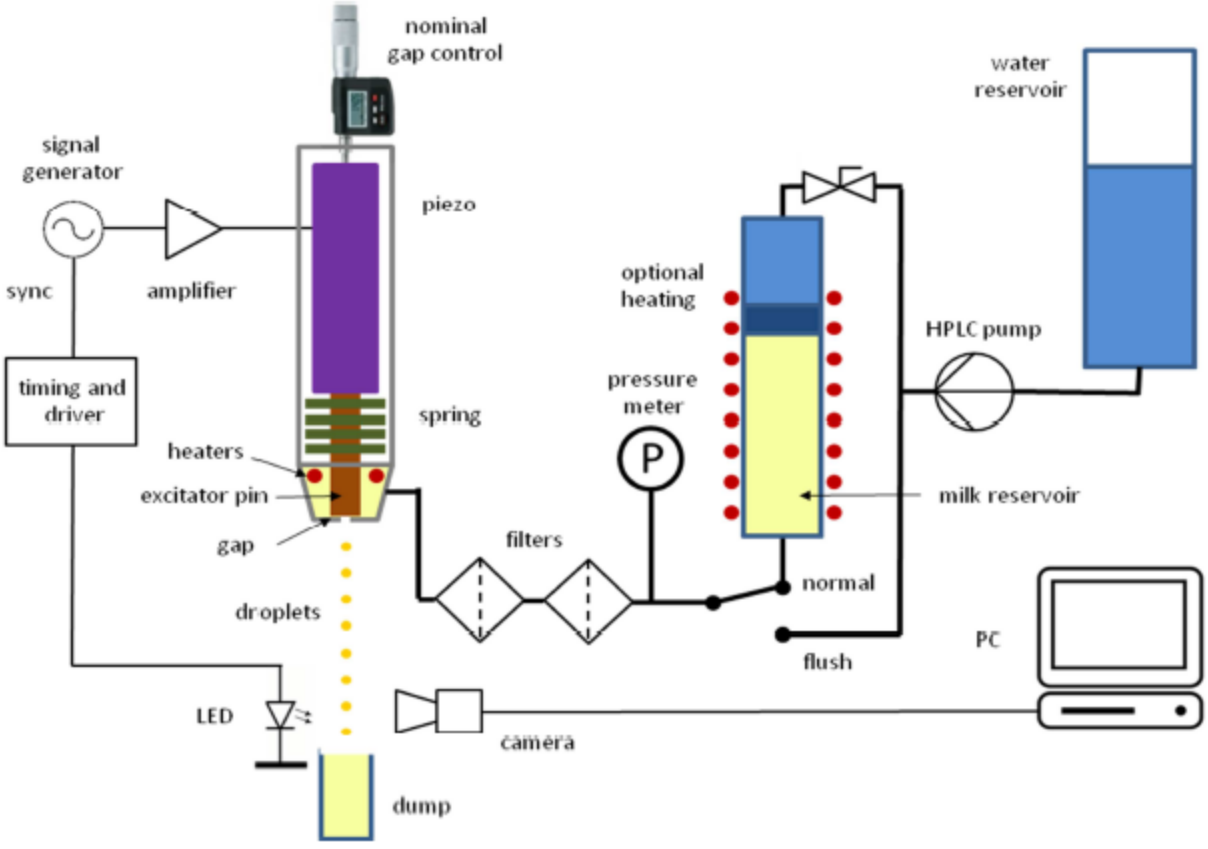

Figure 3.2 *Schematic image of the printing system (TNO, 2014).*

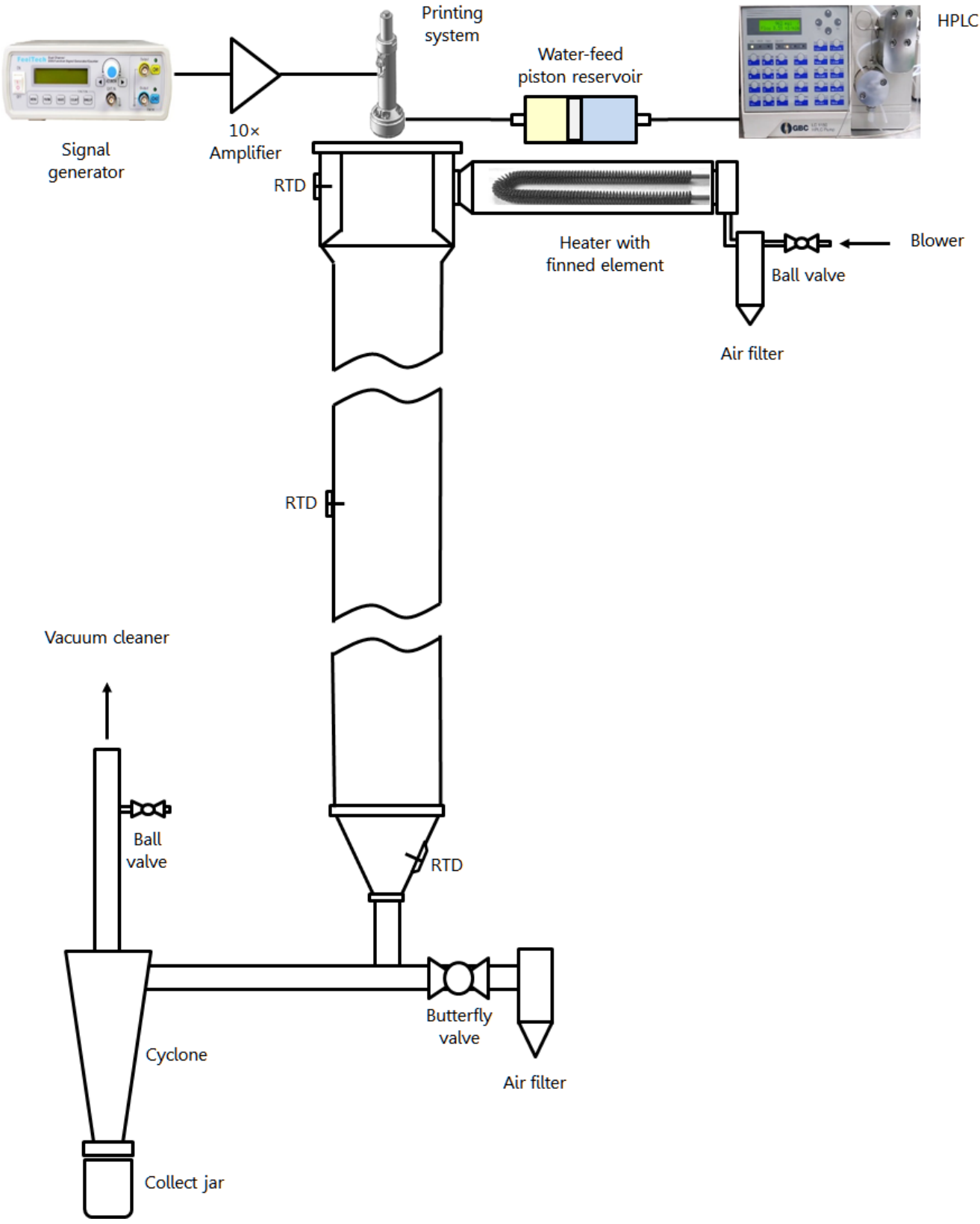

Figure 3.3 *Schematic diagram of the monodisperse droplet drying system.*

3.2.3 Enzyme activity determination (ONPG β-galactosidase assay)

The enzyme activity of lactase was measured within 24 hours of drying, using the ONPG assay (J. Perdana, Fox, Schutyser, & Boom, 2012). The dried lactase samples were re-dissolved in RO water at room temperature at 35% w/w concentration (same as the drying feed) prior to the test. In the assay, 20 μl of the sample solution was added to 980 μl preheated 0.2% ONPG solution and incubated at 40 ℃ in a water bath for 12 min. The enzyme reaction was stopped by adding 1000 μl of 10% Na_2CO_3 solution and removed from the water bath. The sample was immediately transferred to a 2 ml microphotometer cuvette (Thermo Fisher Scientific, Auckland, New Zealand), and the absorbance was measured at 420 nm using a spectrophotometer (Thermo Fisher Scientific, Waltham, United States).

Enzyme activity tests for all samples were carried out in at least triplicate. The absorbance of the drying feed was also measured. The percentage residual activity (% activity) of the enzyme after drying was then calculated by the following equation:

A standard curve of lactase was also prepared to verify the reliability of the assay as shown in Figure 3.4. The original lactase sample (Maxilact L2000) with a total protein (enzyme) content of 3.4% is diluted in 1:5 (0.68% enzyme concentration), 1:10 (0.34% enzyme concentration), 1:15 (0.22% enzyme concentration), 1:20 (0.17% enzyme concentration), 1:30 (0.11% enzyme concentration), 1:40 (0.085% enzyme concentration), 1:50 (0.068% enzyme concentration) and 1:60 (0.055% enzyme concentration) with deionised water, and the enzyme activity was measured. Change in absorbance is linear when the enzyme content is lower than 0.17% (with dilution factor 1:20) and showed a positive correlation with the concentration of lactase solution. When

the enzyme content is too high, the absorbance will keep constant due to insufficient substrate. Therefore, the final enzyme concentration in the drying feed should be lower than 0.17%.

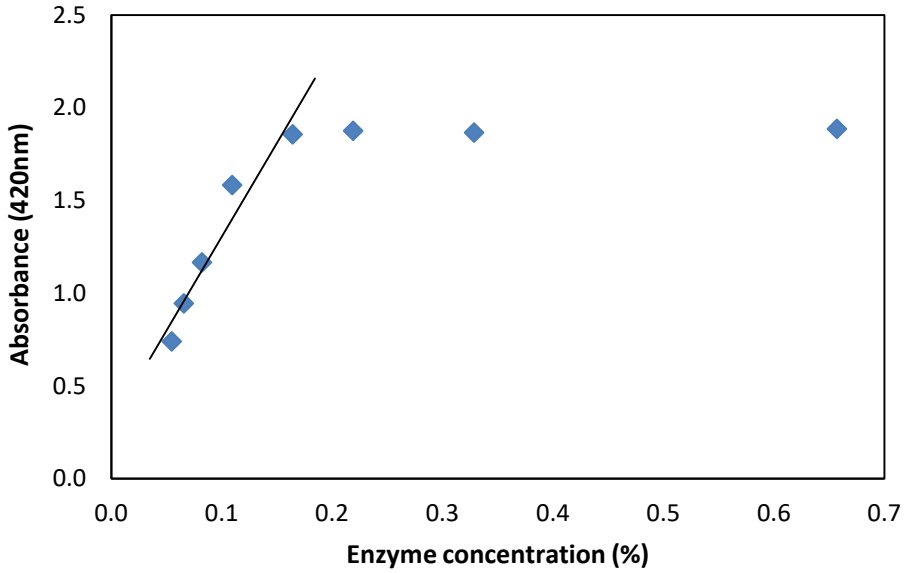

Figure 3.4 *Standard curve of lactase.*

3.2.4 Differential scanning calorimetry (DSC)

The degree of protein denaturation for WPI and egg white was measured by TA DSC Q2000 instrument (TA Instrument, New Castle, DE, USA). The dried sample was re-dissolved in RO water at 35% w/w concentration, mixed at room temperature until completely dissolved. 12-17 mg of the sample solution was transferred into a pre-weighed Tzero DSC pan with hermetic lid (TA Instrument, Switzerland), the weight of the sample was accurately recorded and the pan was then hermetically sealed. The sample pan was placed on the differential thermocouple of DSC Q2000 and scanned from 20 ℃ to 100 ℃ for WPI and to 110 ℃ for egg white at a programmed heating rate

of 10 ℃/min, and then cooled with the rate of 20 ℃/min to 20 ℃. An empty pan was placed as a reference.

Different heating scan rates from 1 ℃/min to 10 ℃/min have been applied in different studies (Anandharamakrishnan et al., 2007; Boye & Alli, 2000; Fitzsimons, Mulvihill, & Morris, 2007; Frydenberg, Hammershøj, Andersen, Greve, & Wiking, 2016; Ma et al., 2013; Sharma, 2012). Different heating rate influences the peak value and peak area of the heat flow curve (Sharma, 2012). Considering the aim of DSC in this study is to compare the heat flow of samples rather than quantitative analysis, coupled with time consumption issue, 10 ℃/min was used in the measurement.

During the measurement of DSC, the remaining undenatured protein in the sample undergoes denaturation. The enthalpy of denaturation (ΔH) appears as a peak in the curve, and its value represents the amount of undenatured protein remaining in the sample. The DSC curve was analysed by TA universal analysis software. The enthalpy value for denaturation (ΔH) was calculated from the area under an extending line with a fixed start and finish point for each sample. The peak temperature of denaturation (T_d) was also computed as the denaturation temperature of the protein.

DSC measurement for each sample was carried out in at least triplicate. The measurement was conducted for the drying feed in the same condition. The percentage of residual un-denatured protein after drying was defined as the percentage non-denatured (% non-denatured) and calculated by the following equation:

3.2.5 Determination of particle size

The particle size distribution of the dried powder was determined by Malvern Mastersizer 3000 instrument (Malvern Instruments Ltd, Malvern, UK). The Mastersizer 3000 uses laser diffraction to measure particle size distribution for both wet and dry dispersions (only dry powder dispersion unit was applied in this study). Sample was dispersed in an air cell by a flow of dry air. A laser beam passes through the cell and the dispersed particles scatter the light creating a scattering pattern. The optics measures the angles and intensity of the scattered light from which the particle size distribution is calculated using Mie Theory.

3.2.6 Determination of moisture content

The moisture content of the dried samples was determined within 24 hours after drying by the air-oven method. The method used in this study is the modification of IDF Standard 26A:1993 (IDF, 1993), refer to Massey University Food Chemistry Lab Manual (Ravindran & Glasgow, 2016). Aluminium moisture dishes used for the measurement were cleaned and dried, and kept in an airtight desiccator at room temperature before use. The weight of the moisture dishes with their matched lids was accurately recorded before the measurement. Approximately 2 g of sample was placed in the dish, and quickly re-weighed with the lid. Subsequently, the dish with the sample was placed in a Contherm solid-state oven 240, Contherm Scientific Limited, Wellington, New Zealand) set at 108 ℃ for 3 hours, with the lid under the dish. The dishes were covered with their lids before removing from the oven and transferred to the desiccators using tongs, cooled down and weighed accurately. Triplicate measurements were taken for each sample.

The moisture content of the sample was determined by the following equation:

Where, $\%\ T.M.$ = % total moisture

w_1 = weight of moisture dish + lid in grams

w_2 = weight of moisture dish + lid + sample (before drying) in grams

w_3 = weight of moisture dish + lid + sample (after drying) in grams

3.2.7 Determination of water activity (a_w)

Water activity is defined as the ratio of the partial vapour pressure of water in a sample to the saturated vapour pressure of pure water at the required temperature. The water activity of the dried powder was determined within 24 hours after drying using AquaLab 4TE water activity instrument (Decagon Devices Inc., WA, USA) at 20 ℃. The powder was uniformly filled into the sample cup until no more than half full. A mesh and a plastic ring were placed on top of the sample to avoid spillage. Three measurements were taken for each sample.

3.2.8 Optical microscopy

The morphology of dried particles was observed using Nikon Alphaphot-2 YS2 microscope (Nikon Instrument Inc., Japan) and Optika SZN2 bright-field Stereomicroscopes (Optika Srl, Bergamo, Italy). A 0.01 mm objective micrometre (Olympus Corporation, Tokyo, Japan) was used as a scale.

3.2.9 Kjeldahl determination

The Kjeldahl determination (AOAC, 2006) was applied in this study as a pre-test for Maxilact to analyse its protein content, in order to determine the amount of sample

required in the enzyme activity test. In the Kjeldahl test, sample was accurately weighed in a digestion tube, 2 Kjeltabs and 18 ml concentrated sulphuric acid was added to the tube. A blank tube with no sample but all other reagents added was used as a reference. The sample and banks tubes were digested in a Foss 2006 Digestor (Foss Analytical, Hillerød, Denmark) at 420 °C until clear. The tubes were then removed from the heating unit and approximately 70 ml of hot distilled water was added to each tube and mixed. The distillation process was conducted in a Foss 2100 Kjeltec Distiller (Foss Analytical, Hillerød, Denmark) with the pre-programmed 'automatic' setting. The distillation product was collected in a 250 ml conical flask with 25 ml 4% boric acid solution (containing bromocresol green and methyl red as the colour indicator). Standard acid (0.1 M HCl) was used for titration to a grey-mauve endpoint. The percentage Nitrogen content was calculated by the following equation:

Where, A = volume of HCl used in the titration in millilitres

B = the molarity of HCl

C = weight of the sample in grams

Chapter 4 Influence of air temperature on the denaturation of proteins during spray drying

4.1 Introduction

As one of the extensively used techniques in the food industry, spray drying has been investigated by a number of researchers in the past decades. Among which, investigation of the effects of process variables and optimization of the operating conditions are the most popular topics. Air temperature is one of the key parameters in spray drying process, which plays an important role in powder quality. However, most of the existing studies for spray drying were using the certain outlet temperature range with different inlet temperature (Anandharamakrishnan et al., 2007; Caliskan & Nur Dirim, 2013), or certain inlet temperature range with recorded outlet temperature (Kha, Nguyen, & Roach, 2010; Mishra, Mishra, & Mahanta, 2014; Samborska et al., 2005). Few works keep the inlet or outlet temperature constant and investigate the effect of the other.

The objective of this study was to investigate the influence of spray drying temperatures on the heat denaturation and other quality properties of protein-based heat labile materials, with either inlet or outlet temperature as the control variable; and to compare the performance of a monodisperse droplet generator spray dryer with a conventional polydisperse atomizer spray dryer. Three proteins or enzyme were selected: lactase, WPI and egg white. The effect of other related variables was also discussed.

4.2 Materials and Methods

4.2.1 Feed preparation

The drying feed was prepared in 35% (w/w) total solid content for each of the three materials. However, the composition varies for each material based on their nature.

Lactase

The lactase feed solution consisted of 35% (w/w) maltodextrin CR10 and 5% (w/w) Maxilact L2000. Due to Maxilact L2000 only has approximately 3.4% (w/w) of total solid, adding 5% of it will not influence the overall solid content of the feed (contributing no more than 0.2% of total solid content). The maltodextrin solution was gently stirred by a laboratory agitator (Qualtech Products Industry Co., Ltd, Shanghai, China) for 1 hour or until completely dissolved. Gentle heat was applied to accelerate dissolving, and the solution was cooled down to room temperature before the addition of Maxilact.

Egg white

The egg white feed solution was made by adding 29% (w/w) of maltodextrin CR10, 21% (w/w) of water, and 50% (w/w) of liquid egg white (containing approximately 12% total solids). The total solid content of the feed was 35% (w/w). Maltodextrin was first dissolved in water with heat and agitation applied until completely dissolved into transparent syrup, and then cooled down to room temperature before adding to liquid egg white. Gentle stirring was applied when adding the maltodextrin syrup to the egg white. The pH of the feed was 8.8 to 9.

WPI

The WPI feed solution was made from 35% (w/w) WPI dissolved in water. Gentle heat (no higher than 50 ℃) and stir were applied during mixing until completely dissolved. When developing the experimental conditions, 20% (w/w) WPI and 15% (w/w) maltodextrin were first used as the drying feed. However, there was no obvious degredation observed. Therefore, considering the potential effect of the carrier, in order to reveal visual changes of protein denaturation, maltodextrin was removed from the feed.

4.2.2 Drying conditions

The drying experiment for each sample was repeated three times. The analysis of the products obtained from each drying run was conducted in at least triplicate as stated previously.

Inlet & outlet air temperature

In the initial design of the experiment, it was considered to use different inlet air temperature as the operating variable. However, pre-experimental results revealed that the effect of inlet air temperature on protein denaturation was inconspicuous compared to the outlet air temperature. Therefore, outlet air temperature was chosen as the variable in the finalised experiment. The inlet air temperature of the spray drying was fixed at 200 ℃. Desired outlet air temperature was achieved by altering liquid feed pump rate. The outlet temperatures and feed pump rates for each sample and each trial were recorded in Table 4.1. The outlet temperature with ± values representing the maximum observed variation from the intermediate value. Before the feed solution was pumped into the drying chamber, distilled water was sprayed into the chamber to start

with in order to reach thermal equilibrium. Each outlet temperature was stabilized at the quoted value for at least 10 min before powder collection. Feed pump rate varies between different runs even though for same sample and same outlet temperature and it is an important parameter which plays a decisive role in the determination of other parameters. Therefore, data for each run was recorded and presented individually in Table 4.1.

Table 4.1 *Experimental conditions used in the spray drying experiments for each sample and their effect on moisture content, water activity and residence time.*

Feed solution	Outlet air temperature (°C)	Pump rate (rpm)	Liquid feed rate (g/ml)	Residence time (s)
Lactase	Trial 1			
	85 ±0.8	31	25.1	15.4
	90 ±0.4	29	23.5	15.4
	95 ±0.7	24.5	19.7	15.3
	100 ±0.8	21	16.8	15.2
	105 ±1.0	20	16.0	15.2
	Trial 2			
	85 ±0.4	24	19.3	15.5
	90 ±0.6	21.5	17.2	15.4
	95 ±0.5	18.5	14.7	15.4
	100 ±0.7	15	11.8	15.3
	105 ±1.0	13.5	10.6	15.2
	Trial 3			
	85 ±0.3	26	21.0	15.5
	90 ±0.4	24	19.3	15.4
	95 ±0.6	17	13.5	15.4
	100 ±0.9	12	9.3	15.3
	105 ±1.0	9	6.9	15.3
WPI	Trial 1			
	82.5 ±1.0	53	44.6	15.3
	92.5 ±0.7	26	21.6	15.3
	102.5 ±0.3	16.5	13.5	15.2
	112.5 ±1.5	9	7.0	15.1

	Trial 2			
	82.5 ±0.2	35	29.2	15.4
	92.5 ±0.7	21.5	17.7	15.4
	102.5 ±0.6	14	11.3	15.3
	112.5 ±1.5	9	7.0	15.1
	Trial 3			
	85 ±1.0	36	30.1	15.4
	95 ±0.7	24	19.9	15.3
	105 ±0.4	15	12.2	15.2
	115 ±1.3	10	7.9	15.1
Egg white	Trial 1			
	85 ±0.4	35	29.0	15.4
	90 ±0.2	30	24.7	15.4
	95 ±0.3	23.5	19.3	15.3
	100 ±0.6	22	18.0	15.2
	105 ±0.4	17	13.8	15.2
	Trial 2			
	85 ±0.7	26	21.4	15.5
	90 ±0.4	23	18.8	15.4
	95 ±0.5	18	14.6	15.4
	100 ±0.5	18	14.6	15.3
	105 ±1.0	19.5	15.9	15.2
	Trial 3			
	85 ± 0.5	41	34.1	15.3
	90 ±0.6	35.5	29.4	15.3
	95 ±0.6	30.5	25.2	15.3
	100 ±1.0	26	21.4	15.2
	105 ±1.2	24.5	20.1	15.1

Flow rate measurement

The liquid feed was pumped through a peristaltic pump. The rotational speed of the rotor and volumetric feed rate conform to linear regression, as shown in Figure 4.1. The regression model is $y = 0.7833x - 0.5833$ ($R^2 = 0.9991$). Mass feed rates as shown in Table 4.1 were acquired by multiplying volumetric feed rate by feed density, which are 1.06, 1.09. 1.08 g/ml for lactase, WPI and egg white feed solution respectively.

Residence time

The residence times of spray drying are given in Table 4.1. They were estimated from the volume of the chamber (Diameter 800 × 620 mm / cone 60 ºas shown in the manual of the dryer) and the drying air rate (80 kg/h at 200 ℃ as shown in the manual). The volume of vapour coming from evaporation and air from atomization were also considered in the calculation of residence time. However, these values were relatively small compared to the volume of drying air, thus didn't contribute much to the residence time.

Assuming the drying air and vapour from evaporation are the ideal gas, whereupon they obey the ideal gas law:

Where P is pressure, V is volume, n is the number of moles, R is the ideal gas constant, and T is temperature.

At constant pressure and number of moles, the volume of a gas is directly proportional to the temperature of the gas. Equation 4.1 can be transformed to:

The molar volume of ideal gas at standard temperature and pressure (273.15 K, 100 kPa) is 22.7 L/mol. The molar volume of gas at the desired temperature can then be calculated by equation 4.2, as well as the density (molar weight was known) and volumetric flow rate (mass flow rate was known) of air and vapour.

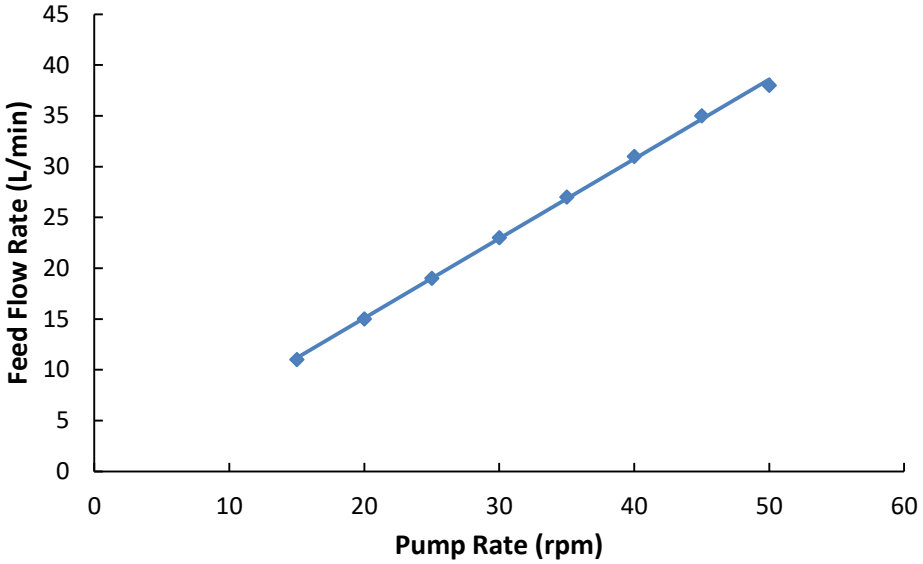

Figure 4.1 *Relationship between rotor pump rate and liquid feed flow rate.*

Drying parameters

Three parameters (drying ratio, productivity, and drying rate) were calculated from the following equations in order to describe the drying process (Samborska et al., 2005).

4.2.3 Data analysis

Data in the tables or figures were the average values of multiple measurements. Error bars or standard errors were indicated where necessary. Statistical analysis of data was conducted by SPSS software (version 23, IBM Corp.). Analysis of variance (ANOVA) was applied to determine the significance of differences between obtained values. Duncan's Multiple Range Test (MRT) was used to measure specific differences

between pairs of means. Normality was checked for each material and temperature point individually before conducting ANOVA. It is found that the most of the data fit the normal distribution. The normality check result is limited by the number of observations. In this study, 3-5 replicates were measured for each sample. Therefore, even 1 or 2 measurements may have a great effect on the distribution of data. Considering the situation stated above and the possible errors caused by the number of measurements, it is assumed that the measurement variables are normally distributed if the number of observations is sufficiently large. In addition, Analysis of Covariance (ANCOVA) for regression models was conducted by Minitab software (version 17.3.1, Minitab, Inc.) to investigate the variance between regressions.

4.3 Results and Discussion

4.3.1 Effects of inlet temperature on the denaturation of lactase

Four inlet air temperature levels (170, 200, 230, 260 ℃) were applied during the spray drying of lactase and the outlet air temperature was maintained at the same level 88 ℃ by adjusting pump rate from 20 to 45 rpm. At higher inlet temperature, a higher pump rate was required in order to achieve same outlet temperature. Figure 4.2 shows the relationship between absorbance obtained from ONPG assay (refer to Chapter 3) and the inlet air temperature. The absorbance values indicate the level of residue lactase activity in the spray dried powder. Statistical analysis shows that the differences in absorbance from different inlet temperature were insignificant ($P > 0.05$). It means with the outlet temperature constant, changing inlet temperature within the range of 170 to 260 ℃ will not greatly affect the residual enzyme activity of spray dried lactase powder. This result agrees with the findings of Kim and Bhowmik (1990) that a higher inlet

temperature only had a minor effect on the heat inactivation. A possible reason is that the extent of heat-related denaturation mainly depends on the combinations of temperature and time. During the constant rate period, the temperature of the spray dried droplets is limited to the wet bulb temperature due to evaporation cooling effect. At the falling rate period, the temperature of droplets will increase and approach the air temperature in the chamber but will not reach the inlet air temperature (Santivarangkna, Kulozik, & Foerst, 2007). The falling rate period is decisive for the heat denaturation, therefore, the temperature of air leaving the drying chamber, which also known as the outlet air temperature, is more important to the degree of denaturation of spray dried products.

In the following sections, the results present are obtained when the inlet air temperature kept constant at 200 ℃ and outlet temperature is changed.

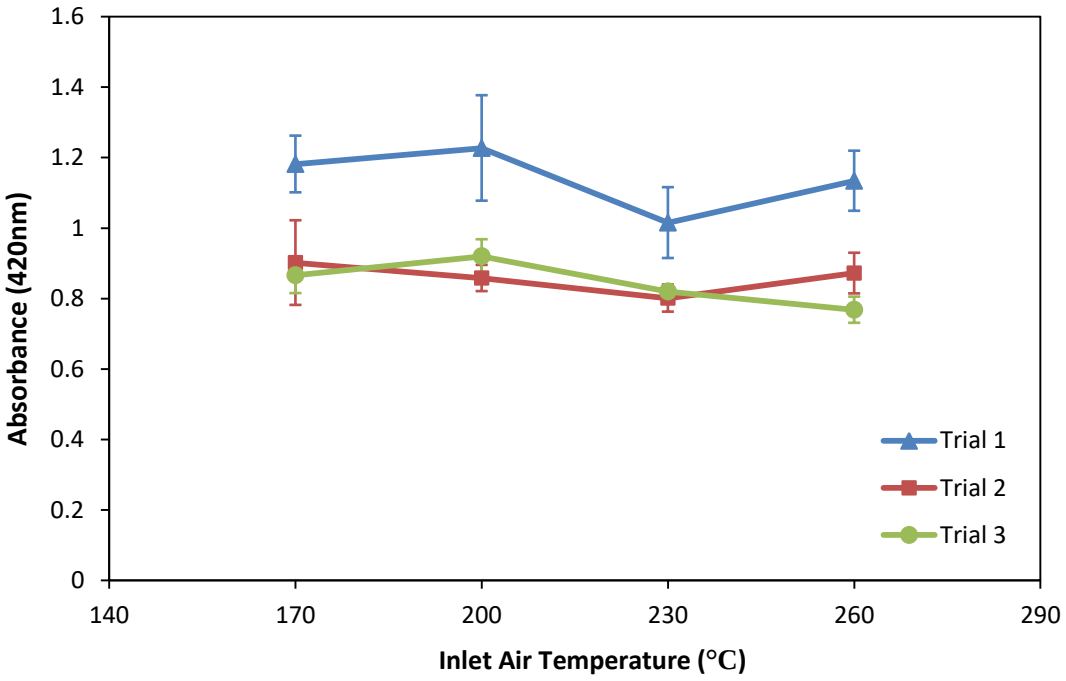

Figure 4.2 *Effect of inlet air temperature on residual lactase activity in spray dried lactase powder indicated by the absorbance in ONPG assay (error bar = 1 standard error).*

4.3.2 Effects of outlet temperature on moisture content and water activity

The average moisture contents of the spray dried powders obtained from different outlet temperature are shown in Figure 4.3 and the values of water activity (a_w) are given in Figure 4.4. Moisture contents for obtained powders are within the range of 1.8% to 5.1%, and water activities are in between 0.06 and 0.18. These values are in agreement with typical values for spray dried products (van't Land, 2011b). Both moisture content and water activity decrease as outlet temperature increases for all of the samples. The changes are statistically significant according to ANOVA results ($P < 0.01$). These trends agree with previously published reports (Anandharamakrishnan et al., 2007; Etzel, Suen, Halverson, & Budijono, 1996; Samborska et al., 2005; Ståhl, Claesson, Lilliehorn, Lindén, & Bäckström, 2002).

Moisture evaporation is an important stage of spray drying and involves a series of heat and mass transfer processes (Silva, Freixo, Gibbs, & Teixeira, 2011a). Heat is transferred from the hot air to the droplets by convection, and the moisture is from the interior to the surface of droplets and to the surrounding air. Higher outlet air temperature provides a larger driving force for heat and mass transfer, which results in greater water evaporation and gives a drier powder.

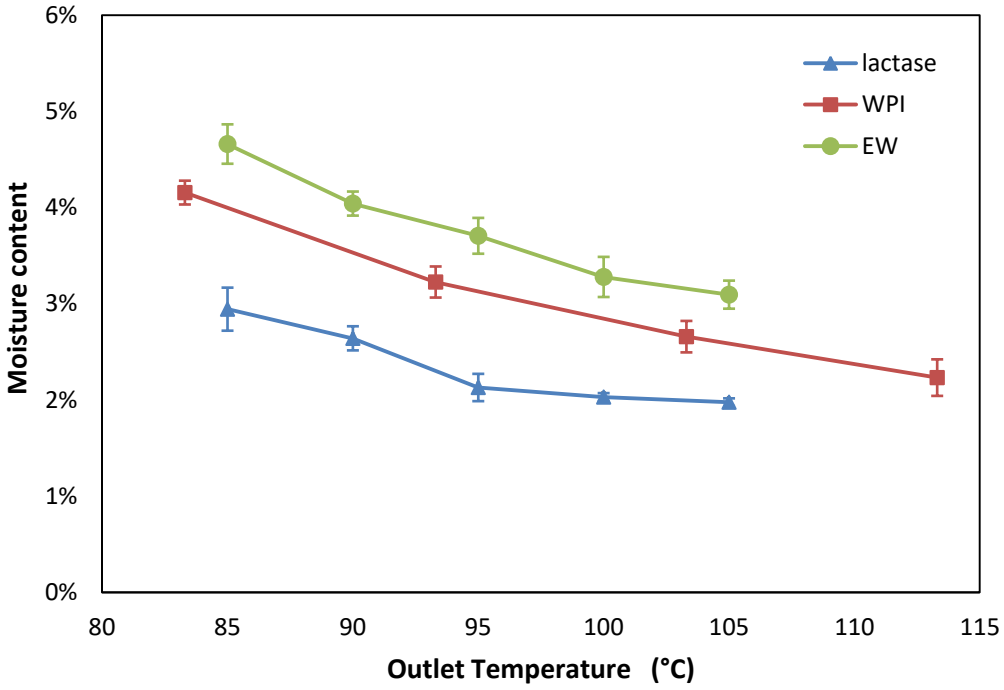

Figure 4.3 *Relationship between outlet temperature and moisture content of the spray dried powder (error bar = 1 standard error).*

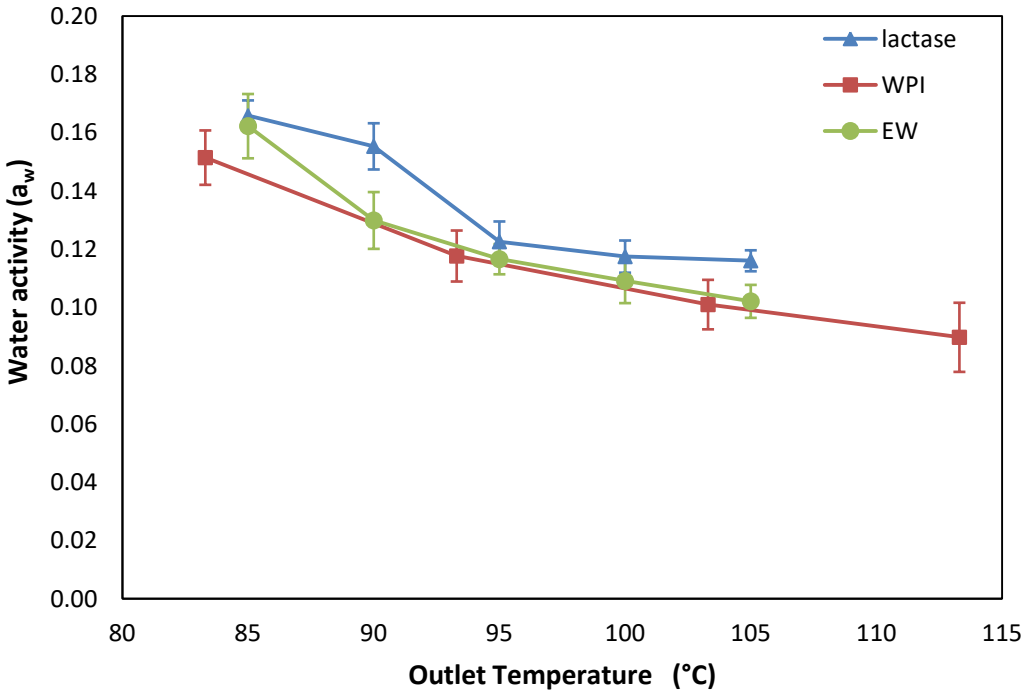

Figure 4.4 *Relationship between outlet temperature and water activity of the spray dried powder (error bar = 1 standard error).*

4.3.3 Effects of outlet temperature on drying Ratio, productivity and drying Rate

Table 4.2 presents the average drying ratio, productivity and drying rate for the three materials at different outlet temperature with their standard errors. It can be observed from the data that drying ratio slightly increases as outlet air temperature increases and generally within the range of 2.7 to 2.8. The drying ratio is inversely correlated to the moisture content of the dried powder. Productivity varied between 0.16 and 0.76 kg/h and drying rate varied from 0.28 to 1.32 kg/h, both of the two parameters are decreasing as outlet air temperature increases. The larger variation observed for WPI is due to WPI being dried across a larger outlet temperature range from 82.5 to 115 ℃, whereas the outlet temperatures for lactase and egg white were within the range of 85 to 105 ℃. Values of productivity and drying rate are mainly related to the feed flow rate according to equation 4.4 and 4.5, which also has a descendant trend with ascending outlet temperature. As stated previously, heat transfer during spray drying is driven by the temperature difference between the droplet and the surrounding air. With the inlet air temperature kept constant, the lower the outlet temperature, the larger the temperature difference, therefore, a greater overall drying rate achieved (Earle & Earle, 1983).

Table 4.2 *Effect of outlet air temperature on drying ratio, productivity and drying rate.*

Feed solution	Outlet air temperature (℃)	Drying ratio	Productivity (kg/h)	Drying rate (kg/h)
Lactase	85	2.77 ± 0.006	0.47 ± 0.036	0.84 ± 0.067
	90	2.78 ± 0.004	0.43 ± 0.039	0.77 ± 0.071
	95	2.80 ± 0.004	0.34 ± 0.040	0.62 ± 0.074
	100	2.80 ± 0.001	0.27 ± 0.047	0.49 ± 0.085
	105	2.80 ± 0.001	0.24 ± 0.057	0.43 ± 0.102

WPI	82.5-85	2.74 ±0.004	0.76 ±0.110	1.32 ±0.189
	92.5-95	2.76 ±0.005	0.43 ±0.025	0.75 ±0.042
	102.5-105	2.78 ±0.005	0.27 ±0.014	0.47 ±0.023
	112.5-115	2.79 ±0.005	0.16 ±0.006	0.28 ±0.011
EW	85	2.72 ±0.006	0.62 ±0.081	1.07 ±0.140
	90	2.74 ±0.004	0.53 ±0.067	0.93 ±0.116
	95	2.75 ±0.005	0.43 ±0.066	0.75 ±0.117
	100	2.76 ±0.006	0.39 ±0.042	0.69 ±0.075
	105	2.77 ±0.004	0.36 ±0.040	0.64 ±0.072

4.3.4 Effects of outlet temperature on the denaturation of proteins and enzymes

The relationship between outlet temperature and the undenatured proteins (calculated as % activity or % non-denatured) retained in spray dried products of lactase, WPI and egg white are shown in Figure 4.5, 4.6 and 4.7 respectively. The definition and calculation of % activity and % non-denatured values can be found in Chapter 3, representing the ratio of residual enzyme activity or undenatured protein in the dried products and that in the original drying feed expressed as a percentage. Data obtained from each of the three trials are presented in the figure; with letters (a-e) indicating the Duncan's Multiple Range Test results for the differences between pairs of means. It can be seen from the three figures that the residual activity of lactase and the undenatured protein in WPI and egg white decreases as the outlet air temperature of spray drying increases. And for each of the three materials, the differences of % activity or % non-denatured at various outlet temperature are statistically significant according to ANOVA results ($P<0.01$). The results correspond with the finding of a number of previous studies that the outlet temperature is the major parameter that affecting the heat

degradation of spray dried products (Anandharamakrishnan et al., 2007; Ananta, Volkert, & Knorr, 2005; Santivarangkna et al., 2007).

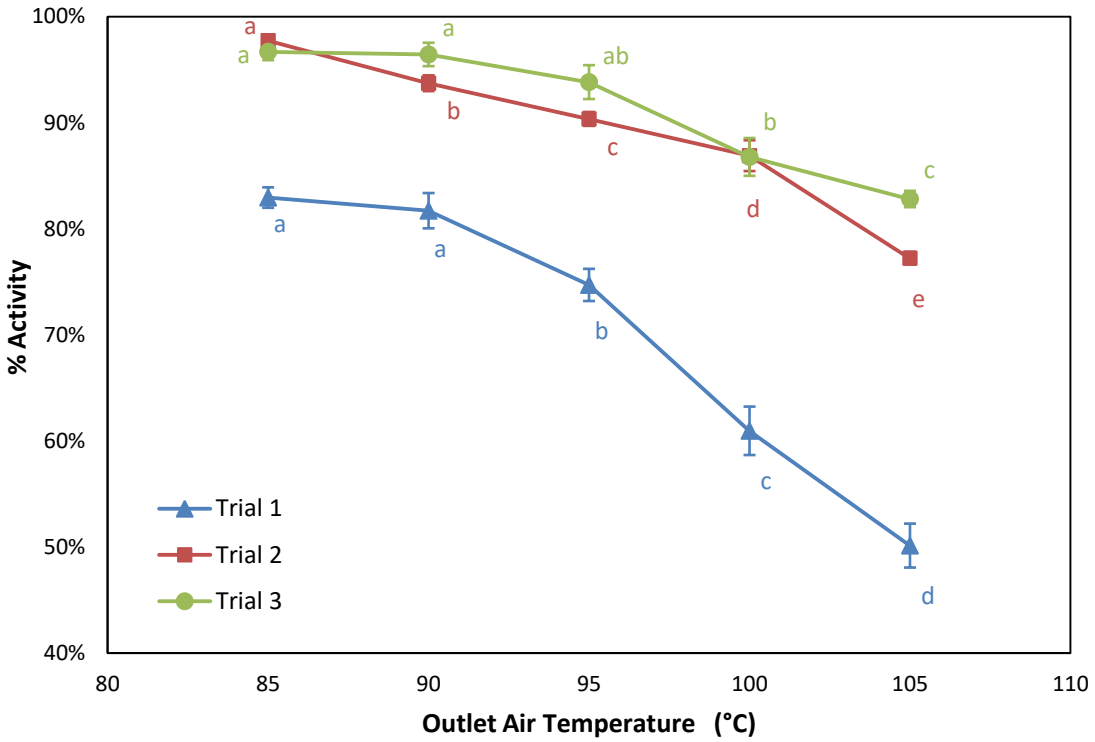

Figure 4.5 *Effect of outlet temperature on the percentage activity of spray dried lactase products (Letters a-e indicate the grouping for the differences between pairs of means according to Duncan's Multiple Range Test, error bar = 1 standard error).*

When the outlet air temperature increased from 85 ℃ to 105 ℃, the activity of lactase changed from 97% to 77% in trial 2 and from 96% to 82% in trial 3. The greater extent of activity change observed in trial 1 from 83% to 50%. The reason for the differences in activity between trial 1 and trial 2 & 3 is that trial 1 was actually conducted 6 months earlier than trial 2 and 3. It is suspected that the activity of lactase has decreased with time due to unstable storage conditions. Therefore, by adding the same amount of enzyme solution to the drying feed, a higher level of active enzymes

existed in the drying feed of trial 1 compared to trial 2 & 3 and resulted in a greater level of denaturation being observed. In addition, the deeper gradient of the curve indicates that the change of activity is more sensitive to temperature.

Based on information provided by the supplier, the lactase product Maixilact L2000 has an optimal reaction temperature of 35-40 ℃. The activity of enzyme starts decreasing when the operating temperature is higher than 40 ℃ and the enzymes become denatured when the temperature exceeds 55-60 ℃. It can be seen from Figure 4.5 that denaturation of lactase occurs at outlet air temperature exceeds 90-95 ℃ (the start points where the differences between means become significant). This implies that when the outlet air temperature reached this level, the temperature of the particles in the chamber starting reaching their denaturation temperature and thermal deformation occurs. However, the relationship between outlet temperature and the change of activity may vary slightly within different trials for the same material. It may be affected by different behaviours of particles, e.g. droplet size and trajectory. As stated previously, conventional spray drying has a non-uniform particle size distribution which will affect the heat and mass transfer of different particles and therefore, influence the temperature of the particles. Hence it is hard to obtain exactly the same drying curve from each drying run, but the overall trend will be consistent.

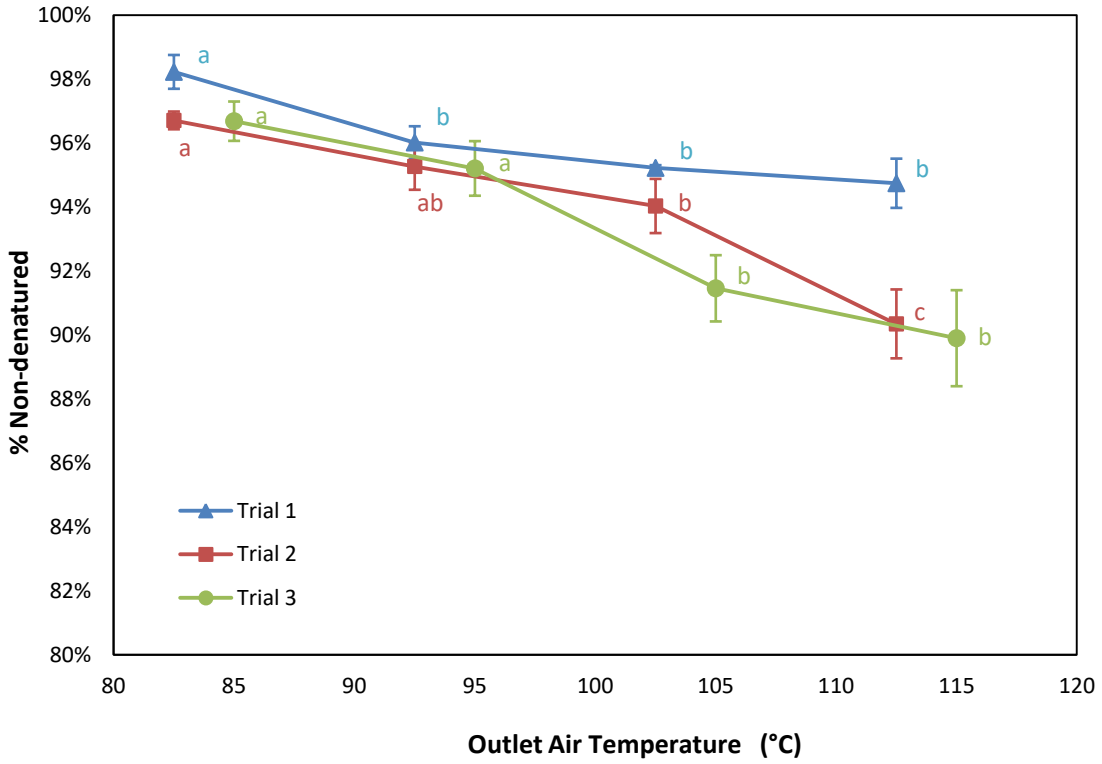

Figure 4.6 *Effect of outlet temperature on the percentage non-denatured value of spray dried WPI products (Letters a-c indicate the grouping for the differences between pairs of means according to Duncan's Multiple Range Test, error bar = 1 standard error).*

The % non-denatured value of WPI decreased from 98% to 90% when the outlet temperature was raised from 82.5 ℃ to 115 ℃. The experiment of WPI proceeded in the largest outlet temperature range; however, the change of % non-denatured value was the smallest. It can be observed from Figure 4.6 that slight level of denaturation of WPI happened when the outlet temperature reached 95-105 ℃. These findings agree with the study of Oldfield, Taylor, and Singh (2005) and Anandharamakrishnan et al. (2007), who found that with the outlet temperature of spray drying lower than 100 ℃ there was no significant denaturation of whey protein being observed. There are two major proteins in whey, α-lactalbumin and β-lactoglobulin. The denaturation temperature for α-lactalbumin is around 62 ℃ and for β-lactoglobulin is around 73 ℃ based on the

DSC thermogram of WPI. Similar thermograms have been reported in several previous studies (Fitzsimons et al., 2007). Whey protein denaturation is less sensitive to outlet temperature compared to lactase and egg white. Higher outlet temperatures and solids concentrations are required to denature whey protein during spray drying. Anandharamakrishnan et al. (2007) have reported that a high level of whey protein denaturation happened when outlet temperature was 200 ℃ and feed concentration was 40%.

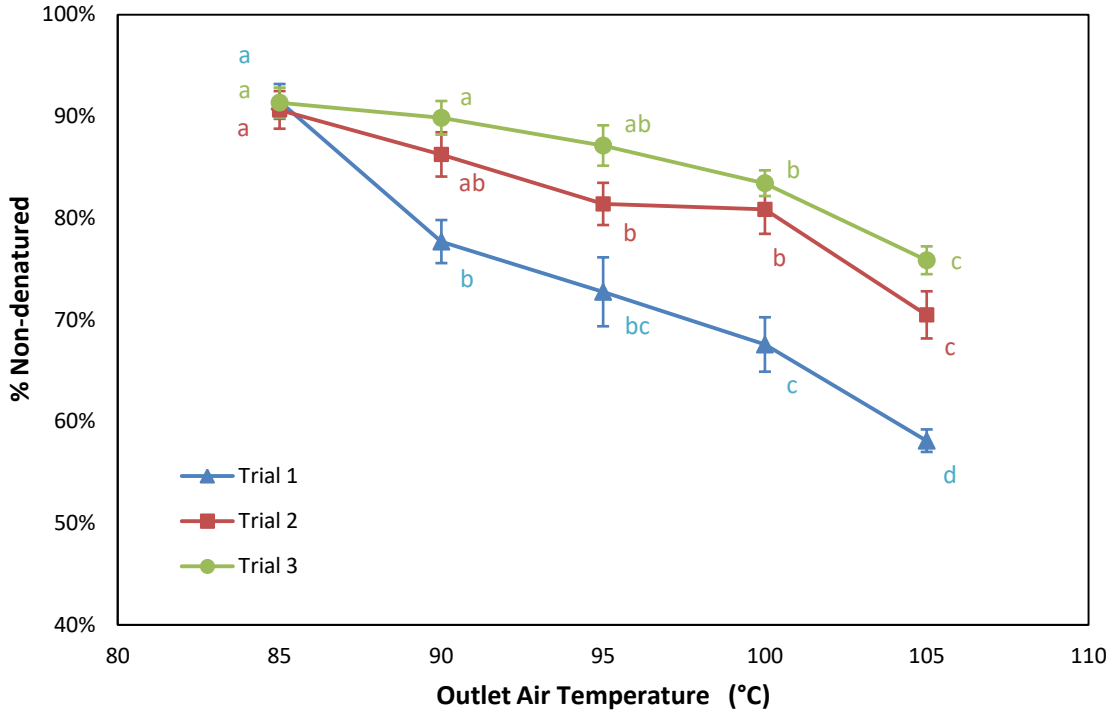

Figure 4.7 *Effect of outlet temperature on the percentage non-denatured value of spray dried egg white products (Letters a-d indicate the grouping for the differences between pairs of means according to Duncan's Multiple Range Test, error bar = 1 standard error).*

The % non-denatured value of egg white protein changed from around 90% to 58%, 70% and 75% respectively for trial 1, 2 and 3 when outlet temperature changed from 85 ℃

to 105 ℃. Denaturation commenced when the outlet temperature in between 90 and 95 ℃ according to Figure 4.7. The most abundant protein in egg white is ovalbumin; it has a denaturation temperature around 84 ℃. Another two major components are conalbumin and ovomucoid. Their denaturation temperatures are around 61 and 70 ℃ respectively. Two endothermic peaks were observed from the DSC thermograph of thermograms of egg white at around 83 ℃ and 70 ℃, which can be assigned to the denaturation of ovalbumin and ovomucoid respectively. Different extents of denaturation were observed from the three trials. Some of the variations may be due to different batches of material since the liquid egg white applied in this experiment was purchased separately before each experiment. Besides, some of the variations may reflect small differences in the spray pattern between trial runs.

4.3.5 Reaction rate kinetic, Arrhenius plot and activation energy

For a general reaction, the rate equation can be expressed by:

$$\frac{dC}{dt} = -k\,C^n \qquad (4.6)$$

Where *C* is the concentration of specific reactant, *t* is time, *n* is the order of reaction and *k* is the reaction rate constant.

For the first order reaction, equation 4.6 can be integrated to:

$$ln\,\frac{C}{C_0} = -k\,t \qquad (4.7)$$

Therefore, the reaction rate constant *k* can be calculated by the following equation:

$$k = -ln\frac{C}{C_0}\cdot\frac{1}{t} \qquad (4.8)$$

The rate constant k is dependent on the temperature, according to Arrhenius Equation:

Where A is the pre-exponential factor, T is the temperature in Kelvin, R is the gas constant, and E_a is the activation energy.

The Arrhenius Equation can be written in a non-exponential form as follows:

Therefore, the slope of the Arrhenius plot (plot $ln\ k$ as a function of $1/T$) is $-E_a / R$, activation energy can then be determined.

The Arrhenius plots for lactase, WPI and egg white are shown in Figure 4.8, 4.9 and 4.10 with regression equations given. It can be observed from the Figures that the regression lines of different trials for each material are generally parallel. The ANCOVA results indicate that for each of the three materials, the differences in slopes of linear regressions between trials are insignificant ($P > 0.05$). The integrated slope for each material was then generated by the software by eliminating the effect of covariates and given in Table 4.3, along with their standard errors and activation energy calculated based on the slopes.

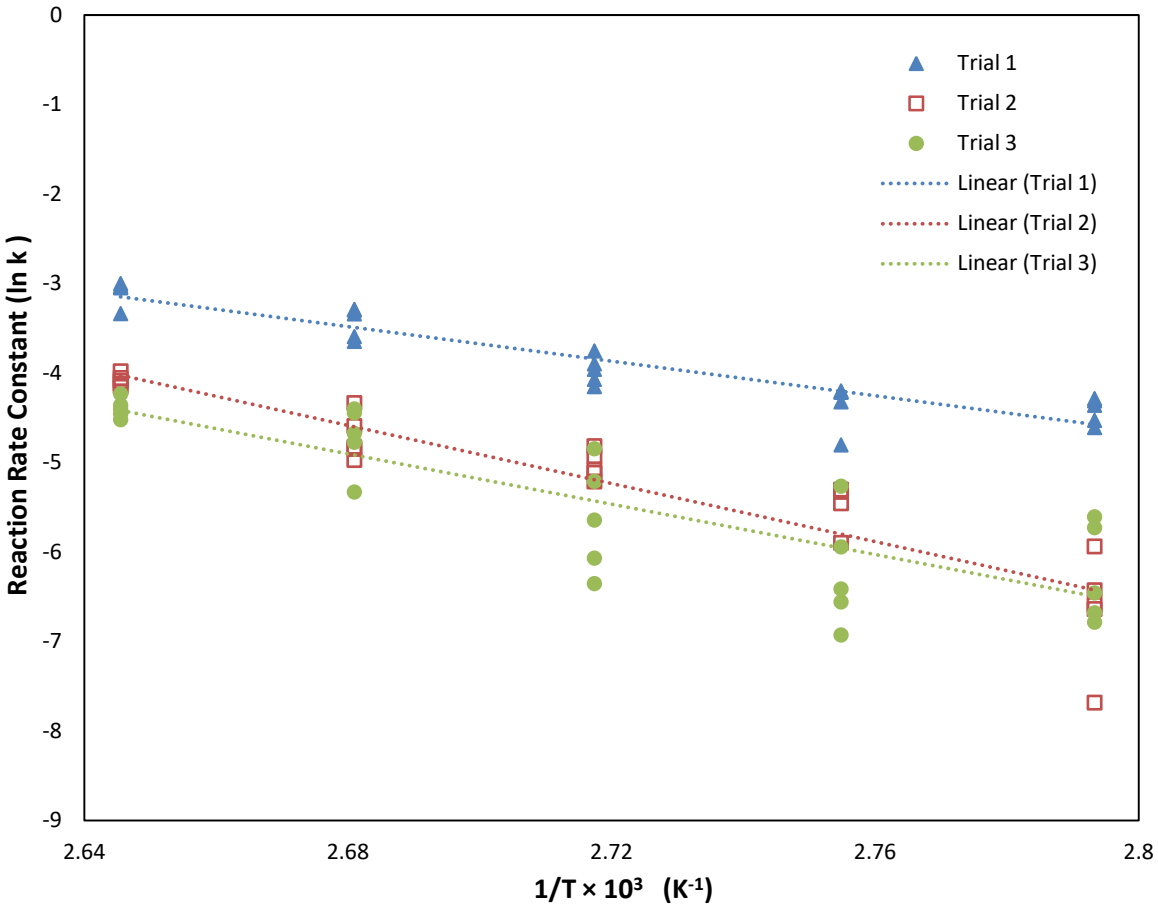

Figure 4.8 *Arrhenius plot for lactase: ln k against 1/T. All of the data points for each trial present in the figure with the linear regression line. Regression models: y = -9.64x + 22.36, R ²= 0.87 (Trial 1); y = -16.26x + 38.98, R ²= 0.85 (Trial 2); y = -14.06x + 32.78, R ²= 0.70 (Trial 3). Integrated slope = -13.298, SE=0.901.*

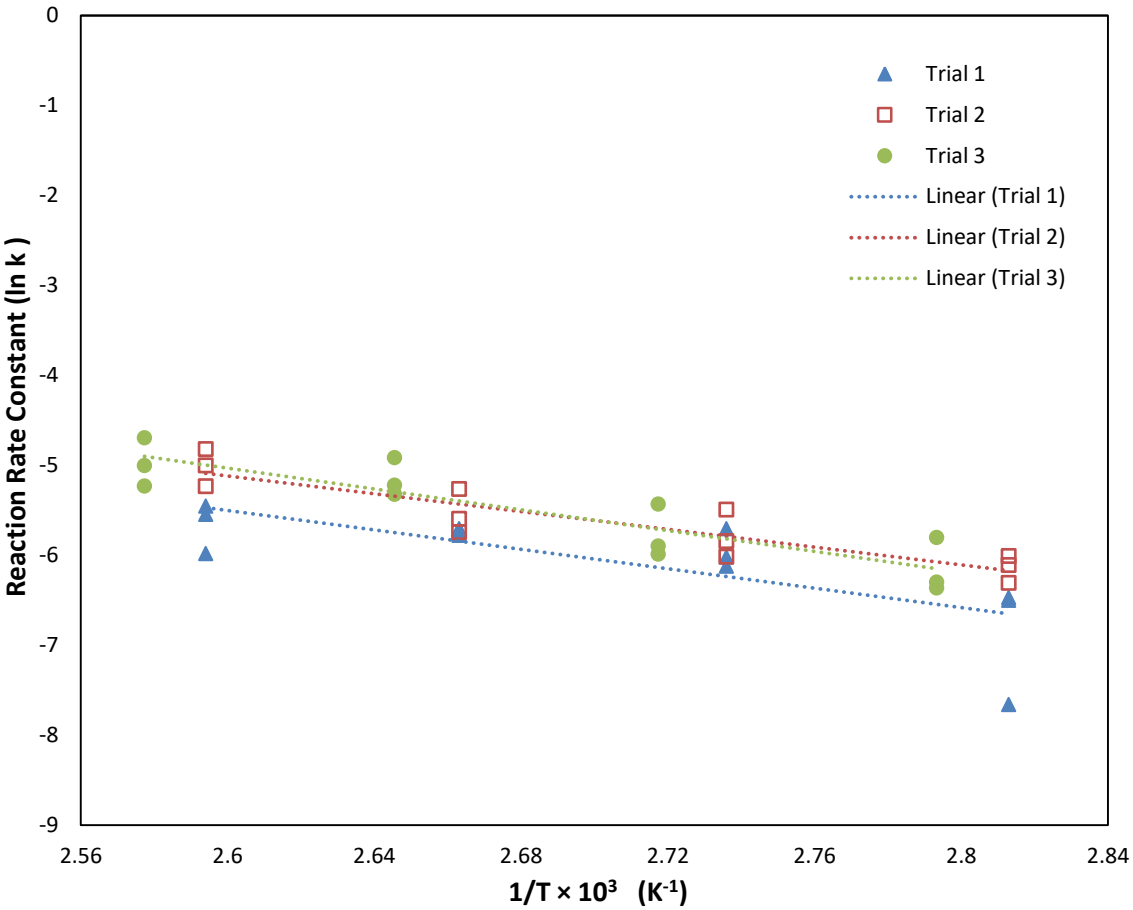

Figure 4.9 *Arrhenius plot for WPI: ln k against 1/T. All of the data points for each trial present in the figure with the linear regression line. Regression models: y = -5.39x + 8.52, R ²= 0.58 (Trial 1); y = -4.95x + 7.75, R ²= 0.81 (Trial 2); y = -5.78x + 10.01, R ²= 0.79 (Trial 3). Integrated slope = -5.371, SE=0.605.*

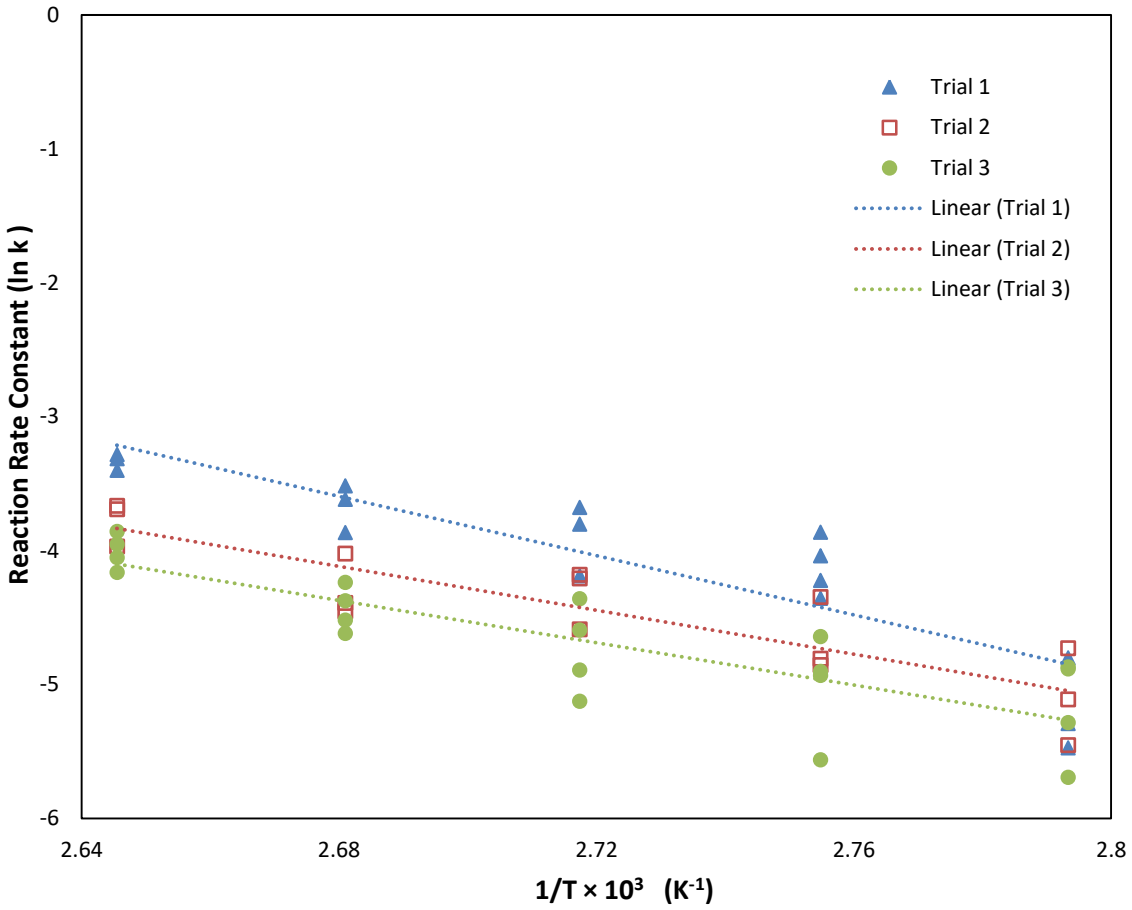

Figure 4.10 *Arrhenius plot for egg white: ln k against 1/T. All of the data points for each trial present in the figure with the linear regression line. Regression model: y = -11.06x + 26.04, R ²= 0.79 (Trial 1); y = -8.19x + 17.83, R ²= 0.77 (Trial 2); y = -7.89x + 16.78, R ²= 0.69 (Trial 3). Integrated slope = -8.949, SE=0.786.*

Table 4.3 *Summary of the integrated slope of linear regressions and activation energy.*

Materials	*Integrated slope*	*Standard error*	E_a (kJ/mol)	*Standard error*
Lactase	-13.298	0.901	110.6	7.5
WPI	-5.371	0.605	44.7	5.0
Egg white	-8.949	0.786	74.4	6.5

Data from Table 4.3 indicates that lactase has the highest activation energy of the three materials, followed by egg white. And the E_a value of WPI is the lowest of the three. Activation energy is the energy required for a specific reaction to start. It can also be thought of as a potential barrier of energy that a reactant must overcome to proceed the reaction (Renneboog, 2015). The lower the activation energy, the faster a reaction happens. The activation energy for a particular reaction is usually determined experimentally (Earle & Earle, 2007). It is influenced by the nature of the reactants and the presence of a catalyst and is independent of the other operating parameters e.g. temperature and pressure. However, for protein denaturation process, a change of temperature dependence may be observed in the Arrhenius plots as reported by several previous studies (Anema & McKenna, 1996; Dannenberg & Kessler, 1988; Hillier & Lyster, 1979). Under the ideal assumption, the activation energy of the same reactant obtained from repeated experiments is expected to be the same. However, the practical situation of a reaction is fairly complex due to the inevitable variations of the reactants and measurement methods.

Different E_a values were observed from the repeated experiments of each material. The results for lactase reveal the largest variance. As state previously, loss of activity occurred during the storage of lactase. Samples applied in trial 1 for lactase experiment were more active, therefore, lower activation energy and faster reaction rate were observed. The variance of E_a values also presents in the results of egg white. It may be due to the fresh liquid egg white samples used in the experiment being purchased from different batches and had different freshness, depend on what was available in the supermarket. The deviation of WPI is relatively narrow, which indicates the nature of WPI is relatively stable, and less degradation happened during storage.

Another factor to be considered when constructing the Arrhenius plot it the goodness-of-fit for the model. It can be seen from Figure 4.8 to 4.10 that the R^2 values for some of the linear models are relatively low. This can be ascribed to the deviation of multiple measurements. One possible reason is that the reaction of protein denaturation with the outlet temperature in spray drying is not simply a first-order reaction. As discussed in the previous section, significant protein denaturation did not occur at low outlet temperature range. The outlet air temperature of spray drying is usually different from the temperature of the particle; the latter has a direct relation to protein denaturation and structure change. Denaturation commenced at outlet temperature 90 to 100 ℃, before which the reaction can be considered to have a different order of reaction. Therefore, constructing the regression model for the entire reaction base on the law of the first-order reaction may introduce deviation to the results.

4.3.6 Particle size distribution of spray drying

The particle size distribution for the powder produced by spray drying is shown in Figure 4.11. A board particle size distribution can be observed in the figure. The D10, D50 and D90 values are 7.2, 31.7, 83.6 μm respectively. The manner in which particle properties influenced by the air temperature depends on the particle size. A wide particle size distribution brings about difficulties in the control of the overall drying process. Particles with different sizes experience different heating history and residence time in the drying chamber, resulting in distinction in powder quality. The variance in powder particle size is on account of the non-uniform size of droplets generated in the atomization process. Therefore, efforts have been made by experts in narrow down the size diversity of droplets coming from the nozzle, in order to achieve better control of the drying process and product quality.

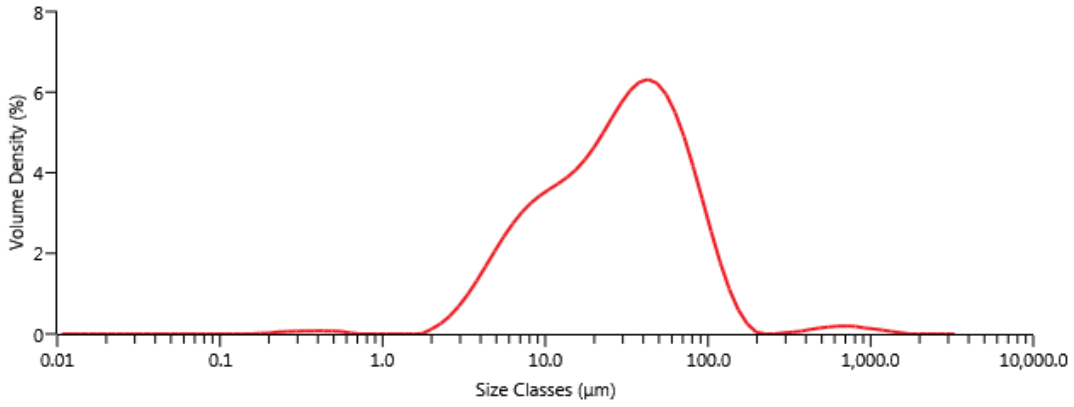

Figure 4.11 *Powder particle size distribution of spray dried lactase powder with outlet temperature 80 ℃.*

4.4 Conclusions

Based on this study, it was found that protein denaturation was closely related to the outlet air temperature during spray drying, but not to the inlet air temperature. With the outlet air temperature of spray drying kept constant and changing the inlet air temperature, no significant protein denaturation was observed. Conversely, with the inlet temperature constant, a higher degree of denaturation was observed at higher outlet temperature. Moisture content and water activity of the powder also decreased as outlet temperature decreased, same trends were also obtained for the productivity and drying rate. Among the three materials, lactase was the most sensitive to outlet temperature, followed by egg white protein; whey protein showed the least level of denaturation during spray drying.

In the next chapter, these three materials will be dried by a novel drying technique known as monodisperse spray drying. In contrast to conventional spray drying, the monodisperse drying involves a single stream of feed solution that breaks down into

droplets with unique size. Results of residual enzyme activity or residual undenatured protein in the dried powders will be compared between the two drying methods, and the feasibility of monodisperse drying as a potential optimized technique of spray drying will be evaluated.

Chapter 5 Investigation of operating parameters for monodisperse drying and their impact on protein denaturation

5.1 Introduction

Monodisperse drying is a novel technique allowing optimization of conventional spray drying. One defect of the conventional spray drying technique is that droplets with various sizes are produced in the atomization process, resulting in different drying experience of particles and bring about product overheating or incomplete drying. Monodisperse drying allows greater control of the droplet size and allows every particle to experience a similar temperature history to produce powders with uniform quality properties. This technology is based on inkjet printing. A continuous liquid jet is generated by a printing head with certain nozzle orifice diameter and broken into uniformly sized droplets. The stream of monodisperse droplets is then heated up in hot air with controllable temperature to dehydrate.

In this chapter, the same three materials (lactase, WPI and egg white) were dried by monodisperse drying. Heat denaturation, particle size and morphology of the products were investigated and evaluated. The effect of air temperature on protein denaturation is discussed. In addition, the design of the experiment, investigation of the process, development of the system and troubleshooting are also demonstrated.

5.2 Experimental set-up

The monodisperse drying system can be divided into two main parts. The first part involves the generation of monodisperse droplet stream from the feed solution; the

second part is drying and powder collection. The structure of the whole experimental system is shown in Figure 5.1. The schematic diagram and the make & manufacturer of the assembly parts of the monodisperse drying system refer to Chapter 3.

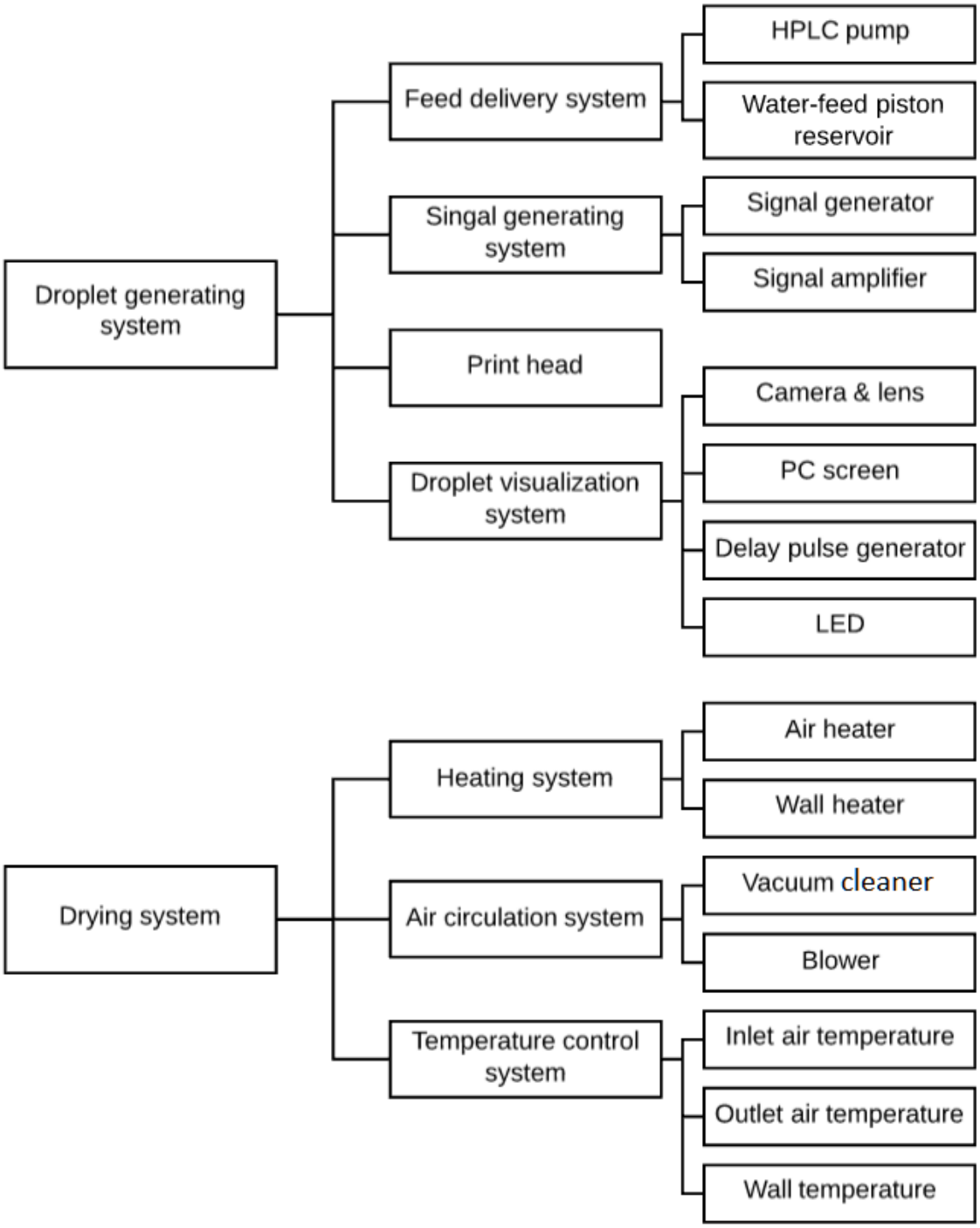

Figure 5.1 *Overall setup of the monodisperse drying system.*

5.2.1 Feed delivery and single droplet generation

The undisturbed and constant-rate fluid flow was achieved by an HPLC pump and a piston reservoir. Water was pumped through the HPLC pump to the water side of the reservoir, pushing the piston from the water side to the feed side and delivered the feed to the printing head. The liquid jet was broken down into single droplets by piezo actuation. The schematic principle of the actuation mechanism is shown in Figure 5.2. A piezo actuator, which is part of the print head assembly, is driven by a signal amplifier. The amplifier takes an analogue input signal from a signal generator, which provides a sinusoidal wave output with controllable amplitude and frequency. The input range of the amplifier is -2V to +12V, and the output range of it is -20V to +120V (10× amplification). Therefore, the amplitude of the signal generator was set to be 7V with a +1.5V offset. The frequency of the wave was adjusted prior to each experiment. Figure 5.3 reveals the images of devices for the droplet generating system.

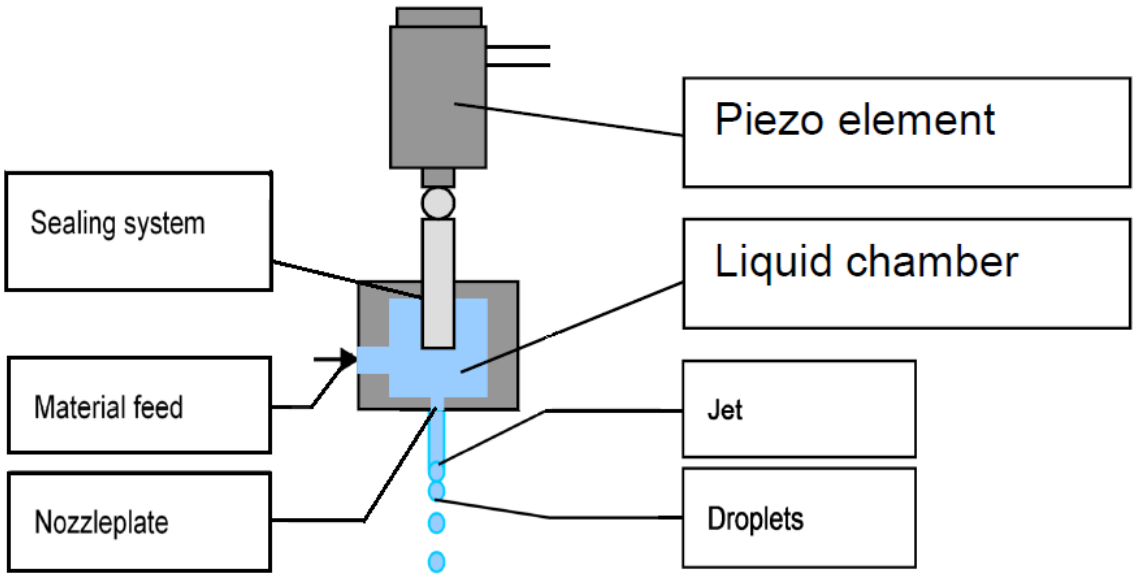

Figure 5.2 *Schematic principle of the actuation mechanism (modified from TNO, 2014).*

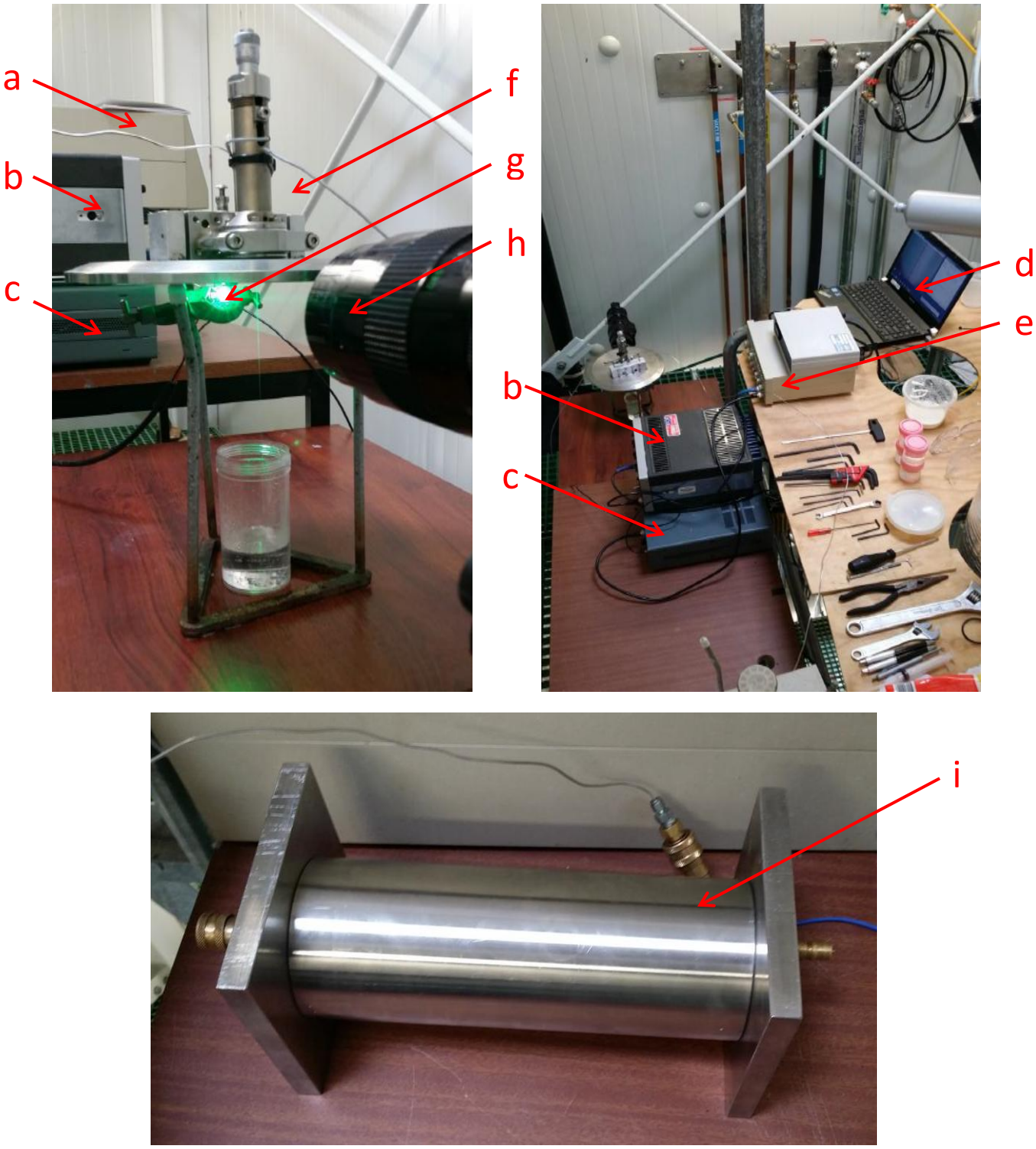

Figure 5.3 *Images of the droplet generating system*

(a: HPLC pump, b: amplifier, c: delay pulse generator, d: PC screen,

e: signal generator, f: print head, g: LED, h: camera & lens, i: piston reservoir).

5.2.2 Droplet visualization

To visualize the droplets, a stroboscopic light was triggered in the same frequency as that for the droplet generation as shown in Figure 5.4. A delay pulse generator was applied to achieve the goal. This unit takes the input from the signal generator and the output connects to the LED illumination. The shutter time of the camera is an order of magnitude lower than the generation rate of the droplets, therefore, it visualizes hundreds of droplets on top of each other. If the droplets are generated steadily, a sharp image will be observed; if the droplet generation is unstable, it will result in a blurry image. The droplet visualization system provides immediate feedback on the performance of the printing system and allows the operator to investigate the optimal settings of the printing operation.

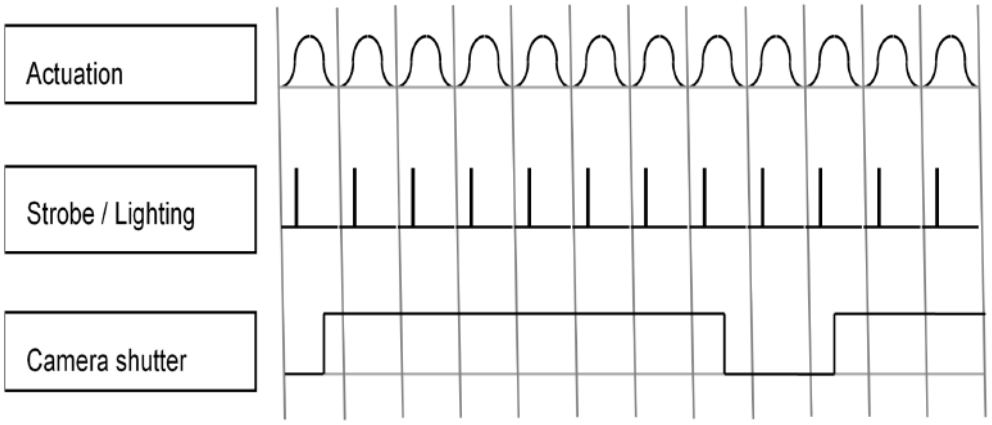

Figure 5.4 *Synchronisation of strobe with actuation mechanism (TNO, 2014).*

5.2.3 Feed preparation

The drying feed of lactase and WPI was prepared in 35% (w/w) total solid content as stated previously in Chapter 4. Changes were made when preparing the drying feed of egg white. 30% (w/w) of total solid content was applied instead of 35%, also reducing

the concentration of maltodextrin. This change is based on the difficulties of pumping the egg white feed solution with the previous concentration through the printing head.

To prevent blocking the nozzle, the feed solution was first pre-filtered through a sieve with selected opening size. The opening size of the sieve was determined based on the size of the nozzle orifice applied in the experiment. For the 80 μm nozzle, a 75 μm sieve was used; and for the 50 μm nozzle, a 45 μm sieve was used. In addition, inline filters were applied to prevent nozzle blockage.

5.2.4 Drying and temperature control

The inlet air temperature was fixed at 200 ℃ for the entire monodisperse drying experiments, whereas the outlet air temperature was controlled by altering the airflow of the vacuum cleaner and blower. Two wall heaters were also set to the specific temperature in advance of the drying experiment to heat up the stack wall and maintain the air temperature in the drying stack. It was hard to adjust the outlet temperature to a certain value and keep it constant within every individual experiment. Therefore, instead of certain outlet temperature values, different settings of airflow were used as the operating variables.

The air circulation of the whole system was driven by a forced draught blower at the top of the dryer, prior to the heater; and an induced draught vacuum cleaner at the bottom of the dryer, connected to the top of the cyclone, as shown in Figure 3.3. The options for adjusting the airflow include turning on or off the vacuum cleaner; and switching between Turbo (high airflow) and Eco (low airflow) mode of the blower. The airflow can also be adjusted by the valves at the exit of the blower and on the by-pass of the cyclone. A flow sensor was installed on the way between the blower pipe and the

heater. It will cut off the heater if the airflow is too low to protect the heater from overheating.

In the design of this experiment, the blower was kept on the low airflow level (Eco mode), and changes were made on whether to turn on the vacuum cleaner. Two temperature sensors were used to monitor the air temperature at the middle and bottom of the tower. Another temperature sensor was placed at the exit of the air heater for indicating the change of air temperature coming straight out from the heater when the airflow altered. The final operating conditions were determined based on a factorial design which will be stated in the next section.

5.2.5 Cleaning of the system

In order to remove proteins that stick to the inside of the stainless steel tubes, 10% NaOH solution was used to clean the piping system from the reservoir to the printing head (TNO, 2014). The whole printing system was first flushed with water sufficiently until clear water came out from the nozzle. Subsequently, the feed side of the piston reservoir was filled with 10% NaOH solution and the system was then flushed with NaOH for a sufficient period of time. The NaOH solution was left in the pipes for overnight and then flushed out thoroughly with water.

In addition, the nozzle was demounted from the printing head and cleaned with an ultrasonic device for at least 30 minutes to clear up any potential inclusion that may block the nozzle in the future experiment. Besides, the bottom parts of the dryer were demounted and cleaned manually with soapy water and rinsed with hot water. The column drying stack can be cleaned by a high-pressure cleaner if necessary.

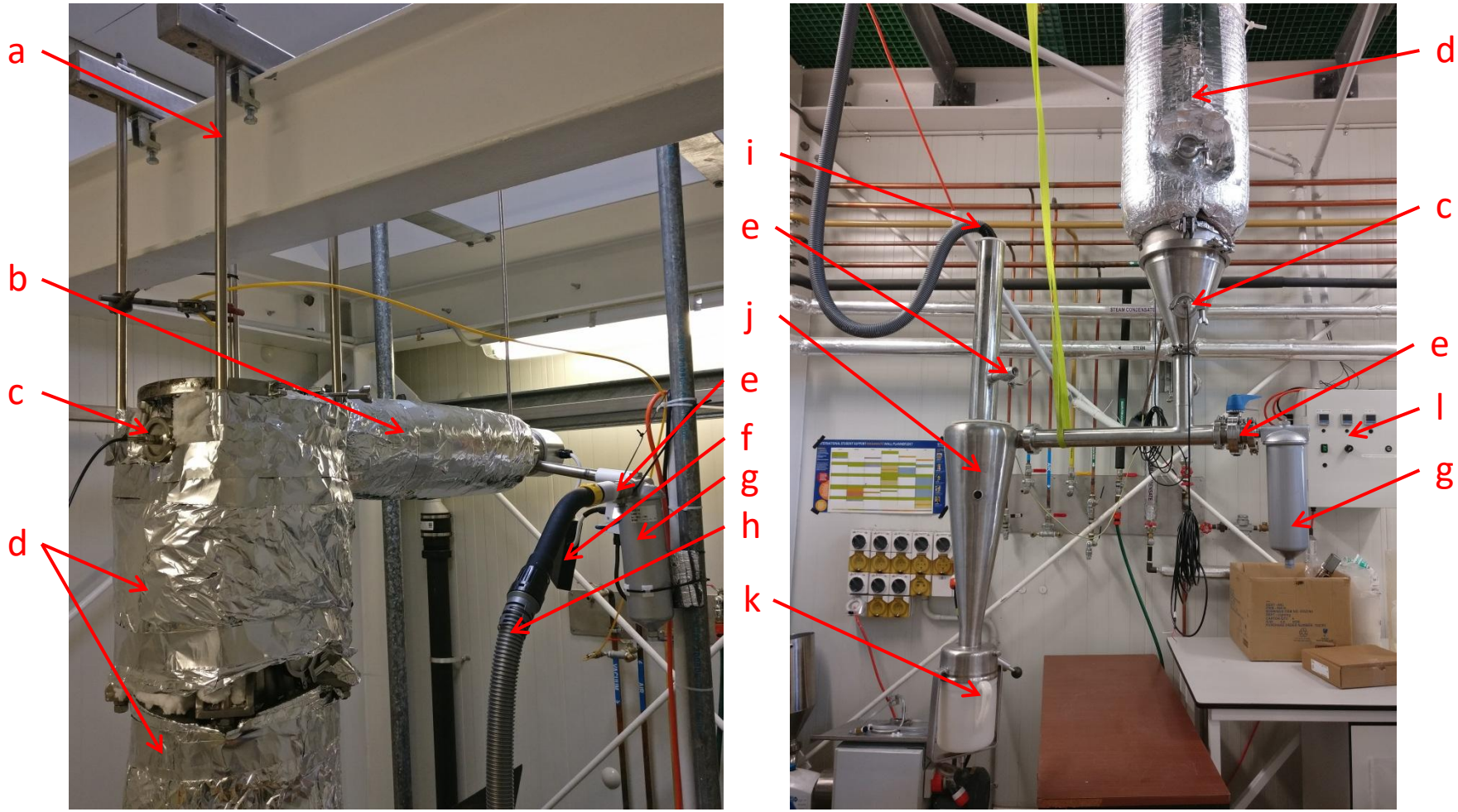

Figure 5.5 *Images of the heating and drying system*

(a: mounting rack, b: inlet air heater, c: RTDs, d: insulations, e: valves, f: air heater switch, g: air filters, h: pipe connected to the blower, i: pipe connected to the vacuum cleaner, j: cyclone, k: collecting jar, l: temperature control panel).

5.3 Operating parameters and factorial design

5.3.1 Factorial design

In order to identify the most important variables of the experiment, a preliminary 2^3 factorial design with one block was designed and conducted using lactase as the drying feed material. The factorial design was generated and analysed by Minitab software. Three factors (A, B and C) were selected to be the feed flow rate, the air flow of the blower and whether to turn on the vacuum cleaner. Each of the factors had two levels as shown in Table 5.1. This design included $2^3 \times ½ = 4$ different experimental conditions and each condition was conducted in duplicates. The full experimental design and results are shown in Table 5.2, in which the response (Y) is the residue lactase activity in percentage.

Table 5.1 *½ Fractional Factorial Design test factors and levels.*

	Factors	High level (+)	Low level (-)
A	Feed flow rate (ml/min)	3.5	3
B	Blower air flow	Low (Eco mode)	High (Turbo mode)
C	Vacuum cleaner	On	Off

Table 5.2 *Full program and results of ½ Fractional Factorial Design.*

Run order	A Flow rate	B Blower air flow	C Vacuum cleaner	Y % Lactase activity
1	-1	-1	1	2.62
2	1	-1	-1	14.38
3	-1	1	-1	14.76
4	1	1	1	14.38
5	-1	-1	1	8.72
6	1	-1	-1	12.78
7	-1	1	-1	12.15
8	1	1	1	8.41

Results of the factorial design indicate that the effect of factor C on enzyme activity is more prominent than factor A and B as shown in Figure 5.6a. Therefore, factor C is selected to be one of the main variables in the subsequent experiment. The interaction plot in Figure 5.6b shows that when factor A or B was on the low level, changing of factor C will result in a larger extent of difference in the response. However, considering the influence of air flow on heater capacity, the lower airflow of the blower will be used in the subsequent experiment.

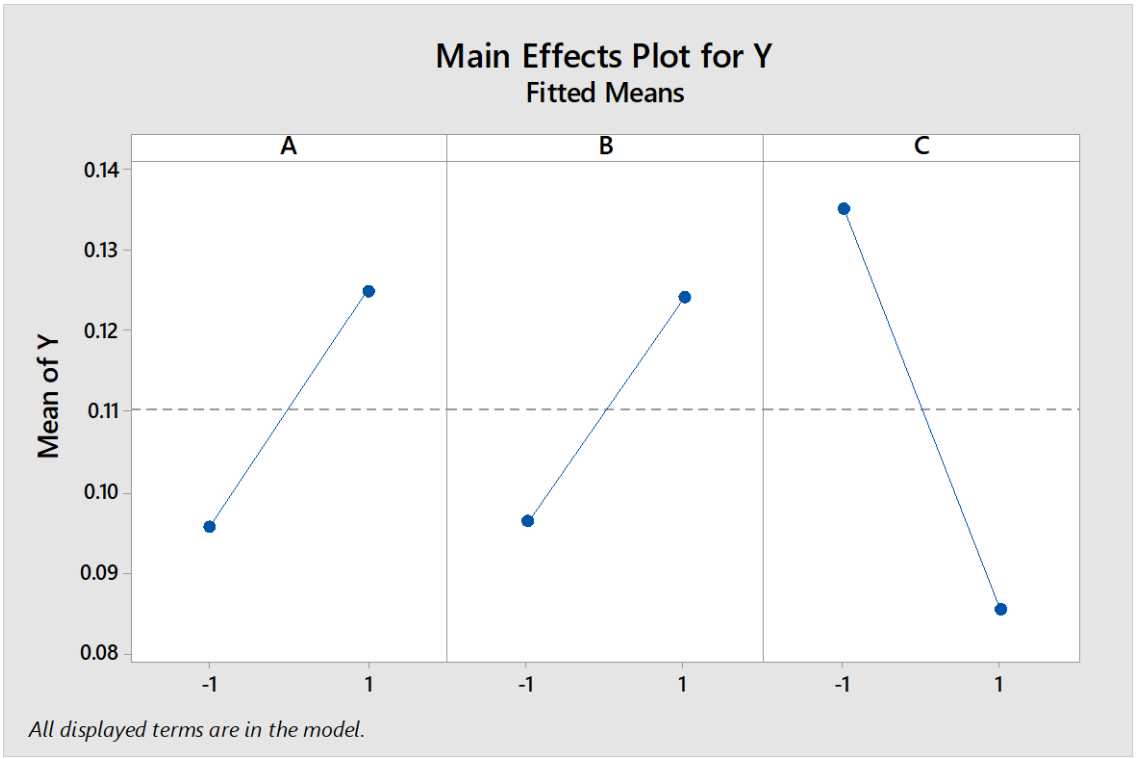

(a)

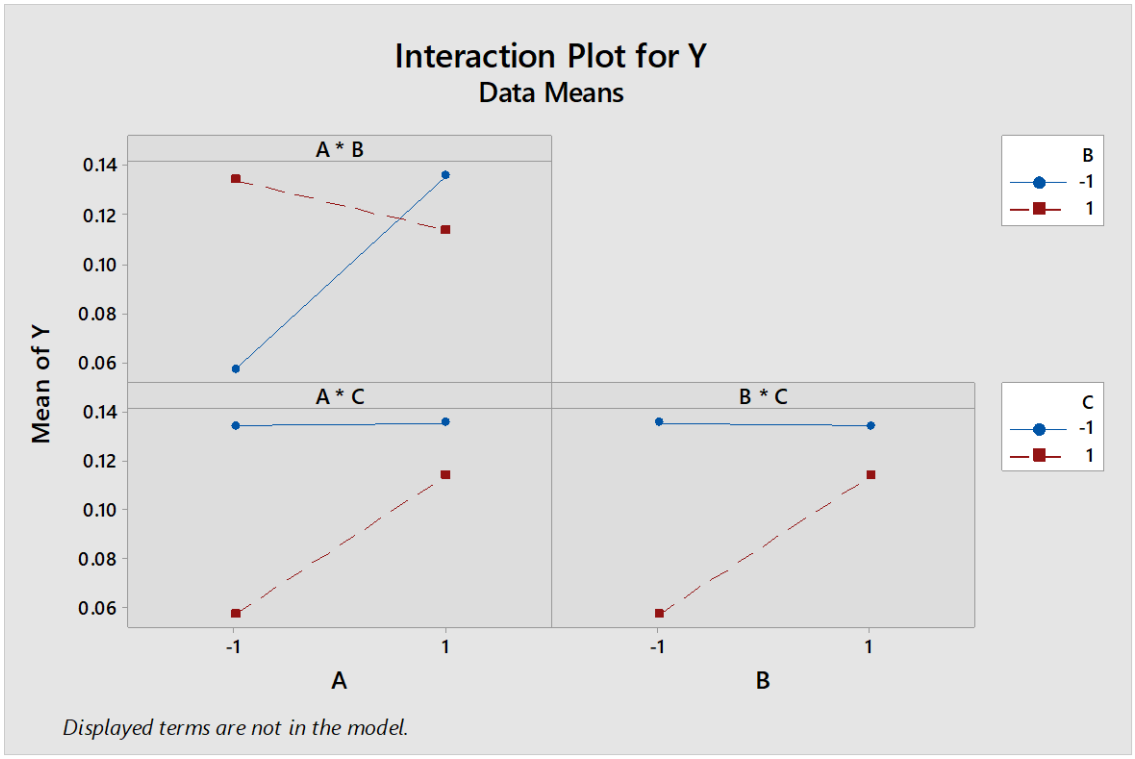

(b)

Figure 5.6 *Analysis results for factorial design from Minitab*

5.3.2 Experimental parameters establishment

Based on the discussion above, the final operating setting is to switch the vacuum cleaner between “off” and “on”, at the mean time, kept the blower at the low airflow level and left the by-pass of the cyclone opened. In the following description, setting 1 (low air flow) represents turning off the vacuum cleaner acting as the exhaust fan and setting 2 (high air flow) represents turning on the vacuum cleaner. Three repeated drying experiments were conducted with each setting for each material. Therefore, six groups of data were obtained for each material. The air temperatures at the middle and the bottom of the tower were recorded in each experiment, as well as the actual wall temperatures and other relevant values.

The operating parameters regarding to the printing system were slightly varied for different materials. However, once the parameters were established, they were held constant for the entire 6 experiments for a certain material. The 80 μm nozzle and a flow rate of 3 ml/min were applied when conducting lactase experiments. This was also the primary setup of the experiment. But for WPI and egg white experiments, the 50 μm nozzle and 4 ml/min flow rate were used, in consideration of the pumpability of these two feed solution. The reasons for choosing these parameters will be stated in the discussion section, along with the impacts of nozzle orifice size, feed flow rate and the properties of feed solution on single droplet generation.

5.4 Development of the system

Since the monodisperse drying technique is a relatively new method, one of the greatest challenges for this study is to make sure the system is working in the desired order. In fact, investigation of the operating conditions and development of the system

in order to achieve steady powder production is one of the main purpose of this study apart from the drying experiment and results themselves. The following two sections introduce the improvements and solutions made to the system involving both technical and operational aspects on account of the problems occurred in the experiment.

5.4.1 Heating system

Improvements were made to the heating system: a previous heating element which causing tripping operation was replaced by a new more robust heating element. The previous heating system consisted of two air heaters (750 W and 1200 W) as shown in Figure 5.7, the lower power one acted as a pre-heater, and the higher power one acted as the main heater. The latter was the one that caused tripping problem due to overheating. This heater was designed to heat up the air from a narrow, enclosed heated surface with the peak operating temperature of 430 ℃. However, this design results in a small surface area and resisted airflow coming through the heater, greatly increasing the risk of overheating. In addition, the air was pre-heated before entering the main heater hence already had a relatively high temperature. It can be observed from Figure 5.6 that colour of the stainless steel surface on both sides of the main heater turned into dark purple and dark blue. By searching the colour-temperature chart of stainless steel, it is found that these colour changes indicate that the surface temperature at the entrance side of the heater reached approximately 380-420 ℃ and at the exit side it reached up to 540 ℃ (BSSA, 2017). Therefore, tripping and overheating is the result of several factors including high pre-heated temperature, restricted air flow, low surface area and the robustness of the heating element itself. In addition, the insulation around the heater will also increase the working load of the heater that resulting in overheating.

In order to attain reliable heating, a new heater with a finned element was used as a replacement. The new heater can handle operating temperature up to 800 ℃ and will heat up the air to the desired temperature in a short period of time with no need for preheating. It is a more robust element with a much larger surface area and can be operated under a low airflow condition, allowing for a maximum amount of heat from the heating element. No more tripping happens after the new heating element was installed and the efficiency of the experiment was greatly enhanced due to rapid heat disbursement.

Figure 5.7 *Images of the previous heating system (a: main heater, b: pre-heater).*

5.4.2 Air flow pattern

In the previous design, the airflow of the system was driven only by a vacuum cleaner connected to the cyclone. The vacuum cleaner acted as an induced draught fan in the system, drawing the air through the heater, the chamber and the cyclone then discharging the spent air to atmosphere. The air flow rate of the vacuum cleaner is not adjustable. The only way to control its airflow is to leak some air from a valve set in between the cyclone and the vacuum cleaner. However, the extent of the adjustment is very limited. There was also evidence of the system drawing in unheated air through leaks at the top of the tower, which also limits the air flow through the air heater.

Improvements were made by introducing an air blower to the system to act as a forced draught fan. In the general design of spray dryer, if the plant is in a large scale, two fans are usually applied to allow a more balanced system. In the design of monodisperse dryer, since the drying chamber is tall and consist of several cylinder stack walls joining together, an exhaust fan and a blower are the preference to balance the air circulation of the entire system. The other advantages of having a blower include balancing the pressure inside the drying chamber, preventing the cold air from leaking in and bringing erratic factors to the system. The blower with multi-regulable levels also introduces more options for adjusting the airflow of the system, which can be useful in controlling the outlet air temperature.

5.4.3 Printing head setup

The printing head was fixed on a disc placed on the top of the drying chamber as shown in Figure 5.8 (upper left) in the original experimental setup. However, burnt product was often found in the nozzle area and sometimes even blocked the nozzle. This

is due to this area being too close to the exit of the air heater, therefore, exposed to extremely high temperature. The hot air coming from the heater can reach the temperature up to 260-320 ℃. A possible solution is to set the printing head apart from the hot area. This is achieved by lifting the printing head up from the metal disc by a transparent cylinder. A customized plastic cylinder with silicon seal on both sides was applied in this study. The new setup of the device can be seen in Figure 5.8 (right). The printing head was held by an adjustable retaining clamp. The printing head, the extension cylinder and the metal disc must be attached tightly without any air leakage otherwise the fluid stream will be affected by the unstable air pressure. A stream of cold compressed air was introduced to cool down the surface of the cylinder, preventing it from overheating. This device also allows the operator to visually adjust the angle of the jet, ensuring it vertically entering the drying tower and reducing its chance of touching the column wall. A straight jet can be observed from Figure 5.8 (lower left).

Figure 5.8 *Images of the previous and modified nozzle setup.*

5.5 Trouble-shooting

The following section lists several common problems encountered when operating the monodisperse drying device, including their probable cause and solution.

5.5.1 Wet and sticky product formation

The genreation of sticky products was one of the greatest problems encountered at the early stage of the experiment. Possible reasons for this problem include low air

temperature, high moisture content of the droplet and re-humidification from moisture condensation.

Water evaporation in the drying droplet is the result of a series of heat and mass transfer processes. It is therefore influenced by the temperature difference and the moisture content of the droplet. The temperature difference between the droplet and the drying medium acts as the driving force of heat transfer. Therefore, the low air temperature will result in insufficient drying and wet product. This problem was overcome by improving the heating system. Adequate heating capacity was insured since the new heater came into service. On the other hand, high moisture content droplet requires higher heat and mass transfer rate. Since the moisture content of the drying feed is constant, the moisture content of a droplet is determined by the size of the droplet. Hence, the larger the droplet, the higher moisture it carries, the more heating is required for water evaporation. The factors affecting droplet size, including nozzle orifice size, feed flow rate and frequency of the signal generator, will be discussed in subsequent sections.

The wet powder may be also caused by water condensation that happens in the downstream of the system. In this monodisperse dryer design, the air stream acts as both drying media and moisture carrier moving all the way along with the product. Condensation may occur on the surface where the temperature is low. The adequate solution is to apply thermal insulation on those surfaces to maintain their temperature.

Apart from those factors stated above, another reason that brings about wet product is the generation of big liquid drips at the beginning of the experiment. Because of the increase of feed flow rate in the HPLC pump and the pressure built-up in the reservoir is a gradual process, it is hard to obtain a jet immediately at the beginning of feed delivery. Therefore, the formation of liquid drops is an inevitable intermediate process. This

problem was uncontrollable when the former printing head setup was used. The drips were too big to be dried thoroughly, thus they will adhere to the bottom of the T-pipe and stick with the subsequent powder to form a honey-like agglomeration. Nevertheless, this problem can be eliminated by applying the new printing head setup introduced in 5.4.3. With the modified setup, the jet can be first stabilized before entering the drying chamber to prevent the "honey" formation.

5.5.2 Block of the nozzle

Nozzle blockage is another common fault of the experiment. It is usually caused by impurities in the feed or burning of the nozzle and can be prevented by pre-filtration of the feed solution and decoupling of the nozzle and hot zone as stated previously. In addition, a filter (20 μm) designed to fit in the flow entry of the printing head was also applied to stop impurity from entering the printing head. It is also vital that the nozzle being cleaned properly and thoroughly after every experiment to make sure the orifice is unobstructed for the next experiment.

In the case that blockage does happen during the experiment, flush the nozzle with water at high flow rate at first. If the block remains, dismount the printing head and the nozzle plate, check the pumpability of the piping system. If the block occurs in the piping system, flush the system with 10% NaOH and then thoroughly with water. If the block is caused by the nozzle, clean the nozzle with ultra-sonic as stated previously.

5.5.3 Low powder yield

Low powder yield is usually relevant to wet product formation as discussed in the previous section. Apart from that, it may also relate to the air flow pattern in the drying chamber. It is found that with the vacuum cleaner off, the powder accumulation is much

slower in comparison with when the vacuum is on. One possible reason is that the airflow of the blower alone is much lower than that of the blower plus vacuum cleaner operating together. Therefore, the airflow with the blower alone may not be sufficient to push all of the powder into the collection jar. Some of the powder may stick onto the surface of the stack wall or the pipes. Furthermore, the air flow from the blower can push a portion of the powder to the opposite end of the T-shape pipe rather than to the cyclone side, since the pressure is positive throughout the assembly. Applying compressed air gun regularly from the opposite end can help to collect this powder but is not efficient. Suggestions for airflow pattern of the system will be discussed later.

5.6 Results and Discussion

5.6.1 Residence time

The residence time of monodisperse drying was estimated based on the volume of chamber and the air flow rate. The air velocity was measured by an anemometer at different positions of the drying chamber. The air flow rate was calculated by multiplying air velocity by area. The average air flow rates for the two settings are 31 m^3/h with the vacuum cleaner off (low air flow) and 64 m^3/h with the vacuum cleaner on (high air flow) respectively. The volume of the drying chamber is 0.3768 m^3. Therefore, the residence time for both settings is estimated to be 45s (low air flow) and 21s (high air flow).

5.6.2 Factors affecting protein denaturation in monodisperse drying

Table 5.3 summarizes the values of wall temperature and air temperature for each monodisperse drying experiment. These data reveal an overall image of the temperature

distribution in the drying tower and play a vital role in the determination of protein denaturation during the drying process. It can be observed from the table that the air temperature in the middle of the drying chamber (abbreviated as middle air temperature in the following content) has the most obvious differences between the two settings. With the vacuum cleaner turned on, the middle air temperature values are generally higher than that when the vacuum cleaner is off. An overall increase in the bottom air temperature of the drying stack is also observed but with lower range compared to the middle air temperature. The bottom wall temperatures keep approximately consistent as they were regulated by the panel-mounted temperature controller. However, the top wall temperatures are substantially higher than its setpoint value, indicating some gain of heat from the heated air in the chamber. The temperature of the air coming out from the heater decreases when the vacuum cleaner switched on due to increased airflow and always higher than the inlet air temperature showing on the control panel, whereas the inlet air temperature read on the panel (measured on the opposite side of the heater) always keeps constant at 200 ℃ under temperature control.

Table 5.3 *Recording of temperature values during monodisperse drying.*

Settings	**Temperature (℃)**					**% Enzyme activity / % Non-denatured protein**
	Wall Top Half	Wall Bottom Half	Air Middle	Air Bottom	Air Heater Exit	
			Lactase			
Low air flow	120-129	99-103	91-96	70-73	265-270	19.81%
	122-126	105	90-100	63-67	330	16.15%
	129-131	98-107	98-102	70-73	263-274	14.76%
High air flow	123-128	103-107	91-105	67-68	260-280	13.29%
	130	103	106-108	68-70	270-274	8.72%
	112-114	102-103	112-114	74-76	263	2.52%
			WPI			
Low air flow	113-115	106-108	93-96	63-65	290-306	68.15%
	121-126	103-108	97-102	64-67	341	45.12%
	126-129	103-107	100-108	65-68	340	42.28%
High air flow	122-128	102-107	102-112	76-77	285	28.09%
	119-127	102-107	108-116	75-80	220-240	27.84%
	126-131	102-107	114-117	70-77	288-291	24.30%
			Egg White			
Low air flow	120	102	98-100	64	286-298	62.68%
	112-113	102-108	99-106	63-65	330-335	46.68%
	109-112	103-104	106-108	63-64	320-330	38.36%
High air flow	114-118	104-108	107-112	67-69	260	31.35%
	117-121	103-106	109-113	68-70	265-267	26.97%
	114-121	107-109	128-130	80-82	290	16.85%

Figure 5.9, 5.10 and 5.11 present the relationship between the middle air temperature and the % activity of monodisperse dried lactase, or % non-denatured values of WPI and egg white respectively. It can be seen from the figures that the % activity / % non-denatured values of the powder obtained from setting 2 (high air flow) are generally lower than that from setting 1 (low air flow). The differences are statistically significant ($P < 0.01$) for all of the three materials according to ANOVA results. In addition, the %

activity / % non-denatured values decreases as the middle air temperature increases. The extent of decrease in these values is determined by the range of middle air temperature. Greatest range of temperature change is observed in egg white experiment from 100 to 130 ℃. Therefore, largest extent of % non-denatured value change is obtained from 67% to 12%. The % non-denatured value of WPI decreases from 68% to 22% when the middle air temperature increases from 94 ℃ to 116 ℃. Lactase has the narrowest range of % activity change from 21% to 2% when the middle air temperature changes from 93 to 113 ℃. The low initial point indicates that greater extent of activity loss occurred during the drying process for lactase. Therefore, lactase is more sensitive to drying temperature compared to WPI and egg white.

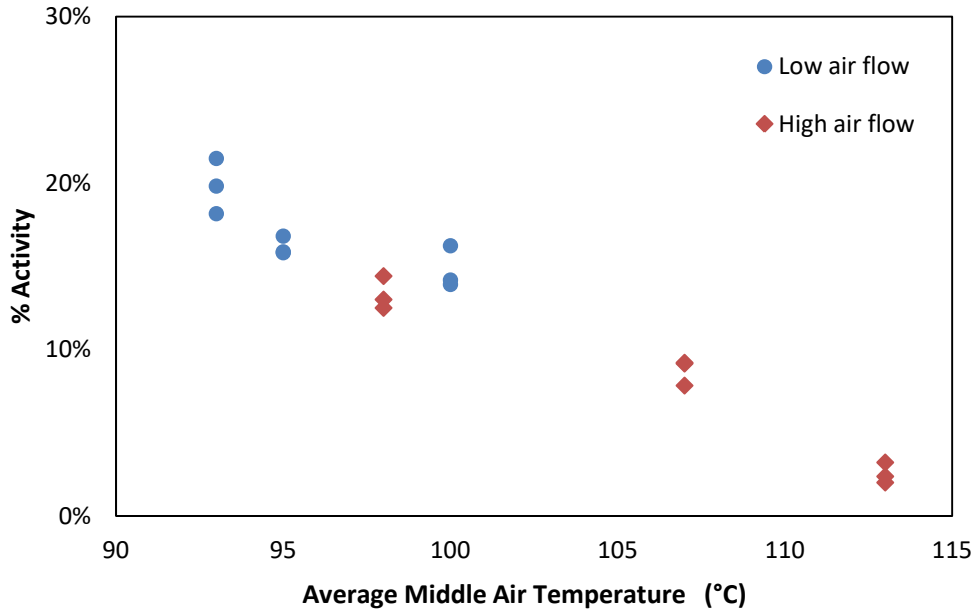

Figure 5.9 *Effect of middle air temperature on the percentage enzyme activity of monodisperse dried lactase products (setting 1: low air flow; setting 2: high air flow).*

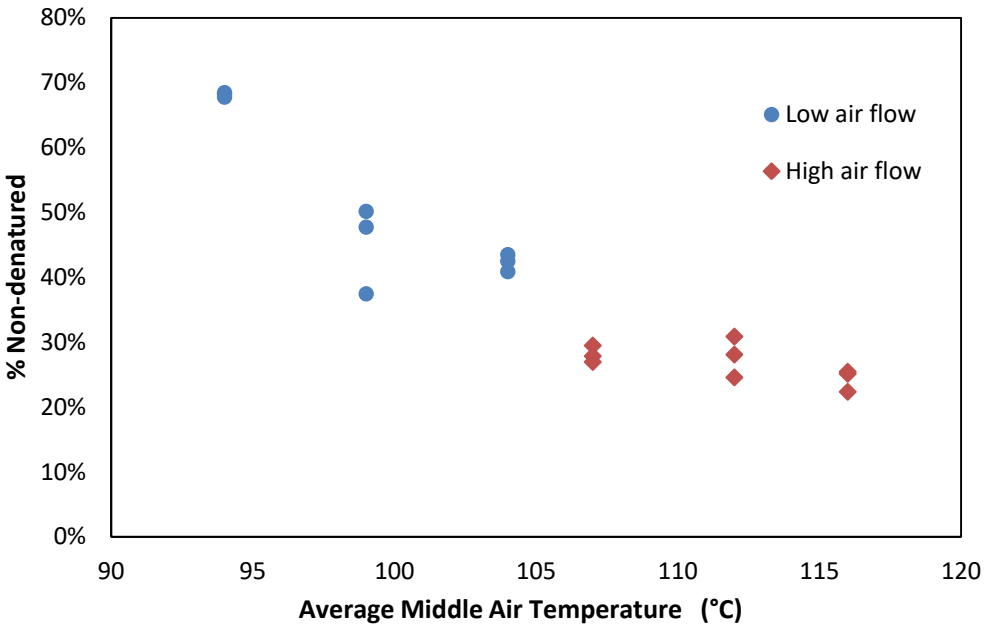

Figure 5.10 *Effect of middle air temperature on the percentage non-denatured value of monodisperse dried WPI products (setting 1: low air flow; setting 2: high air flow).*

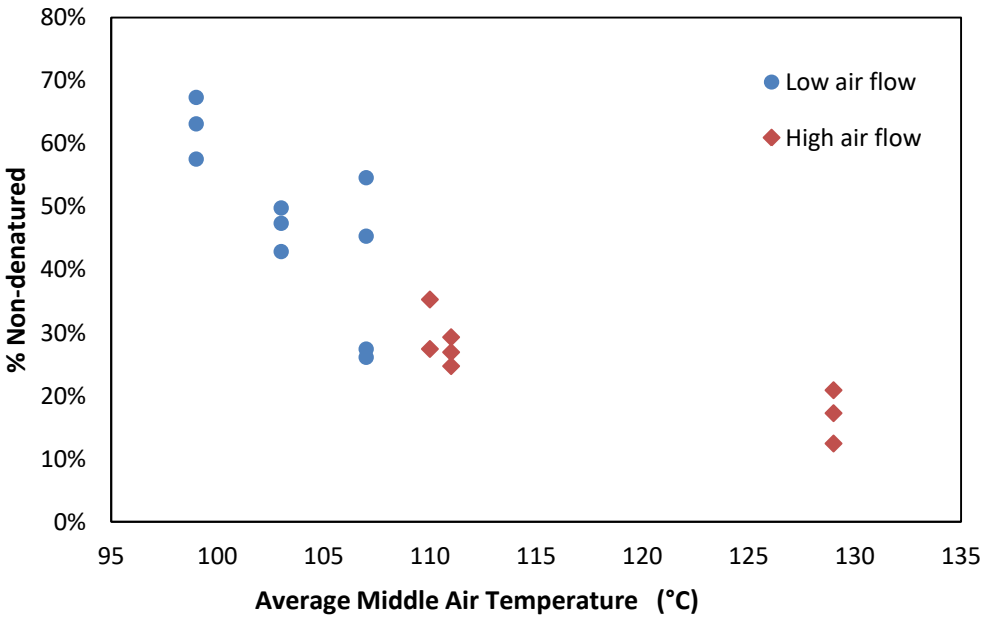

Figure 5.11 *Effect of middle air temperature on the percentage non-denatured value of monodisperse dried egg white products (setting 1: low air flow; setting 2: high air flow).*

The air temperature inside the drying tower is affected by the airflow that controlled by the vacuum cleaner and the blower. When the vacuum cleaner was off, the air flow rate inside the drying tower was relatively low and the residence time was high. With turning on the vacuum cleaner, the air flow rate increased, resulting in decreased air temperature at the exit of the heater (not the final inlet air temperature). However, as the inlet air temperature was automatically controlled by the PID controller, continuous heating will be applied to the system to offset the influence of increasing airflow and to keep the panel inlet temperature at a constant level 200 ℃. On the other hand, since the vacuum cleaner has the higher air flow rate in comparison with the blower, more hot air was driven from the upper area of the tower to the lower site due to the negative pressure. As a result, the air temperature at the middle and bottom of the tower increased when turning on the vacuum cleaner.

The tendency that the protein denaturation level of the dried product decreases as the air temperature increases is consistent with the findings from spray drying experiment that stated previously in Chapter 4. The level of residual undenatured proteins in the monodisperse dried product is determined by the entire air temperature distribution inside the drying tower. The reason for selecting middle air temperature as the abscissa is that both middle and bottom air temperature change with the same trend but the middle air temperature has more distinct variation when switching between the two settings. Precise outlet air temperature control of the system is a great challenge in this experiment. As a result, an interval of air temperature was obtained instead of a specific temperature point. Recommendations regarding narrow down this temperature interval will be included in the next chapter.

Residence time is another potential factor that may affect the degree of protein denaturation in the dried product. In this experiment, setting 1 (low air flow) has longer residence time, lower air temperature but lower degree of protein denaturation compare to setting 2 (high air flow). The results indicate that the effect of residence time is much smaller than that of air temperature in monodisperse drying. More denaturation occurred when the droplets were exposed to high temperature for a shorter time than to low temperature for a longer time.

The comparison between spray drying and monodisperse drying techniques will be discussed in the next chapter.

5.6.3 Arrhenius plot and activation energy

Arrhenius plots for the three materials Figure 5.12, 5.13 and 5.14 were created based on the reaction rate kinetics as stated in the previous chapter. The linear regression and Analysis of Covariance (ANCOVA) were analysed by Minitab software. It is noteworthy that a change in temperature dependence can be observed for WPI and egg white when the air flow is at the low level (setting 1). Similar tendencies were reported in the studies of Anema and McKenna (1996); Dannenberg and Kessler (1988) and Hillier and Lyster (1979). Different reaction kinetic values and thermodynamic parameters are given by protein denaturation reactions and subsequent aggregation reactions, which is the reason for the change of temperature dependence in Arrhenius plots of protein denaturation. At the low temperature range, protein unfolding acts as the rate-determining process, resulting in higher E_a values; and at high temperature range, aggregation process acts as the rate determining process, resulting in lower E_a values (Anema & McKenna, 1996).

ANCOVA results indicate that the difference of regression slopes between the two settings for lactase is statistically insignificant ($P > 0.05$). In addition, the difference of regression slopes between setting 1 at high temperature range and setting two is insignificant ($P > 0.05$). The integrated slopes were calculated by the software at the temperature ranges where the differences between slopes are insignificant. Corresponding E_a values were then calculated and shown in Table 5.4 on the basis of the Arrhenius Equation as described in Chapter 4.

The trend of slope in the Arrhenius plots is generally consistent with the expectation. However, the goodness-of-fit for some of the regression models is not satisfactory. The fit of model is limited by the number of data points. The more data points present, the closer the predicted model fits the actual model. In this experiment, only three sets of data were measured for each setting, the change in a single data point may bring about significant change in the linear regression model. Therefore, there is a greater chance to have a large random error. Furthermore, the actual point when the change in temperature dependence occurs cannot be accurately determined with only three temperature points. To achieve the comprehensive image of Arrhenius plots and improve the fit of regression models, more repeat experiments are suggested in the design of the further experimental plan.

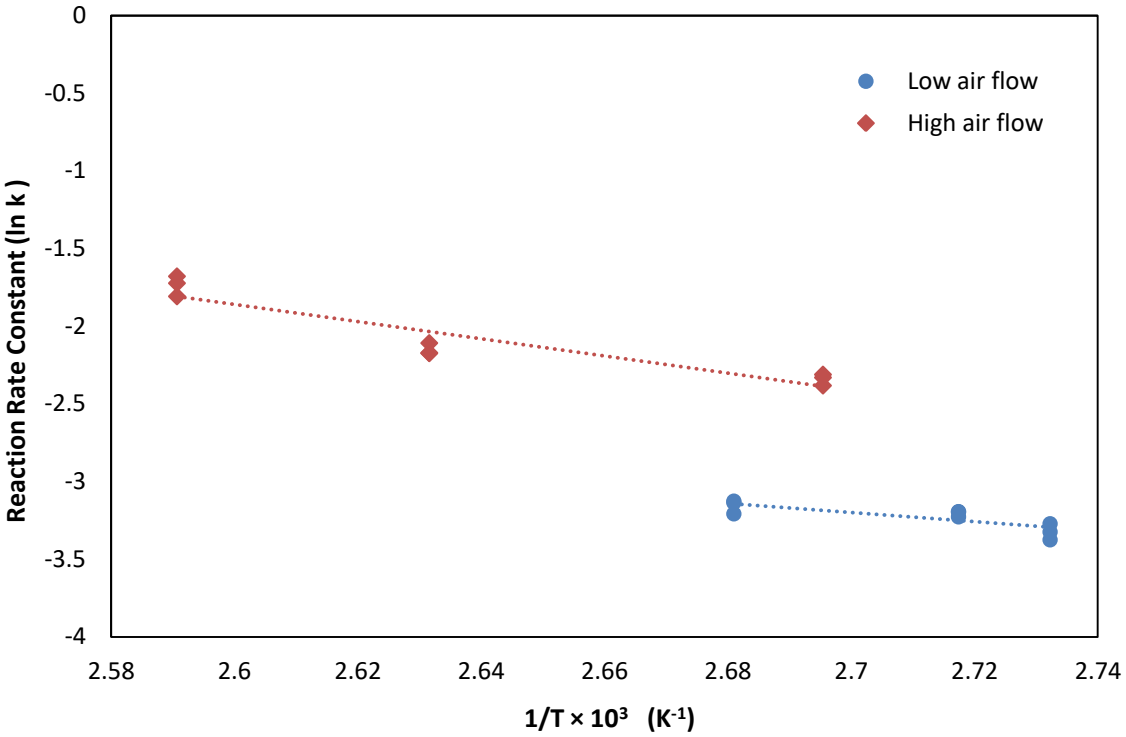

Figure 5.12 *Arrhenius plot for monodisperse dried lactase: ln k against 1/T.*

Regression model: y = -2.90x + 4.62, R^2= 0.65 (Setting 1: low air flow, 93-100 ℃);

y = -5.53x + 12.51, R^2= 0.87 (Setting 2: high air flow, 98-113 ℃).

Integrated slope = -5.002, SE = 0.617.

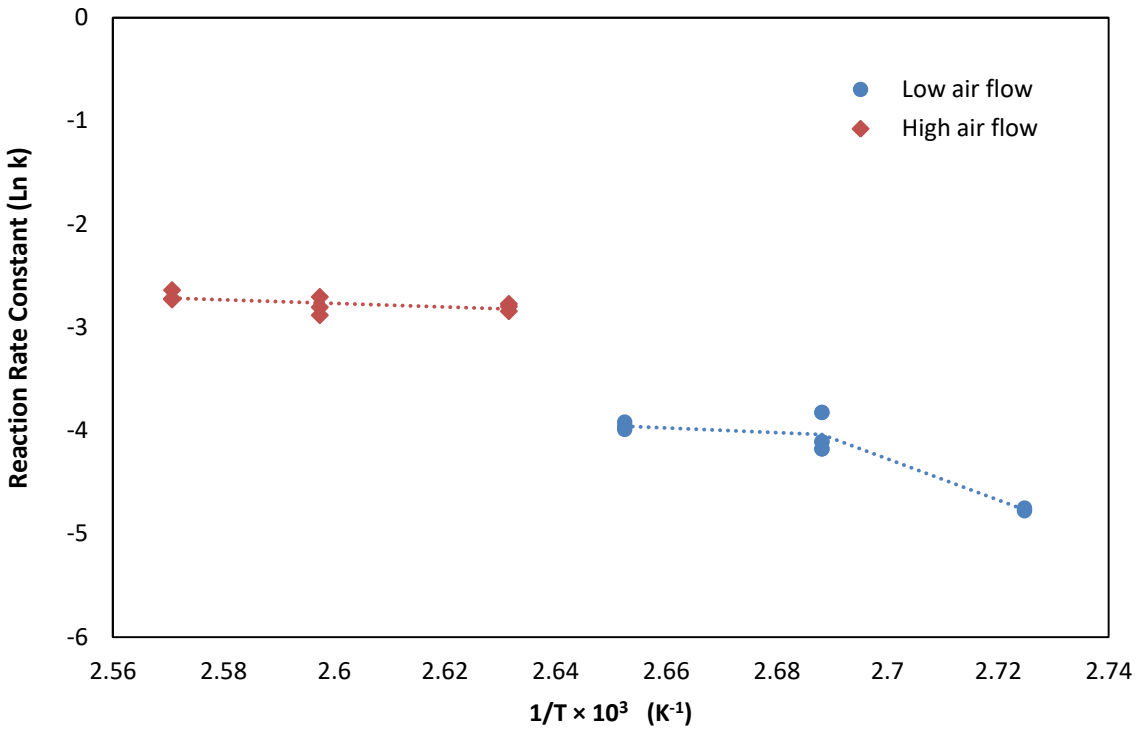

Figure 5.13 *Arrhenius plot for monodisperse dried WPI: ln k against 1/T.*

Regression model: y = -19.89x + 49.43, R ²= 0.92 (Setting 1: low air flow, 94-99 ℃);

y = -2.25x + 2.02, R ²= 0.12 (Setting 1: low air flow, 99-104 ℃);

y = -1.7071x + 1.6713, R ²= 0.36 (Setting 2: high air flow, 107-116 ℃).

Integrated slope for high temperature range = -1.85, SE = 1.06.

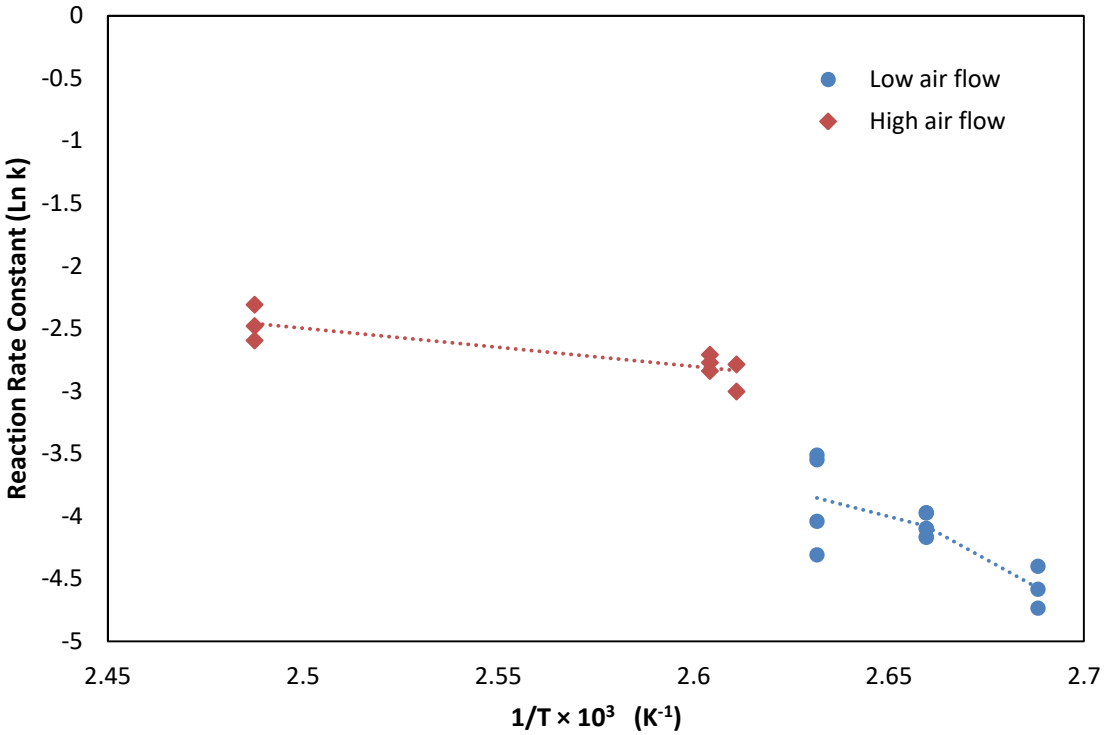

Figure 5.14 *Arrhenius plot for monodisperse dried egg white: ln k against 1/T. Regression model: y = -17.25x + 41.80, R ²= 0.83 (Setting 1: low air flow, 93-103 ℃); y = -8.11x + 17.48, R ²= 0.16 (Setting 1: low air flow, 103-107 ℃); y = -3.05x + 5.13, R ²= 0.74 (Setting 2: high air flow, 110-129 ℃). Integrated slope for high temperature range = -3.29, SE = 1.32.*

Table 5.4 *Summary of activation energy with different temperature ranges*

Materials	*E_a (kJ/mol)*	*Temperature (℃)*
Lactase	41.6	93-113
WPI	165.4	94-99
	15.4	99-116
Egg white	143.4	93-103
	27.4	103-129

5.6.4 Impacts of nozzle orifice size, feed viscosity, feed flow rate and frequency on droplet formation

The size of the monodisperse droplets is an important parameter in the determination of particle size and the properties of dried products. The size of droplets was adjusted prior to drying experiment and is influenced by the nozzle orifice size, the frequency of signal generator, the feed flow rate and the feed viscosity. To prevent the droplet from joining each other, the distance between them should be at least twice the diameter of the droplets (TNO, 2014).

Droplet diameter is primarily determined by the size of the orifice. Droplet diameter is generally 2 to 3 times of the nozzle orifice diameter as stated by TNO (2014). The selection of orifice size should take the liquid properties (e.g. viscosity) into consideration. Droplet formation is governed by a number of forces including gravitational force, inertial force, surface tension force, and viscous force (Wu et al., 2011). When the liquid feed has a high viscosity, using a nozzle orifice with a large diameter and low flow velocity will result in the formation of liquid dripping instead of liquid jet due to the governance of gravitational force and surface tension force (Liu, 1999; Wu et al., 2007). Therefore, for a viscous liquid, smaller nozzle orifice and high flow velocity should be applied. The effects of feed flow rate and viscosity on droplet formation will be discussed later.

Figure 5.15 presents the influence of disturbance frequency on droplet size. As it can be observed from the figure, high frequency produces droplets with smaller size and smaller distance in between the droplets when feed flow rate is the same. This finding is consistent with the results from TNO (2014) and Wu et al. (2011). It was also found that when the frequency is too high or too low, the droplet breaking-up process is irregular.

Frequency between 8 and 14 kHz is a proper range to acquire well separated and regular droplets for the rheology of the solution under investigation.

Figure 5.16 shows the relationship between feed flow rate and droplet size. It can be seen from the figure that at the same frequency, the space between droplets becomes wider as feed flow rate increases, at the meantime the droplet size slightly increases. The reason can be explained as that when the jet velocity increases, the surface tension force is augmented and produces greater attraction between the droplets that makes them join each other. Therefore, larger breakup force is required to break them up (Liu, 1999).

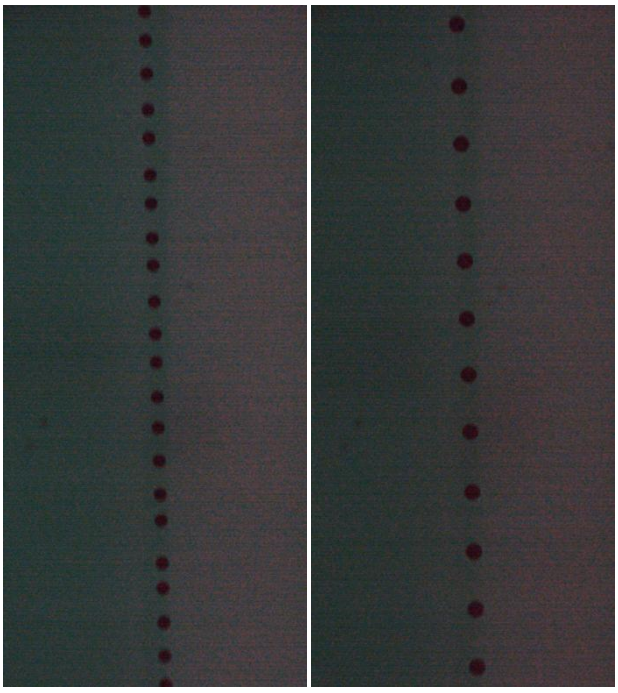

Figure 5.15 *Effect of frequency on droplet size. Left: 13.2 kHz, Right: 12.8 kHz (Feed: lactase with 3 ml/min flow rate).*

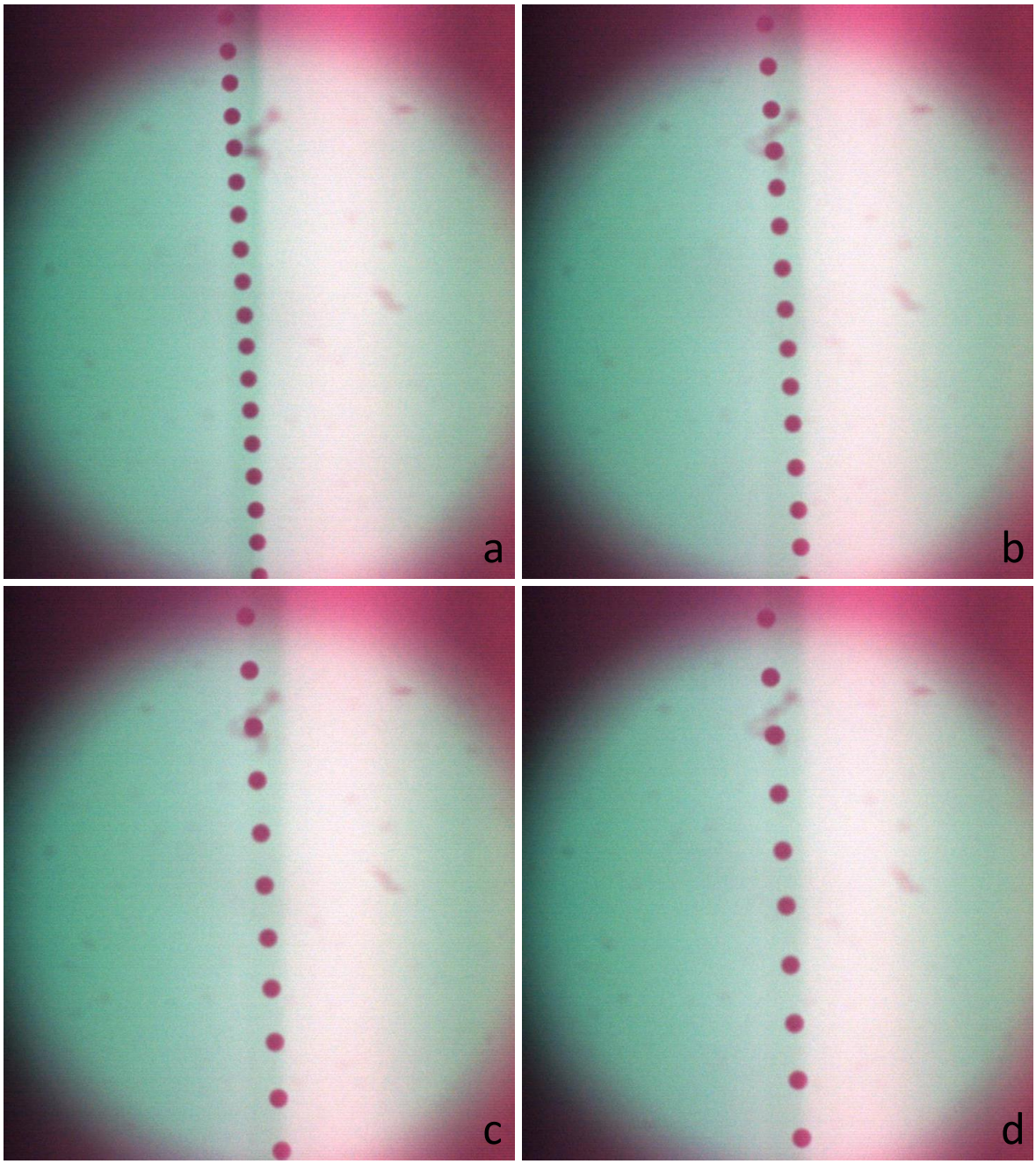

Figure 5.16 *Effect of feed flow rate on droplet size. a: 2 ml/min, b: 2.5 ml/min, c: 3 ml/min, d: 3.5 ml/min (Feed: water at frequency of 7.5 kHz).*

In addition, the feed solution with high viscosity requires higher breaking up force to acquire monodisperse droplets, which means higher disturbance frequency is required. On the other hand, bigger droplets are generated for viscous liquid at the same

disturbance frequency. This is due to high viscosity increases the viscous force and surface tension thereby increases the resistance of droplets to break-up (Wu et al., 2007).

Wu et al. (2011) have demonstrated same trends in their study in terms of the effect of frequency, feed flow rate and feed viscosity on monodisperse droplet production.

5.6.5 Particle size distribution and morphology of monodisperse dried products

The particle size distribution for the powder obtained from two different sizes of nozzle orifice is shown in Figure 5.17. The D10, D50 and D90 values for 50 μm and 80 μm nozzles are relatively 140, 239 and 366 μm, and 320, 490 and 766 μm. It can be seen from the figure that the size distribution of monodisperse dried particles is relatively narrow. The comparison of particle size between monodisperse drying and conventional spray drying will be included in the next chapter.

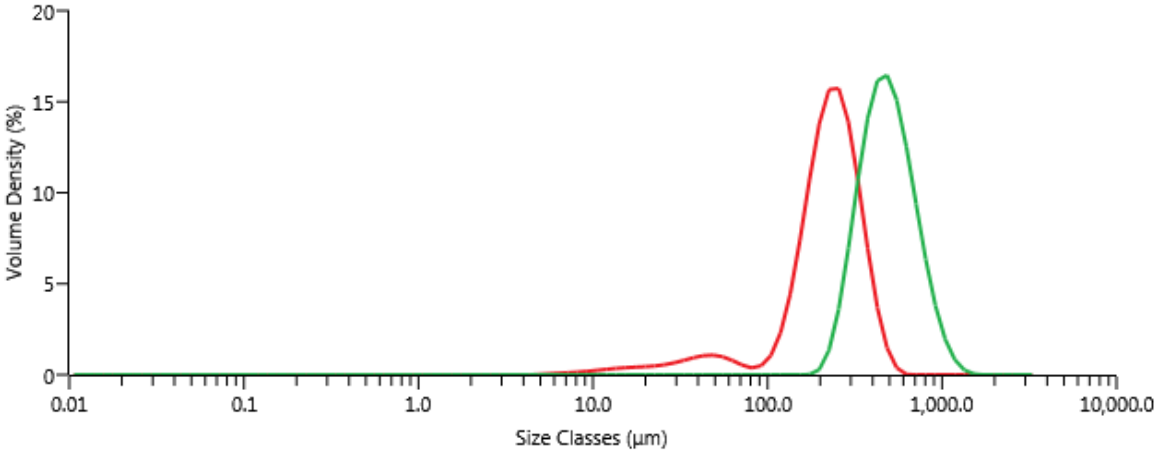

Figure 5.17 *Powder particle size distribution for monodisperse dried lactase powder obtained from nozzles with different diameters (red line: 50 μm nozzle, middle air temperature 110 ℃; green line: 80 μm nozzle, middle air temperature 100 ℃).*

As stated previously, the size of droplet is usually 2 to 3 times of the size of nozzle orifice, and shrinkage of droplets will occur during drying process due to loss of moisture; thus the diameter of the dried particle should be even smaller. However, the size of particles measured is approximately 5 to 6 times of the size of nozzle orifice according to the results. By observing the microscope images of the particles (Figure 5.18) it can be seen that coalescence of droplets occurs during the drying process, which accords with the large droplet size.

There are several reasons that can cause the coalescence. Wu et al. (2011) have defined a phenomenon called semi-monodisperse which represents the situation that a pair of initially monodisperse smaller droplets get closer when travelling down and recoil together into bigger droplets after travelling for a period of time. This phenomenon defined in their study is in the premise of no interference from the environment and happens at a certain frequency, considering to be a transition state between random and monodisperse.

In an actual experimental system, the falling liquid jet may be affected by various factors; for instance, turbulence, gravitational force and surrounding airflow. The turbulence of jet can be triggered by the pressure and flow fluctuation of the HPLC pump and may lead to differences in velocity of droplets. The effects of surrounding air can be explained by the phenomenon called “drag”. Drag is an aerodynamic force generated when a solid object moving through a fluid. Drag force acts in a direction opposite to the relative motion of the moving body (Ruban & Gajjar, 2014), resulting in reduced pressure behind the moving droplet. If two droplets move in the same direction in the surrounding fluid, drag force of the former one tends to drag the latter one to join itself if they are too close to each other. In addition, once the adjacent droplets join to each other and become a bigger droplet, the velocity of the coalescence droplet

increases and tend to catch the next droplet to form bigger and bigger droplets. As a result, a coalescence of multiple particles formed as it can be observed in Figure 5.18.

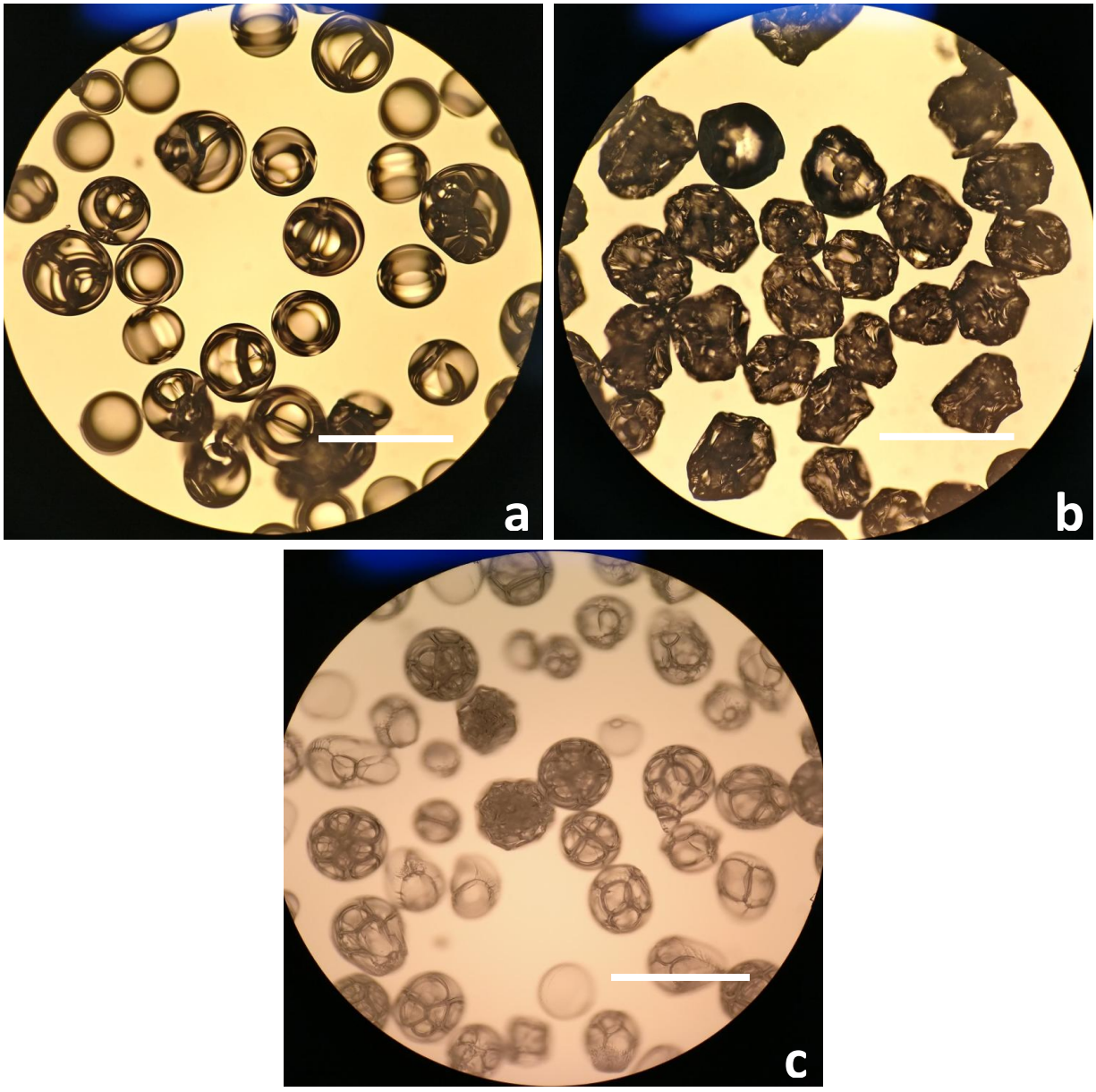

Figure 5.18 *Light micrograph for monodisperse dried powder. a: WPI (35% T.S., 50 µm nozzle, middle air temperature 116 ℃), b: lactase (35% T.S., 80 µm nozzle, middle air temperature 107 ℃), c: egg white (30% T.S., 50 µm nozzle, middle air temperature 110 ℃) (100 × magnifications, 5 µm scale bar).*

In terms of particle morphology, WPI (Figure 5.18a) and egg white (Figure 5.18c) particles exhibit hollow spheres with agglomeration of several particles; fragments of spheres can also be observed. Nevertheless, lactase particles exhibit irregular convex-concave morphology with corrugated edge; it is also hard to recognize whether they have a hollow interior. The hollow interior of droplets is formed by the air expansion in the droplet during the drying process (Kamlesh C. Patel & Chen, 2008). Rogers, Wu, et al. (2012) and Rogers, Fang, et al. (2012) have reported their conjectures about the relationship between high internal temperature and hollow particles; and on the other hand, 'buckled' particles are considered to be related to the lower internal temperature condition. In this experiment, 'buckled' particles, as shown in Figure 5.18b, were observed in lactase powders which had a larger size of feed droplet and experienced lower air temperature during the drying process, therefore, the interior temperature of lactase particle is more likely lower than that of WPI and egg white particles. Therefore, the conjectures from Rogers et al. (2012) are corroborated in this study.

5.7 Conclusions

In conclusion, the effect of outlet air temperature on protein denaturation in monodisperse drying generally agrees with the results from spray drying. Lactase is the most sensitive to air temperature of the three materials. The extent of protein denaturation increases with outlet air temperature increases. It is noteworthy that the air temperature in the drying tower for monodisperse drying is a continuous state due to the height of the tower, and the residence time is also much higher than spray drying. Therefore, the effect of air temperature on the product is a result of the entire temperature history rather than the temperature at one point. In addition, the difference

in effects between two settings of the experiment (with or without exhaust fan) on protein denaturation is significant. With the exhaust fan (vacuum cleaner) on, the air temperature at the middle and bottom of the drying chamber increases, resulting in a greater extent of protein denaturation.

The size of droplets generated from the printing head is determined by the nozzle orifice diameter, disturbing frequency, feed viscosity and feed flow rate. To prevent wet products, droplet size needs to be well adjusted. It is summarized that the application of smaller nozzle orifice diameter (50 μm), higher frequency (over 12 kHz) and higher feed flow rate (4 ml/min) is more beneficial to achieve well separated monodisperse droplet and dried product for a viscous feed material. However, it is found that the dried particles are usually the agglomeration of several particles and having bigger particle size than expected. This was concluded to be caused by differential drag force and unexpected turbulence of the system.

The results indicate that the products obtained from monodisperse drying encountered larger extent of thermal degradation compare to spray drying, which is contrary to our expectation. The comparison of spray drying and monodisperse drying and possible reasons will be discussed in the next chapter, along with the recommendations for improving the current monodisperse drying method.

Chapter 6 Overall discussion and recommendations for future work

6.1 Overall discussion

Spray drying is a process where the liquid feed is sprayed into small droplets and rapidly dried as it comes in contact with a stream of hot air (Toledo, 2007). The atomization process of spray drying causes generation of droplets of different sizes. With a wide range of droplet size distribution, overheating of small particles may occur and give rise to problems in powder collection (Watson & Harper, 1988). One possible reason is that the small particles are lighter and more likely to stay in the drying chamber for a longer time (Schmitz-Schug, Kulozik, & Foerst, 2016b). Therefore, one possible direction to optimize the spray drying process is to narrow down the range of droplet size distribution. Based on this theory, monodisperse drying technique which aims to produce particles with uniform size is introduced. The design of monodisperse droplet generator allows for the precise control of the feed system to produce a stream of small droplets with the same size. What we expected from this technique is that each of the particles experiences the same drying history and result in similar quality properties of the dried products (Rogers, Fang, et al., 2012). If the drying conditions are properly controlled, overheating of particles due to the variation in droplet size should be eliminated.

A comparison of particle size between spray drying and monodisperse drying is shown in Figure 6.1. It can be observed from the figure that monodisperse drying has a much narrower size distribution but larger particle size compared to conventional spray drying. The reasons for having large particle size were discussed in the previous chapter, including particle coalescence due to drag force and particle expansion due to high

interior temperature. The similar morphology effect of the monodisperse dried powder was observed in the drying of skim milk by Rogers, Fang, et al. (2012) and Rogers, Wu, et al. (2012). However, no particle coalescence was found in their study. Rogers, Fang, et al. (2012) have reported that 'puffed' hollow particles are more likely to be formed at high temperature conditions, which is consistent with the results in this study. They also observed loss of solubility and heat damages from the monodisperse dried powders operated at high air temperature.

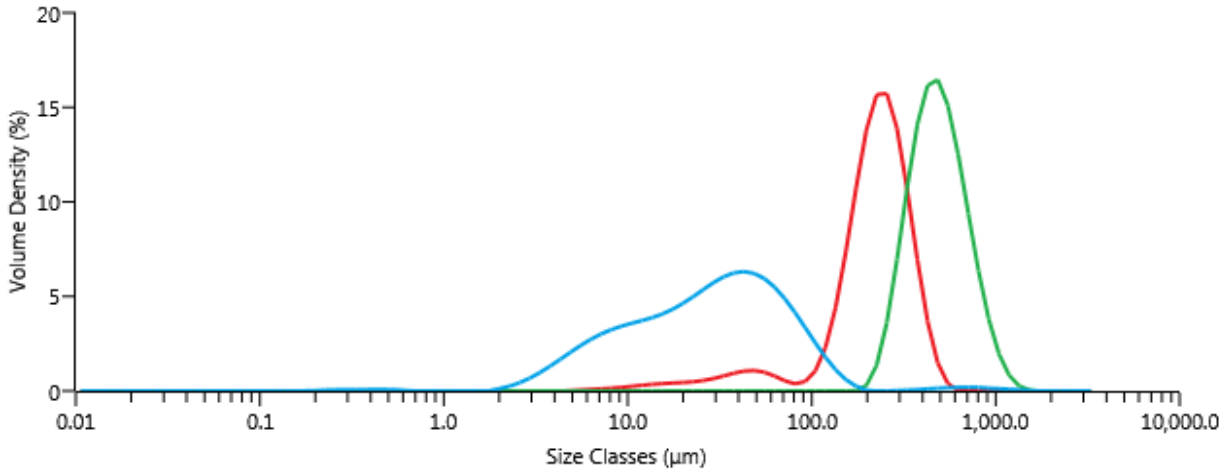

Figure 6.1 *Powder particle size distribution for spray dried and monodisperse dried lactase (blue line: spray drying, outlet air temperature 80 ℃; red line: 50 µm nozzle, middle air temperature 110 ℃; green line: 80 µm nozzle, middle air temperature 100 ℃).*

The comparison in residual non-denatured protein of the powders obtained from spray drying and monodisperse drying is shown in Figure 6.2. An overall trend can be seen from the figures that the residual % activity of enzymes and % non-denatured values of proteins decrease as the outlet air temperature increases. Monodisperse dried lactase particles have a lowest interior temperature but a higher extent of activity loss,

indicating that lactase has a higher thermal sensitivity. Whereas monodisperse dried egg white powders have a highest overall % non-denatured value compared to the other two materials. One possible reason is that egg white feed solution is the only one made in 30% (w/w) total solid content while the other two feed solutions both have a total solid content of 35% (w/w). Decreasing in feed solid content results in an increased level of undenatured protein remaining in the dried product (Anandharamakrishnan et al., 2007).

It can also be observed that for all of the three materials, the powders obtained from monodisperse drying encountered higher extent of protein denaturation compared to spray drying. These findings reject the expectation that monodisperse drying will improve the quality of the dried products. Two dominating parameters that affect the quality of monodisperse dried powders are air temperature and residence time. Particles exposed to a high temperature for a prolonged period of time is considered to be the main reason for severe heat degradation that occurred in monodisperse drying (Toledo, 2007). As stated previously, spray drying has a residence time of approximately 15 seconds and outlet air temperature between 85 and 115 ℃, whereas monodisperse drying has a longer residence time 21 and 45 seconds for high and low air flow rate settings respectively. The temperature profile in the drying tower has been reported in Chapter 5. The drying tower has a height of 12 meters. The air temperature at the top of the tower is 200 ℃. The air temperature is 100-130 ℃ in the middle of the tower and 67-80 ℃ at the bottom of the tower for high air flow setting; 90-108 ℃ in the middle and 63-73 ℃ at the bottom of the tower for low air flow setting. The longer time the particles remaining in the high temperature air, the greater risk of overheating exists.

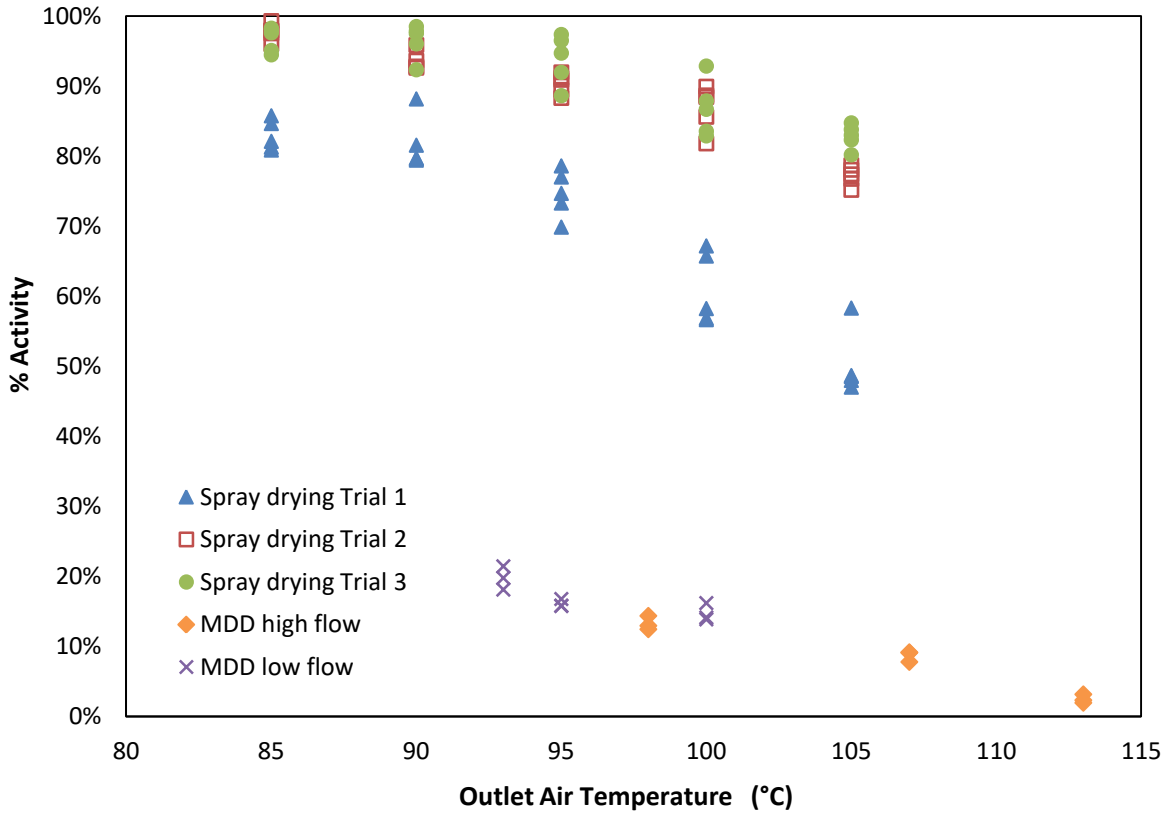
100%
90%
80%
70%
60%
50%
40%
30%
20%
10%
0%
% Activity
80
85
90
95
100
105
110
115
Outlet Air Temperature (°C)
Spray drying Trial 1
Spray drying Trial 2
Spray drying Trial 3
MDD high flow
MDD low flow

(a)

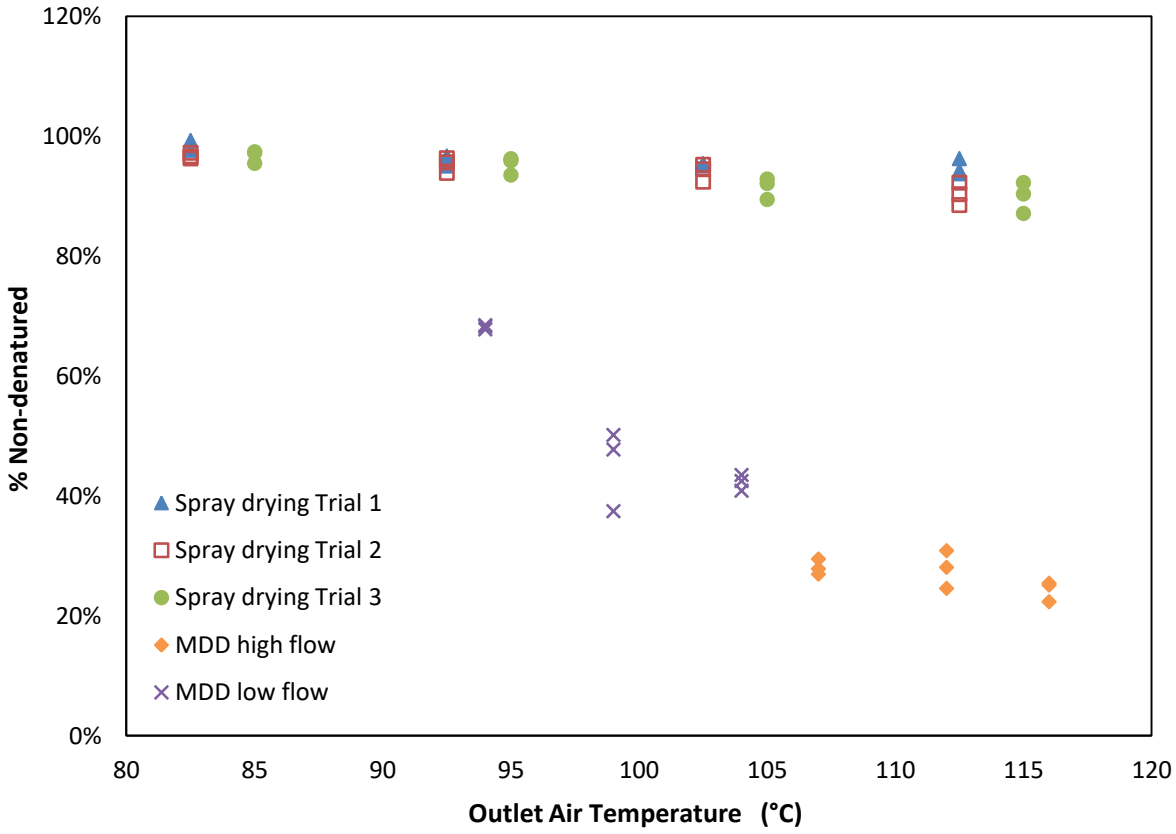
120%
100%
80%
60%
40%
20%
0%
% Non-denatured
80
85
90
95
100
105
110
115
120
Outlet Air Temperature (°C)
Spray drying Trial 1
Spray drying Trial 2
Spray drying Trial 3
MDD high flow
MDD low flow

(b)

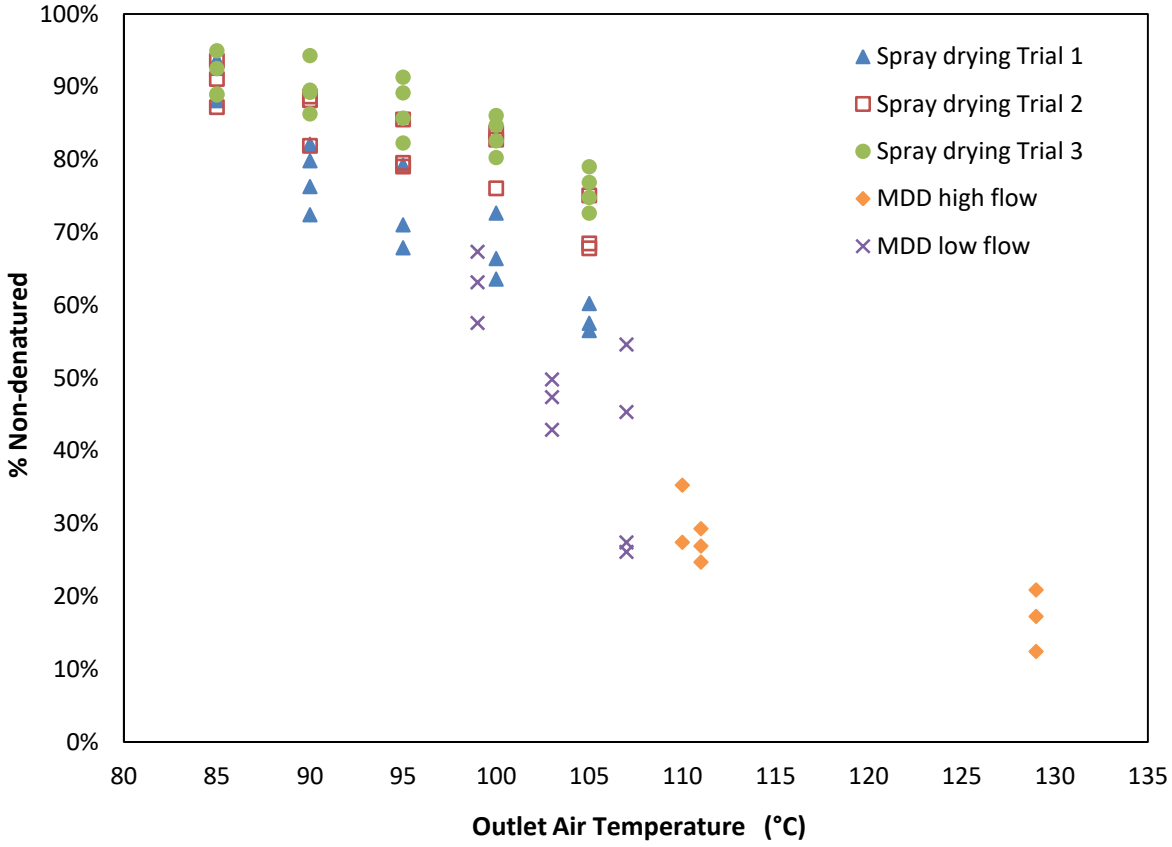

(c)

Figure 6.2 *Comparison between spray drying and monodisperse drying on the percentage activity of dried powders for (a) lactase, percentage non-denatured values for (b) WPI and (c) egg white; and outlet air temperature (middle air temperatures are presented for monodisperse drying)*

It is speculated that during monodisperse drying the droplet loses moisture rapidly at the beginning of the drying process and form a solid crust with a wet core. The temperature of the particle remains at the wet bulb temperature of the drying air at this stage; therefore, minor heat damage will occur. This is also the stage when the coalescence of particles occurs. It can then explain why multivesicular hollow particles are observed in the micrographs of monodisperse dried powders. If coalescence happens before solid crust formation, merging of liquid droplets will occur and it is not likely to

form a particle with multi vesicle. If coalescence happens afterwards, the particle surface will be too dry to stick together. As moisture migration and formation of the solid crust continue, the movement of moisture from the interior to the surface of the particle is hindered. Subsequently, the temperature of the particle increases and boiling of internal moisture occurs to form a multivesicular hollow particle. Boiling of the internal moisture takes place at a relatively high air temperature condition, and results in heat damage to the heat sensitive components.

In order to optimize the experimental parameters and achieve better product quality, improvements can be made in the aspect of feed flow rate, inlet air temperature and air flow control to reduce the time of product contacting with high temperature air. Optimization of operating conditions will be given in the next section.

Table 6.1 *Comparison of activation energy obtained from different techniques*

	Spray drying		*Monodisperse drying*	
Materials	E_a (kJ/mol)	*Outlet air temperature (℃)*	E_a (kJ/mol)	*Middle air temperature (℃)*
Lactase	110.6	85-105	41.6	93-113
WPI	44.7	85-115	15.4	99-116
Egg white	74.4	85-105	27.4	103-129

Table 6.1 summarizes the activation energy values obtained from the two methods. Differences in the activation energy in the different temperature range for each material can be observed from the table. As discussed previously, the dependence of reaction rate of protein denaturation on temperature is affected by the temperature range (Anema & McKenna, 1996). Therefore, lower activation energy is obtained at the high temperature range from monodisperse drying.

The accuracy of E_a values obtained from monodisperse drying experiment is also affected by the number of data points and the order of reaction. Too few temperature points present in the Arrhenius plot of monodisperse drying impacts the reliability of the regression model. The actual order of reaction may not be 1, which may also influence the accuracy of regression. In addition, the air temperature used in the calculation of E_a in monodisperse drying is the middle air temperature, which cannot exactly reflect the actual temperature of the particles in the chamber and may also lead to error in calculation.

6.2 Optimization and Recommendations

Based on what has been discussed above, there are several suggestions for optimizing the experimental parameters for the monodisperse drying to achieve better product yield and quality in the future studies:

- Have both of the vacuum cleaner (induced draught fan) and the blower (forced draught fan) on to ensure a more balanced airflow system and help powder collection. With the vacuum cleaner on, the air temperature in the drying tower will be increased. In the meantime, more precise air temperature control is required. The air temperature is affected by the pattern of the air flow. The current system only allows very limited airflow adjustment for the vacuum cleaner, and it can be improved by installing a ball valve at the exit of the vacuum cleaner. By adjusting this valve and the one located at the exit of the blower, more control levels for the airflow will be introduced, thereby altering the air temperature and residence time.

- Apart from adjusting the airflow in the tower, there are several other approaches to lower the air temperature in the drying tower including increasing the feed flow rate and reducing the inlet air temperature. It is noteworthy that when adjusting these parameters, the drying capacity should be taken into consideration. Pre-experiments are required to investigate the proper conditions that preventing inadequate drying and sticky powder.
- To prevent particle coalescence, it is suggested to increase the distance between the monodisperse droplets to at least 2-3 times of the particle diameter. For the current setting, the droplet visualization system is by the side of the drying tower. The printing system is first demounted from the top of the drying tower to be adjusted until having desired monodisperse droplet stream and then mounted to the top of the tower. One way to improve the system is to lift up the camera to the top of the drying tower, making sure it can capture the image of droplets when the printing system is working normally on the top of the drying chamber through the transparent cylinder. Better monitoring of the droplet morphology and immediate regulation are insured in this way of setting.
- More repeats of experiments are required for further studies to investigate the more accurate relationship between air temperature and product quality.

References

Adhikari, B., Howes, T., Bhandari, B., & Truong, V. (2000). Experimental studies and kinetics of single drop drying and their relevance in drying of sugar‐rich foods: A review. *International Journal of Food Properties, 3*(3), 323-351.

Al Zaitone, B. A., & Tropea, C. (2011). Evaporation of pure liquid droplets: Comparison of droplet evaporation in an acoustic field versus glass-filament. *Chemical Engineering Science, 66*(17), 3914-3921.

Ameri, M., & Maa, Y.-F. (2006). Spray drying of biopharmaceuticals: stability and process considerations. *Drying technology, 24*(6), 763-768.

Anandharamakrishnan, C., Rielly, C., & Stapley, A. (2007). Effects of process variables on the denaturation of whey proteins during spray drying. *Drying technology, 25*(5), 799-807.

Anandharamakrishnan, C., Rielly, C. D., & Stapley, A. (2008). Loss of solubility of α-lactalbumin and β-lactoglobulin during the spray drying of whey proteins. *LWT-Food Science and Technology, 41*(2), 270-277.

Ananta, E., Volkert, M., & Knorr, D. (2005). Cellular injuries and storage stability of spray-dried Lactobacillus rhamnosus GG. *International Dairy Journal, 15*, 399-409. doi:10.1016/j.idairyj.2004.08.004

Anema, S. G., & McKenna, A. B. (1996). Reaction kinetics of thermal denaturation of whey proteins in heated reconstituted whole milk. *Journal of Agricultural and Food Chemistry, 44*(2), 422-428.

AOAC. (2006). *Official Methods of Analysis of the Association of Official Analytical Chemists* (18th ed.). Gaithersburgs, MD.

Ayadi, M., Khemakhem, M., Belgith, H., & Attia, H. (2008). Effect of moderate spray drying conditions on functionality of dried egg white and whole egg. *Journal of Food Science, 73*(6).

Boye, J., & Alli, I. (2000). Thermal denaturation of mixtures of α-lactalbumin and β-lactoglobulin: a differential scanning calorimetric study. *Food Research International, 33*(8), 673-682.

Brenn, G., Rensink, D., Tropea, C., & Yarin, A. (1997). Investigation of droplet drying characteristics using an acoustic-aerodynamic levitator. *International Journal of Fluid Mechanics Research, 24*, 633-642.

Brennan, J. G. (2011). Evaporation and Dehydration. In J. G. Brennan & A. S. Grandison (Eds.), *Food Processing Handbook* (pp. 77-130): Wiley-VCH Verlag GmbH & Co. KGaA.

BSSA. (2017). Heat tint (temper) colours on stainless steel surfaces heated in air. Retrieved from https://www.bssa.org.uk/topics.php?article=140

Caliskan, G., & Nur Dirim, S. (2013). The effects of the different drying conditions and the amounts of maltodextrin addition during spray drying of sumac extract. *Food and Bioproducts Processing, 91*(4), 539-548. doi:https://doi.org/10.1016/j.fbp.2013.06.004

Campbell, L., Raikos, V., & Euston, S. R. (2003). Modification of functional properties of egg‐white proteins. *Molecular Nutrition & Food Research, 47*(6), 369-376.

Chen, X. D. (2004). Heat-mass transfer and structure formation during drying of single food droplets. *Drying technology, 22*(1-2), 179-190. doi:10.1081/drt-120028226

Costa-Silva, T. A., Nogueira, M. A., Fernandes Souza, C. R., Oliveira, W. P., & Said, S. (2011). Lipase production by endophytic fungus Cercospora kikuchii: stability

of enzymatic activity after spray drying in the presence of carbohydrates. *Drying technology, 29*(9), 1112-1119.

Dannenberg, F., & Kessler, H. G. (1988). Reaction kinetics of the denaturation of whey proteins in milk. *Journal of Food Science, 53*(1), 258-263.

Dijkstra, C. E., Larkin, O. J., Anthony, P., Davey, M. R., Eaves, L., Rees, C. E., & Hill, R. J. (2011). Diamagnetic levitation enhances growth of liquid bacterial cultures by increasing oxygen availability. *Journal of The Royal Society Interface, 8*(56), 334-344.

Earle, R. L., & Earle, M. D. (1983). Drying.Unit operations in food processing (2nd ed.): NZIFST. Retrieved from http://www.nzifst.org.nz/unitoperations/drying.htm.

Earle, R. L., & Earle, M. D. (2007). *Fundamentals of food reaction technology.* : Cambridge : Royal Society of Chemistry, 2007.

Etzel, M., Suen, S.-Y., Halverson, S., & Budijono, S. (1996). Enzyme inactivation in a droplet forming a bubble during drying. *JOURNAL OF FOOD ENGINEERING, 27*(1), 17-34.

Fang, Y., Rogers, S., Selomulya, C., & Chen, X. D. (2012). Functionality of milk protein concentrate: Effect of spray drying temperature. *Biochemical Engineering Journal, 62*, 101-105. doi:http://dx.doi.org/10.1016/j.bej.2011.05.007

Farid, M. (2003). A new approach to modelling of single droplet drying. *Chemical Engineering Science, 58*(13), 2985-2993.

Filkova, I., Huang, L. X., & Mujumdar, A. S. (2007). Industrial spray drying systems. In A. S. Mujumdar (Ed.), *Handbook of industrial drying* (pp. 215-254). New York: CRC Press.

Fitzsimons, S. M., Mulvihill, D. M., & Morris, E. R. (2007). Denaturation and aggregation processes in thermal gelation of whey proteins resolved by differential scanning calorimetry. *Food Hydrocolloids, 21*(4), 638-644. doi:http://dx.doi.org/10.1016/j.foodhyd.2006.07.007

Frydenberg, R. P., Hammershøj, M., Andersen, U., Greve, M. T., & Wiking, L. (2016). Protein denaturation of whey protein isolates (WPIs) induced by high intensity ultrasound during heat gelation. *FOOD CHEMISTRY, 192*, 415-423.

Fu, N., Woo, M. W., & Chen, X. D. (2011). Colloidal transport phenomena of milk components during convective droplet drying. *Colloids and Surfaces B: Biointerfaces, 87*(2), 255-266.

Fu, N., Woo, M. W., & Chen, X. D. (2012). Single Droplet Drying Technique to Study Drying Kinetics Measurement and Particle Functionality: A Review. *Drying technology*(15).

Fu, N., Zhou, Z., Jones, T. B., Tan, T. T. Y., Wu, W. D., Lin, S. X., . . . Chan, P. P. Y. (2011). Production of monodisperse epigallocatechin gallate (EGCG) microparticles by spray drying for high antioxidant activity retention. *International Journal of Pharmaceutics, 413*(1–2), 155-166. doi:http://dx.doi.org/10.1016/j.ijpharm.2011.04.056

Gharsallaoui, A., Roudaut, G., Chambin, O., Voilley, A., & Saurel, R. (2007). Applications of spray-drying in microencapsulation of food ingredients: An overview. *Food Research International*.

Gibbs, F. B., Kermasha, S., Alli, I., & Mulligan, C. N. (1999). Encapsulation in the food industry: a review. *International journal of food sciences and nutrition, 50*(3), 213-224.

Groenewold, C., Möser, C., Groenewold, H., & Tsotsas, E. (2002). Determination of single-particle drying kinetics in an acoustic levitator. *Chemical Engineering Journal, 86*(1), 217-222.

Heldman, D. R., & Hartel, R. W. (1997). Dehydration. *Principles of food processing* (pp. 177-218). New York: International Thomson Publishing.

Hillier, R. M., & Lyster, R. L. (1979). Whey protein denaturation in heated milk and cheese whey. *Journal of Dairy Research, 46*(1), 95-102.

Höhne, G. W. H., Hemminger, W. F., & H.-J., F. (2004). *Differential scanning calorimetry* (2nd ed.). Berlin Heidelberg: Springer.

IDF. (1993). Provisional Standard 26A: Dried milk and cream - Determination of water content. *International Dairy Federation, Brussels, Belgium*.

Jelen, P. (1985). Processes for Food Preservation. *Introduction to food processing*. Reston, Va.: Reston Pub. Co.

Kastner, O., Brenn, G., Rensink, D., & Tropea, C. (2001). The acoustic tube levitator–a novel device for determining the drying kinetics of single droplets. *Chemical engineering & technology, 24*(4), 335-339.

Kessler, H. G. (1981). *Food engineering and dairy technology*. Freising, Germany: Verlag A. Kessler.

Kha, T. C., Nguyen, M. H., & Roach, P. D. (2010). Effects of spray drying conditions on the physicochemical and antioxidant properties of the Gac (Momordica cochinchinensis) fruit aril powder. *JOURNAL OF FOOD ENGINEERING, 98*(3), 385-392. doi:https://doi.org/10.1016/j.jfoodeng.2010.01.016

Kim, S. S., & Bhowmik, S. R. (1990). Survival of Lactic Acid Bacteria during Spray Drying of Plain Yogurt. *Journal of Food Science, 55*(4), 1008-1010. doi:10.1111/j.1365-2621.1990.tb01585.x

Lepock, J. R. (2005). How do cells respond to their thermal environment? *International journal of hyperthermia, 21*(8), 681-687.

Lin, R., Woo, M. W., Fu, N., Selomulya, C., & Chen, X. D. (2013). In Situ Observation of Taurine Crystallization via Single Droplet Drying. *Drying technology*(13-14).

Liu, H. (1999). *Science and engineering of droplets : fundamentals and applications*: Norwich, NY : Noyes Publications, 1999.

Lorenzen, E., & Lee, G. (2012). Slow motion picture of protein inactivation during single‐droplet drying: A study of inactivation kinetics of l‐glutamate dehydrogenase dried in an acoustic levitator. *Journal of Pharmaceutical Sciences, 101*(6), 2239-2249.

Ma, S., Zhao, S., Zhang, Y., Yu, Y., Liu, J., & Xu, M. (2013). Quality characteristic of spray-drying egg white powders. *Molecular biology reports, 40*(10), 5677-5683.

Meerdink, G., & Van't Riet, K. (1991). Inactivation of thermostable α-amylase during drying. *JOURNAL OF FOOD ENGINEERING, 14*(2), 83-102.

Mezhericher, M., Levy, A., & Borde, I. (2007). Theoretical Drying Model of Single Droplets Containing Insoluble or Dissolved Solids. *Drying technology, 25*(6), 1035-1042. doi:10.1080/07373930701394902

Mezhericher, M., Levy, A., & Borde, I. (2008a). Heat and mass transfer of single droplet/wet particle drying. *Chemical Engineering Science, 63*, 12-23. doi:10.1016/j.ces.2007.08.052

Mezhericher, M., Levy, A., & Borde, I. (2008b). The Influence of Thermal Radiation on Drying of Single Droplet/Wet Particle. *Drying technology, 26*(1), 78-89. doi:10.1080/07373930701781686

Mezhericher, M., Levy, A., & Borde, I. (2010). Theoretical Models of Single Droplet Drying Kinetics: A Review. *Drying technology, 28*(2), 278-293. doi:10.1080/07373930903530337

Mishra, P., Mishra, S., & Mahanta, C. L. (2014). Effect of maltodextrin concentration and inlet temperature during spray drying on physicochemical and antioxidant properties of amla (Emblica officinalis) juice powder. *Food and Bioproducts Processing, 92*(3), 252-258. doi:https://doi.org/10.1016/j.fbp.2013.08.003

Mondragon, R., Jarque, J. C., Julia, J. E., Hernandez, L., & Barba, A. (2012). Effect of slurry properties and operational conditions on the structure and properties of porcelain tile granules dried in an acoustic levitator. *Journal of the European Ceramic Society, 32*(1), 59-70.

Oldfield, D. J., Taylor, M. W., & Singh, H. (2005). Effect of preheating and other process parameters on whey protein reactions during skim milk powder manufacture. *International Dairy Journal, 15*, 501-511. doi:10.1016/j.idairyj.2004.09.004

Pajander, J. P., Matero, S., Sloth, J., Wan, F., Rantanen, J., & Yang, M. (2015). Raman Mapping of Mannitol/Lysozyme Particles Produced Via Spray Drying and Single Droplet Drying. *Pharmaceutical Research*(6), 1993. doi:10.1007/s11095-014-1592-z

Patel, K. C., & Chen, X. D. (2008). Drying of aqueous lactose solutions in a single stream dryer. *Food and Bioproducts Processing, 86*(3), 185-197. doi:http://dx.doi.org/10.1016/j.fbp.2007.10.013

Patel, K. C., Wu, W. D., & Chen, X. D. (2007). *Review on generation of monodisperse sprays for manufacturing micron-size uniform particles using a spray drying technique.* Paper presented at the The Proceedings of the 5th Asia-Pacific Drying Conference: (In 2 Volumes).

Perdana, J., Fox, M. B., Schutyser, M. A., & Boom, R. M. (2013). Mimicking spray drying by drying of single droplets deposited on a flat surface. *FOOD AND BIOPROCESS TECHNOLOGY, 6*(4), 964-977.

Perdana, J., Fox, M. B., Schutyser, M. A. I., & Boom, R. M. (2012). Enzyme inactivation kinetics: Coupled effects of temperature and moisture content. *FOOD CHEMISTRY, 133*(1), 116-123. doi:http://dx.doi.org/10.1016/j.foodchem.2011.12.080

Ravindran, R., & Glasgow, S. (2016). *Food Chemistry Laboratory Manual*. Massey University, Palmerston North: Institute of Food, Nutrition and Human Health.

R é, I. M. (1998). Microencapsulation by spray drying. *Drying technology, 16*(6), 1195-1236.

Renneboog, R. M. M. (2015). Activation Energy: Salem Press.

Rogers, S., Fang, Y., Lin, S. X. Q., Selomulya, C., & Chen, X. D. (2012). A monodisperse spray dryer for milk powder: Modelling the formation of insoluble material. *Chemical Engineering Science, 71*, 75-84. doi:http://dx.doi.org/10.1016/j.ces.2011.11.041

Rogers, S., Wu, W. D., Lin, S. X. Q., & Chen, X. D. (2012). Particle shrinkage and morphology of milk powder made with a monodisperse spray dryer. *Biochemical Engineering Journal, 62*, 92-100.

Rotstein, E., & Crapiste, G. H. (1997). Design and Performance Evaluation of Dryers. In K. J. Valentas, E. Rotstein, & R. P. Singh (Eds.), *Handbook of Food Engineering Practice* (pp. 125-166): CRC Press.

Ruban, A. I., & Gajjar, J. S. B. (2014). *Fluid dynamics*: Oxford : Oxford University Press, 2014.

Samborska, K., Witrowa-Rajchert, D., & Gonçalves, A. (2005). Spray-drying of α-amylase—The effect of process variables on the enzyme inactivation. *Drying technology, 23*(4), 941-953.

Santivarangkna, C., Kulozik, U., & Foerst, P. (2007). Alternative Drying Processes for the Industrial Preservation of Lactic Acid Starter Cultures. *Biotechnology Progress, 23*(2), 302-315.

Schmitz-Schug, I., Kulozik, U., & Foerst, P. (2016a). Modeling spray drying of dairy products–Impact of drying kinetics, reaction kinetics and spray drying conditions on lysine loss. *Chemical Engineering Science, 141*, 315-329.

Schmitz-Schug, I., Kulozik, U., & Foerst, P. (2016b). Modeling spray drying of dairy products – Impact of drying kinetics, reaction kinetics and spray drying conditions on lysine loss. *Chemical Engineering Science, 141*, 315-329. doi:10.1016/j.ces.2015.11.008

Schutyser, M. A. I., Perdana, J., & Boom, R. M. (2012). Single droplet drying for optimal spray drying of enzymes and probiotics. *Trends in food science & technology*(2).

Sharma, D. (2012). Non-isothermal unfolding/denaturing kinetics of egg white protein. *Journal of thermal analysis and calorimetry, 109*(3), 1139-1143.

Silva, J., Freixo, R., Gibbs, P., & Teixeira, P. (2011a). Spray-drying for the production of dried cultures. *International Journal of Dairy Technology, 64*(3), 321-335. doi:10.1111/j.1471-0307.2011.00677.x

Silva, J., Freixo, R., Gibbs, P., & Teixeira, P. (2011b). Spray drying for the production of dried cultures. *International Journal of Dairy Technology, 64*(3), 321-335.

Sloth, J., Kiil, S., Jensen, A. D., Andersen, S. K., Jørgensen, K., Schiffter, H., & Lee, G. (2006). Model based analysis of the drying of a single solution droplet in an ultrasonic levitator. *Chemical Engineering Science, 61*(8), 2701-2709.

Ståhl, K., Claesson, M., Lilliehorn, P., Lindén, H., & Bäckström, K. (2002). The effect of process variables on the degradation and physical properties of spray dried insulin intended for inhalation. *International Journal of Pharmaceutics, 233*(1), 227-237. doi:https://doi.org/10.1016/S0378-5173(01)00945-0

TNO. (2014). Enabling the drying process to save energy and water, realising process efficiency in the dairy chain - Small scale single nozzle ink for printing dairy. *Enthalpy*.

Toledo, R. T. (2007). Dehydration. *Fundamentals of food process engineering* (3rd ed.). New York: Springer.

van't Land, C. M. (2011a). Introduction *Drying in the Process Industry* (pp. 1-7): John Wiley & Sons, Inc.

van't Land, C. M. (2011b). Spray Drying *Drying in the Process Industry* (pp. 133-162): John Wiley & Sons, Inc.

van Deventer, H., Houben, R., & Koldeweij, R. (2013). New atomization nozzle for spray drying. *Drying technology, 31*(8), 891-897.

Vehring, R. (2008). Pharmaceutical particle engineering via spray drying. *Pharmaceutical Research, 25*(5), 999-1022.

Watson, E. L., & Harper, J. C. (1988). Dehydration. *Elements of food engineering* (2nd ed.). New York: Van Nostrand Reinhold

Werner, S. R. L., Edmonds, R. L., Jones, J. R., Bronlund, J. E., & Paterson, A. H. J. (2008). Single droplet drying: Transition from the effective diffusion model to a modified receding interface model. *Powder Technology, 179*, 184-189. doi:10.1016/j.powtec.2007.06.009

Woo, M. W., & Bhandari, B. (2013). Spray drying for food powder production. In B. Bhandari, N. Bansal, M. Zhang, & P. Schuck (Eds.), *Handbook of food powders : processes and properties* (pp. 29-56). Oxford: Woodhead Publishing.

Wu, W. D., Lin, S. X., & Chen, X. D. (2011). Monodisperse droplet formation through a continuous jet break‐up using glass nozzles operated with piezoelectric pulsation. *AIChE Journal, 57*(6), 1386-1392.

Wu, W. D., Patel, K. C., Rogers, S., & Chen, X. D. (2007). Monodisperse droplet generators as potential atomizers for spray drying technology. *Drying technology, 25*(12), 1907-1916.

Yamamoto, S., & Sano, Y. (1992). Drying of enzymes: enzyme retention during drying of a single droplet. *Chemical Engineering Science, 47*(1), 177-183.

Yarin, A., Brenn, G., Kastner, O., & Tropea, C. (2002). Drying of acoustically levitated droplets of liquid–solid suspensions: evaporation and crust formation. *Physics of Fluids (1994-present), 14*(7), 2289-2298.